2020

Analysing and improving the applicability of Precast Concrete Sandwich Panels

Master Thesis Civil Engineering:
Structural Engineering – Concrete Structures

BRAM SCHROOTEN - 4734440

bram_schrooten@hotmail.com

Lievense | WSP // TU Delft

Graduation Committee:

Dr. ir. Y. Yang (Chair)	TUD | Concrete Structures
Dr. ir. E. O. L. Lantsoght	TUD | Concrete Structures
Prof. dr. ir. J. G. Rots	TUD | Structural Mechanics
Ing. R. Mink	Lievense | WSP | Building Structures

Abstract

Precast Concrete Sandwich Panels (PCSPs) are composite panels consisting of two concrete layers, surrounding an intermediate insulation layer. When these panels are load-bearing, truss-connectors are used to increase the cooperation between the concrete layers. The advantages of these floors are that they possess a high bending resistance, with relative high stiffness and low-weight values. However, the full behaviour of these panels are still unpredictable up until this day. Although researchers have found models that predict the linear behaviour, these are too difficult to be applicable in practice. Non-linear behaviour is still hard to predict, as Finite Element models are still unable to perfectly imitate the cracking behaviour. When these types of floors will be applied into a fully pre-fabricated structures, it is useful to know what type of forces can be expected on those floors, to ensure the structural validity of this structure.

As such, it is necessary to increase the applicability of PCSPs. In this report, this is done by a multitude of methods: a literature study is performed, an advanced, non-linear Finite Element model and simple linear analytical model are developed, and calculations have been performed on a design-structure from Lievense | WSP. The literature study is performed to gain insight into the unique behavioural aspects of PCSPs, and to find where the current issues arise regarding the already-present prediction models. After the most important aspects of these floors have been determined, an advanced Finite Element model is developed to predict both the linear and non-linear behaviour of PCSPs. This FE-model has the possibility to include the non-linearity of all materials. In order to verify the correctness of the full behaviour of this model, it has been compared to experiments from literature. Additionally, the simple linear analytical model is developed, with the goal to make PCSPs easy-to-use in practice, so that people without knowledge about the background-calculations are still able to make use of these floors. This analytical model is compared to the linear version of the FE-model. On top of this, the Reinbouw project from Lievense | WSP is used to analyse what the bottlenecks are in their current design of a fully prefabricated structure. Based on these bottlenecks, a calculation is done to find the required resistances of the PCSPs to ensure a structurally verified structure. Both the linear prediction model and the Reinbouw project are combined at the end, where an advice is given on the PCSP-design in the Reinbouw project. All of these methods have the goal of increasing the applicability of PCSPs.

From the literature study, it was concluded that the main difficulty in calculating and predicting the behaviour of PCSPs was caused by the interaction between the concrete and intermediate layer. This was especially the case in the non-linear part of the floor. In this part, earlier-developed prediction models were not able to predict the detailed tension-stiffening behaviour of the concrete, causing an over- or under-estimation of the PCSP-stiffness of around 20% in the worst cases. The developed FE-model in this research was able to perfectly predict the linear bending behaviour. However, this model started showing deviations from some experiments in the non-linear phase of around 20%, similar to earlier-developed models from literature. Luckily, the model could still be used to understand the general non-linear behaviour. This showed that most of the truss-connectors were showing plasticity after a considerable load, which decreased the composite bending behaviour of the floor even before large cracking occurred in the lower wythe. In regards to shear-experiments, the linear phase of the FE-model did not predict the behaviour correctly, over-estimating the stiffness around six times higher.

The linear analytical model shows perfect results compared to the linear FE-model, both with and without the application of truss-connectors. Only dimensions, strengths and stiffnesses of the different elements are required for the model to predict the stiffness and the accompanied stresses

of these elements. Without the application of truss-connectors, Increasing the concrete thickness of the PCSPs from 60 to 140 mm would decrease the composite factor for a value of around 0.28. Increasing the span length from 4000 to 8000 mm would increase the composite factor for around 0.31. The effect of increasing the insulation thickness from 40 to 80 mm depends on the concrete thickness, where the reduction of the composite factor is 0.02 and 0.06 for a concrete thickness of 60 and 140 mm respectively. When truss-connectors are applied, most PCSP-designs will possess a composite factor of above 0.95 when 12 mm diameter bars are being used every 800 mm. However, when concrete wythes with a thickness of 140 mm or higher are being used, the increase in composite-action due to the application of trusses decreases significantly. When 140 mm and 60 mm thick concrete wythes are used, the composite factor is reduced from 0.96 to 0.91 respectively.

From the Reinbouw project, many different bottlenecks could be found in the design. The most essential part for the PCSP-floors was the applied axial forces, that cause shear forces along the span of the floor due to the connection-method in the floor-design. This shear force is increased if certain pile-foundations are weakened, of which the magnitude has been determined in this report. With regards to the bending behaviour of the PCSPs in the Reinbouw project, the linear prediction model was used to give advice on their design-choices with regards to truss connectors and prestressing.

As such, this research has made an effort to increase the applicability of PCSPs using different methods. The current issues and behaviours of non-linear prediction models have been analysed, while also developing linear models to ensure easy application of these floors in designs. Lastly, an analysis has been done to find design-requirements for PCSPs in unconventional structures that might become more common in the future.

Table of Contents

1. Introduction

1.1. Problem statement

Precast concrete sandwich panels (PCSPs) consist of three layers; two outer concrete layers called "wythes" and one middle insulation-layer. When a PCSP is used as a load-bearing element, diagonal truss-connectors are present to connect the two concrete wythes, resulting in a high level of "composite-action", which describes the level of cooperation between the concrete wythes. A visualisation of these floors are shown in Figure 1-1. This lay-out results in a floor-system with a high bending-resistance, while also being relatively low-weight and energy-efficient. However, PCSPs display complex behaviour. Due to this, and a lack of appropriate design codes and testing methods, experimental findings are being used, which are backed by simplified analytical solutions. However, these solutions do not reflect the real behaviour of PCSPs, as they assume either full or no composite action (Ekenel, 2014).

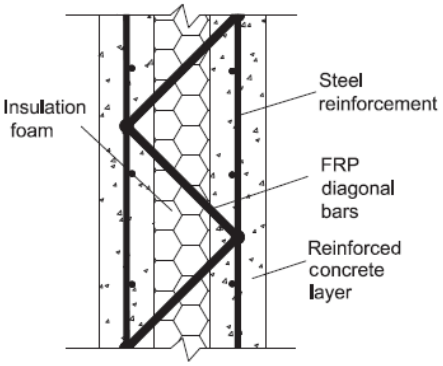

Figure 1-1: Lay-out PCSPs

These PCSPs will be used in a project of Lievense | WSP. (Mink, Discussion about the Reinbouw mid-rise project, 2019). Lievense | WSP is asked to design an apartment building which uses as many prefab elements as possible. The base-design for this is shown in Figure 1-2. The different elements used are prefab walls (green) and PCSPs (orange/green). Next to these prefab elements, a large repetitive unit that includes all important installations is placed in the middle of the apartments (blue). As the structure consists of only pre-fabricated elements, the structure essentially functions as a house of cards. Because the present connections do not cause a sufficient stiffness, diaphragm action is responsible for the stability of the building. Additionally, the elements that possess this diaphragm action must be able to resist the applied forces, which are increased due to the unique structural characteristics. If these unique characteristics are not analysed thoroughly, a failure similar to the one at Eindhoven Airport might occur, where the temperature-effect on the floors partly caused the failure of the entire structure (NOS.nl, 2017).

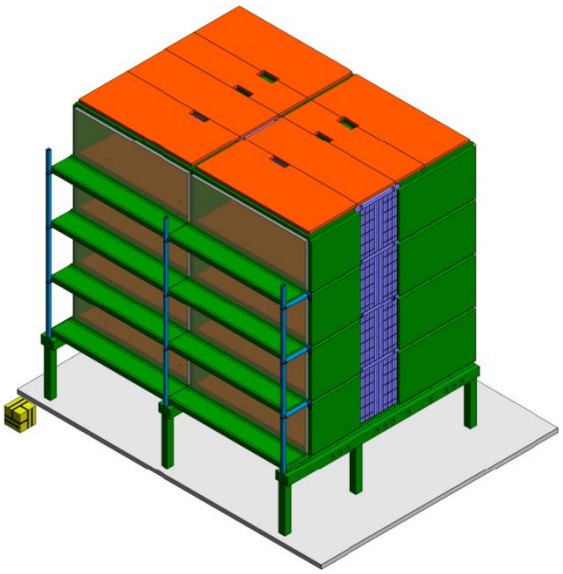

Figure 1-2: Concept of the prefabricated apartments by Lievense | WSP

For the majority of general designs, accurate models are available to predict the behaviour of an element. However, for more advanced floor-types like hybrid precast concrete lattice girders, there was a lack of comprehensive test data, which limited the development of these types of models for the construction-phase severely. In order to obtain more information, multiple specimens were subjected to experiments. A broad range of sensors were used to measure all important parameters, while previous experiments on these types of floors had seemingly not performed this type of analysis (Newell & Goggins, 2019). Without these types of detailed analyses, accurate modelling and optimisation can be difficult.

In order to provide further insights into the behaviour of PCSPs, a theoretical model has been developed which accounted for partial shear interaction. This model has also been analysed using a parametric study, and compared to test results from literature. In this comparison, excellent agreement was found between the model and test results, until cracking occurred (Hamed, 2016). However, this theoretical model seems to possess a large and complicated theoretical background. Even in the linear behaviour, it seems that this model cannot be applied in general practice, as a lot of knowledge about this background is required to understand and apply the model. The parametric study that was done by Hamed caused an increase of insight in the behaviour, but did not result in an increase of applicability of these floors. Regarding the non-linear phase, the cracked RC wythes possess a different tension stiffening behaviour than the ones modelled. The two identical concrete panels also behave differently from each other after cracking (Hamed, 2016). If this post-cracking behaviour is not analysed further, a similar failure can occur, e.g. at Eindhoven Airport, due to unexpected weaknesses or deformations.

Regarding the linear behaviour and the prediction of it, no publicly available calculation-method is found for the determination of the composite effect of PCSPs. As mentioned before, the theoretical model requires a lot of knowledge about mechanics to be able to apply it. In general, people in practice want to use simple expressions to find the behaviour of an element. Although the understanding of the linear behaviour is present at the moment, no effort has been made to change this understanding into a simplified method.

In order to correctly predict the post-cracking behaviour of PCSPs, a more accurate and more particular tension stiffening model needs to be developed (Hamed, 2016). For an initial understanding of the non-linear behaviour of PCSPs, a finite element (FE) model must be developed, that considers the tension-stiffening behaviour of the entire floor-element. An FE-analysis has been developed before, that was able to describe the partial composite behaviour (Salmon et al., 1997). However, non-linearity was still missing from this analysis (Hamed, 2016), while non-linear effects can often lead to serviceability failures in concrete structures when it is not understood (Hopkins et al., 2017).

A non-linear FE-model has been developed, based on the research of Hamed (2016). This model was able to correctly follow the aforementioned theoretical model. Additionally, it showed comparable results with some experiments within acceptable boundaries, although possibility for improvement in the model is still present (Huang & Hamed, 2019). Additionally, these experiments only load the structure in the bending direction. In the project of Lievense | WSP, a combination of vertical loads and shear forces will be present. A combination of an improvement and extension of the model is required to increase its applicability.

In conclusion, there is a clear shortage of applicability of PCSPs. An easy-to-use model to predict the bending-behaviour is also not open to the public yet. Without these models, PCSPs will not become a conventional floor-system, even with all the advantages that they bring. Additionally, the non-linear behaviour also requires more research, as some elements are still missing or incorrectly predicted in earlier-developed models. As prefabricated structures become more and more prevalent in The Netherlands, it's also important to analyse the change in flow of forces due to the weaker connections between floors and walls. These are all elements that must be taken into account before PCSPs can be used comfortably in practice.

1.2. Research aim

The aim of this research is to predict the behaviour of precast concrete sandwich panels better and more easily. In order to do so, information has to be acquired on known behaviours of similar types of floors and how sandwich panels are different from these known behaviours. It is also essential to

understand what kind and magnitude of forces are applied to PCSPs in practice. With the use of modelling software like DIANA, Technosoft and SCIA, it is hoped that simple expressions can be set up to predict the complete behaviour.

1.3. Research questions

Based on aforementioned aim, the main research question is formulated as follows:

How can simple expressions be set-up for the behaviour of precast concrete sandwich panels, and to what extent can these expressions be applied to a fully pre-fabricated structure?

As can be seen, this research-question contains a clear theoretical and practical part. Firstly, the theoretical part is divided into different phases with related sub-questions:

Phase A: Analysing the known information of loading-behaviour and precast concrete sandwich panels

- **A.1** What is the loading-behaviour of other concrete elements?
- **A.2** How do PCSPs differ from these other concrete elements?
- **A.3** Which differences (A.2) are expected to have the biggest influence on the behaviour of PCSPs?

Phase B: Developing a FE-model including non-linear behaviour of precast concrete sandwich panels

- **B.1** How can the different elements of PCSPs be applied to an advanced, non-linear FE-model?
- **B.2** What is the real influence of the differences (A.3) on the loading-behaviour of PCSPs?

Phase C: Checking the performance and robustness of the FE-model

- **C.1** How well does the FE-model perform on PCSPs, similar to the PCSP used to fit the model?
- **C.2** Regarding robustness, what are the weakest elements of the prediction model?
- **C.3** Which (important) parameters were overlooked at the start of the research (A.2/3)?

Phase D: Developing the prediction model

- **D.1** In which ways can the prediction model be developed?
- **D.2** Which of these ways are the most efficient and/or useful?
- **D.3** What insights can be gained from the prediction model?

The practical part is done in collaboration with Lievense | WSP and their prefabricated Reinbouw project. Parallel to the theoretical part, calculations will be done to gain insight in the Reinbouw project. These calculations are also split in four parts, following the same phases at the theoretical part:

- **A.P** What is the flow of forces of the Reinbouw project?
- **B.P** What is the required pile-foundation to achieve an equal sagging in the building?
- **C.P** What are the resulting shear forces due to horizontal loads?
- **D.P** How will the present shear-forces combine in a fully prefabricated structure?

In the end, both the theoretical and practical elements of this thesis will be combined. In this final phase, the prediction model developed in the theoretical part will be applied to the practical Reinbouw project:

- **E.** To what extent can PCSPs be used and optimized for the Reinbouw project?

1.4. Research methods

A visualisation of all different phases and their dependence can be found in Figure 1-3. The blue boxes and arrows visualise the process of the research, while the other colours define various elements that increase the applicability of PCSPs in practice. In this thesis, two main paths are followed: a theoretical part, which includes structural mechanics and the individual behaviour of PCSPs, and a practical part, which includes a study into the Reinbouw Project, to gain insight into the requirements of PCSPs in building designs like the Reinbouw project. For each phase, different methods are required, which are all explained below the figure.

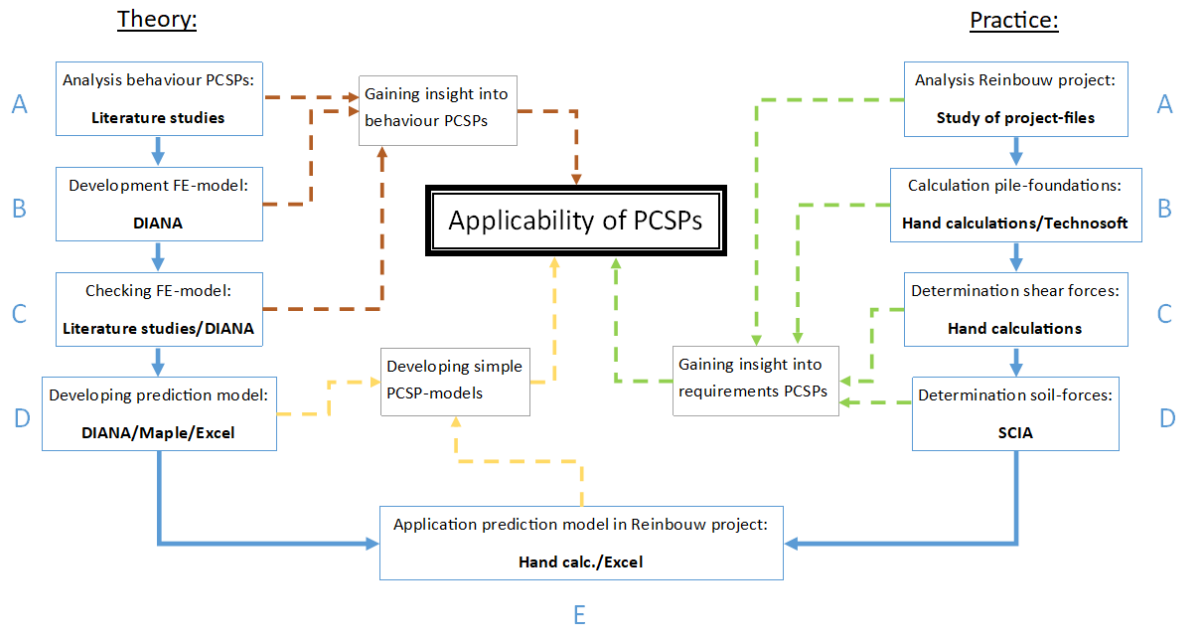

Figure 1-3: Flowchart research methods

Related to the theory-aspect of this thesis, phase A conducts literature studies on both general bending behaviour and PCSPs. During discussions about this Master's Thesis with experts of concrete, a combination of both literature studies and interviews resulted in a well-founded decision on the most important differences between usual tension-stiffening behaviour and that of PCSPs.

Phase B commences with developing the prediction model, which is done in a Finite Element Modelling (FEM) program (DIANA) for the most part. Some analysis takes place outside this software, e.g. comparing the results of the model to the experimental results of a PCSP-design.

Phase C is a comparison study of the first iteration of the prediction model and experimental results of multiple similar PCSP-designs. Some of the PCSP-designs will be significantly different, to test robustness. This will therefore be an comparison between FEM programming and literature results. After this analysis is completed, insights are gained by checking the FE-model and the initially expected results from phase A.

Phase D uses both Maple and Excel to develop an analytical prediction model for PCSPs. The FE-model from Phase C is used to compare these models, so that a broad set of floor-designs can be compared. After this development and comparison, the analytical Excel-model is used to gain more insight into the effect of the main parameters on the stresses in PCSPs.

For the practical part, all calculations are done in collaboration with Lievense | WSP. Firstly, the practical part starts off with an analysis of the expected flow of forces in the entire structure. Afterwards, hand calculations and Technosoft are being used in phase B to calculate the required foundation piles of this structure. Based on this lay-out, stiffness calculations can be done by hand, and wind-loads on each cross-section can be calculated. The relative stiffnesses are also used as input in SCIA, to calculate the resulting stresses when soil settlement is present. Finally, both the theoretical and analytical part are combined into phase E, where Lievense | WSP is advised on their use of PCSPs, based on the gained insight and prediction model from the theoretical part.

1.5. Scope and limits of research

In regards to the non-linear FE-model, no model has been able to predict multiple experiments correctly. As the goal is to gain more insight into the non-linear bending-behaviour, some advanced aspects of behaviour will not be taken into account. Creep, relaxation, and settlements are all elements that will not be computed or analysed in the FE-model. Additionally, only already done experiments are being used as comparison-material for the FE-model. No experiments are done for this research specifically.

While an analysis will be conducted on the forces and displacements caused by a conceptual prefabricated building, the FE-analysis only includes one floor-element. The forces and displacements from the SCIA-analysis can be used to gain insight into what kind of loads are applied on the structures, but the FE-model and analytical model will focus on local forces only.

Moreover, this research cannot take into account some important elements of PCSPs, mainly due to the boundaries of the methods that were chosen. Firstly, non-linear FE-modelling cannot analyse all important aspects of PCSPs. One of the main elements missing from these kinds of models is robustness against procedural errors. Experimental results have shown that construction details have an important role on PCSPs, for the weakest parts of the panel are dependent on this (Bush & Stine, 1994). Additionally, aspects such as faulty concrete pouring and misplaced reinforcement could decrease the stiffness or resistance of a PCSP element.

Additionally, the analytical prediction model is solely applicable to the linear part of PCSPs. Non-linearity is not included, and when strength-limits are reached, the model is not trustworthy anymore. Even though there is a possibility that other floor-elements will show comparable results when the model is used, there is no proof that this will work for all elements. The model also possesses some simplifications in regards to dimensions; the only possible design is two identical concrete wythes with one intermediate layer including insulation and truss-connectors. Finally, because models have always been developed by scientists, these models will be lacking information they are not aware of. Even in the case where the author analyses all papers on PCSPs, there might still be features about PCSPs that are unknown to anyone in this field of research. These unknown features are hard to locate as only experiments from earlier studies are used, on which the prediction model will be based. A visualisation including some examples is given in Figure 1-4.

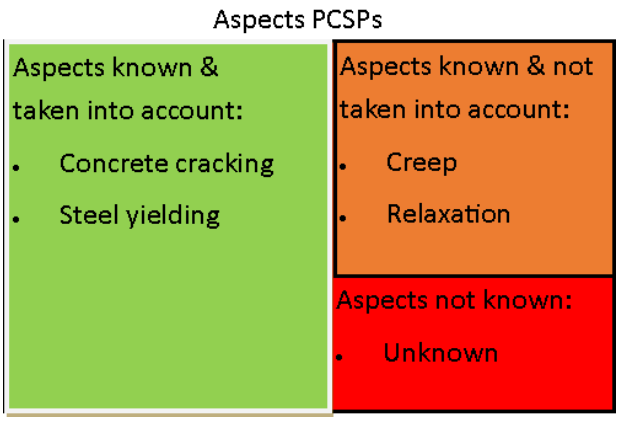

Figure 1-4: Diagram showing the boundaries of PCSP-aspects

2. Literature study

2.1. Theoretical background of PCSPs

The linear way in which our buildings and their materials are built and used, is no longer sustainable. Because of this, efforts have been made to increase the sustainability of building-designs. Circularity principles have begun to be incorporated into sustainability applications only recently (Kubbinga, et al., 2019). Still, The Netherlands are one of the leading countries which, regarding circularity, already think about the re-use of materials the most (Gruijl, 2019).

A PCSP, as already shown in Figure 1-1, consists of two reinforced concrete layers called wythes, with a layer of insulation in between. Often, especially when these panels are load-bearing, truss shear connectors are also applied to attach the two concrete wythes. Due to this lay-out, they are very light-weight and efficient as wall-elements. Only more recently, their application as roof or floor panels has been researched (Hopkins et al., 2017). Floor panels will be loaded in bending mainly. However, shear forces will also occur through the PCSPs in the design of Lievense | WSP, due to the prefabricated nature of the structure.

Aiming to apply the most circularity possible, client Reinbouw asked Lievense | WSP to design an apartment building with as many prefabricated concrete elements as possible. They also wish to minimise the use of wet connections. The concept that Lievense | WSP designed, has already been displayed in Figure 1-2. In Figure 2-2, a side cross-section of the Reinbouw project can be found. Additionally, the top view of the ground floor can be found in Figure 2-1. Apart from three protruding walls, the entire ground floor consists of columns. These columns are not able to resist shear forces caused

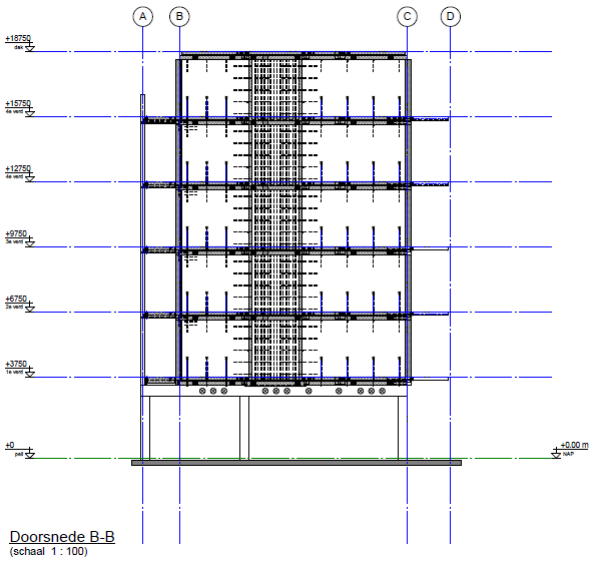

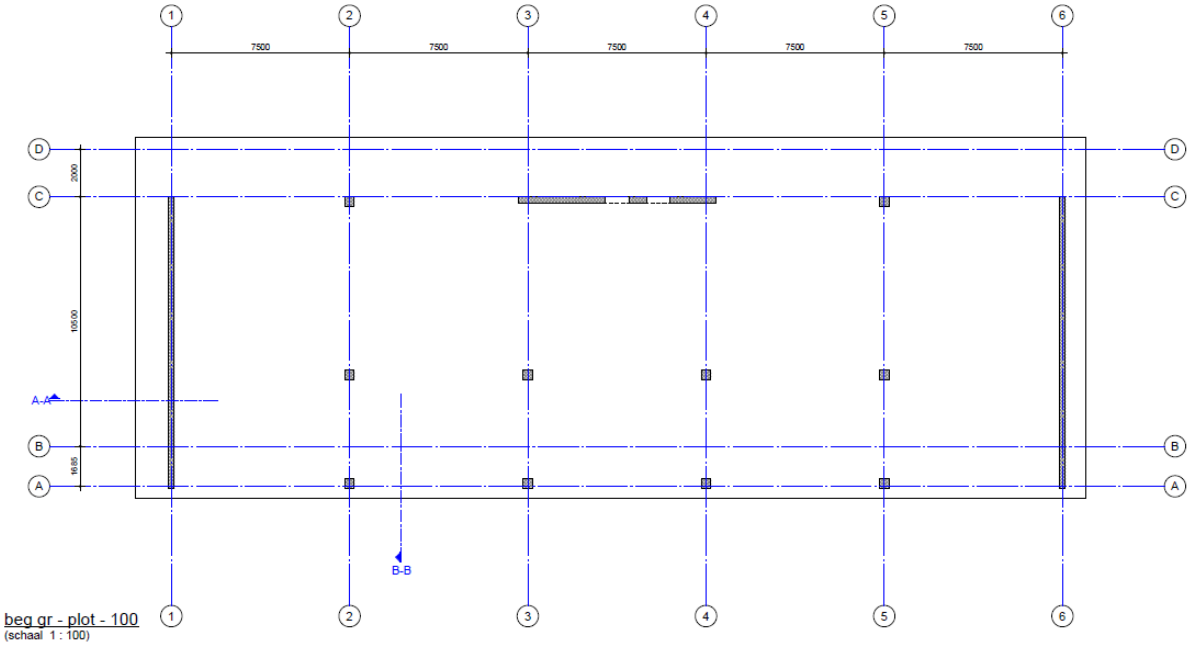

Figure 2-1: Top view ground floor Reinbouw project

by wind-loads or unequal settlements. Thus, these forces must be transferred to the sides of the buildings. Apart from this additional transfer, the connections between floor and walls are weaker than non-prefab structures. As the floors are only connected with steel connectors as shown in Figure 2-3, the rotational stiffness from the frame-structure is relatively low. This will cause a further unequal rotation in the structure, resulting in more forces being transferred to the diaphragm walls.

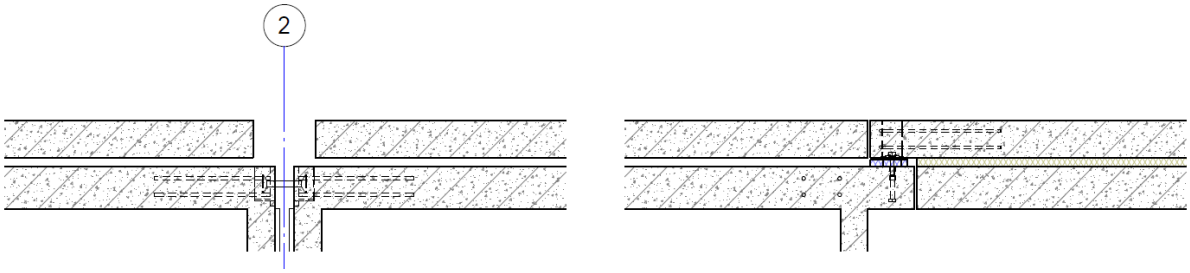

Figure 2-3: Steel connectors in floors

On top of wind loads, the Reinbouw project is also very sensitive to foundation setting (Mink, Discussion about the Reinbouw mid-rise project, 2019). As mentioned before, the stiffness of the frame structure is relatively weak. If a certain group of pile foundations sag significantly more than others due to weaker soil, this unequal deflection will result in stresses in the unit-walls. Most importantly, as shown in Figure 2-4, door-openings in the unit walls result in a very thin concrete part above these openings. This causes both a low shear-resistance and low stiffness of these elements, requiring other elements of the building to help support this foundation setting. This is mostly done by the floor-elements: Precast Concrete Sandwich Panels (PCSPs). If the effect of foundation setting on the resistance and stiffness of PCSPs is not considered well enough, a failure similar to Eindhoven Airport might occur. Here, a newly built parking garage collapsed, partly because the temperature-effect on the floors was not taken into account sufficiently, while the production of the floors also had some errors (NOS.nl, 2017) (Hellenberg Hubar et al., 2019).

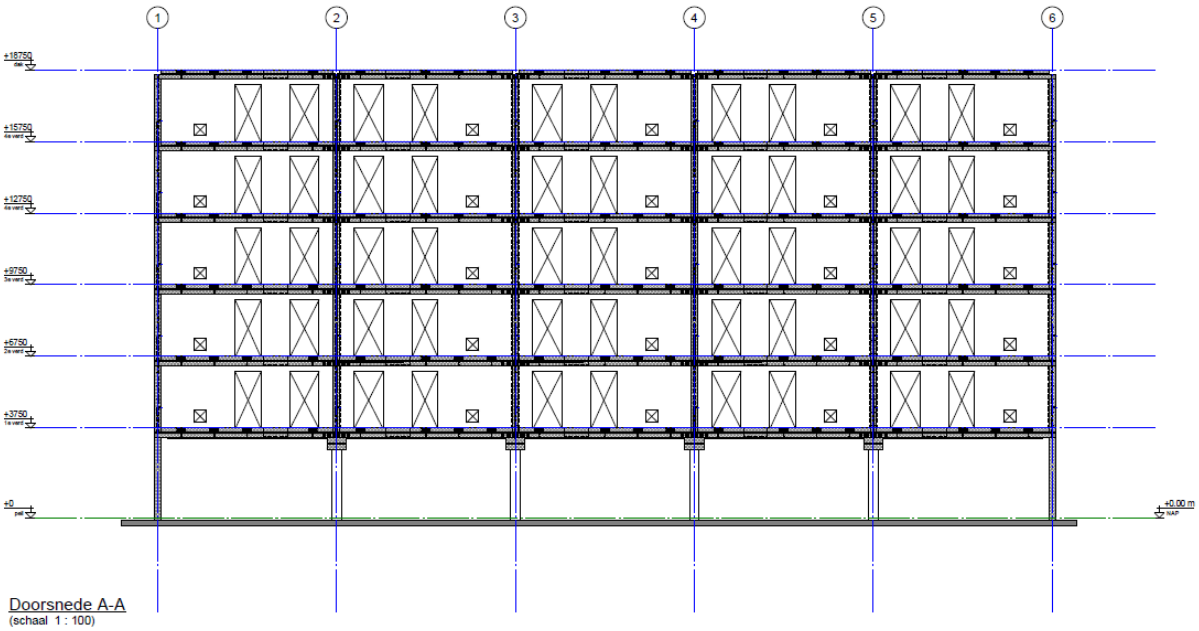

Figure 2-4: Front view Reinbouw project

This research will focus on the precast concrete sandwich panels. In the case of an in-plane shear force– by either a bending moment or a direct shear force – a PCSP without truss shear connectors can still resist some load in this direction. This is related to the shear surface between the wythes and the insulation-layer possessing some resistance. However, in order to significantly increase the resistance of the element, truss shear connectors have to be added. If these changes are implemented, the resistance of PCSPs can possibly be doubled (Choi et al., 2015). The (bending) stiffness also significantly increases, based on a principal called composite action, as shown in Figure 2-5. Fully composite behaviour means that multiple layers all behave as one "unit", where the plane of the entire element remains straight. Non-composite behaviour is based on that all layers behave and bend independently on each other. However, PCSPs behave somewhere in between fully and non-composite, which is called partially composite. Depending on how many shear connectors are applied, this composite action either increases or decreases. However, fully composite behaviour for PCSPs is essentially never expected, as this requires an inefficient number of connectors (Hamed, 2016).

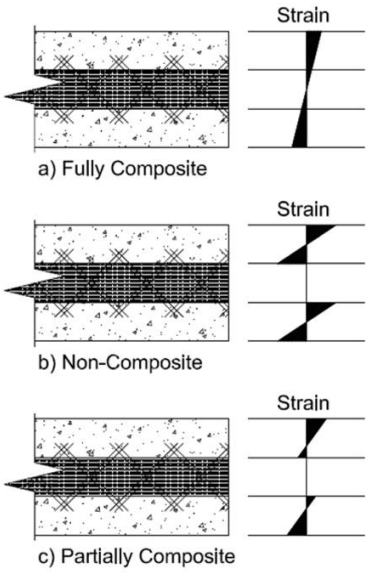

Figure 2-5: Different types of composite action (Salmon et al., 1997)

A multitude of shear connector types can be used. FRP shear connectors have been preferred lately, due to their lower thermal conductivity, which prevents thermal bridging. However, these connectors also have a lower stiffness compared to steel, which influences the behaviour of the PCSPs severely (Hopkins et al., 2017). Thus, it is clear that many studies have been done on PCSPs as both wall and floor-elements.

However, Hamed remarked that most of the studies done on PCSPs do not take this partially composite behaviour into account, which is a very important feature of PCSPs. He developed a theoretical model that takes this behaviour into account, and which "accounts for the axial and bending rigidities of reinforcement (RC) layers and their potential cracking" (Hamed, 2016). When comparing the results of this model to experimental results, excellent agreement exists up until the cracking of concrete wythes. In this phase, the model misses an appropriate tension-stiffening model. In order to find the right model, the cause of post-cracking behaviour must be understood first. A finite element model can be developed to create a PCSP-framework. This framework can be compared to different experimental results, to find the main influences of the post-cracking behaviour.

Throughout the years, multiple studies have been conducted on the finite element analysis of PCSPs. Initial research was only in the linear phase and did not take the structural interaction and the cracking wythes into account (Salmon et al., 1997), while it was known that the overall behaviour of PCSPs is non-linear and ductile (Einea A. et al., 1994). Even the more recent analyses have not been able to predict the post-cracking response, while the linear behaviour was correctly predicted (Bajracharya et al., 2013).

Last year, a non-linear model was developed to continue the partially-composite research done by Hamed (Huang & Hamed, 2019). Even though the non-linear FE model was able to correctly follow the theoretical model, it still did not follow the post-cracking response of experimental results. Multiple experiments were compared, and while all experiments compared well with the model in the linear phase, the non-linear phase was only correctly predicted in only one experiment.

Regarding the linear behaviour, some issues are present as well. Although previously-mentioned mathematical models and FE-models help with gaining insight into the linear behaviour of PCSPs, the required theoretical background to understand these advanced models is high. These types of models are impractical to use by everyone that wants to apply PCSPs to their design. Additionally, although some parameter-study is done in the previously-mentioned research (Hamed, 2016), no clear individual influence per parameter is analysed. In order for PCSPs to be used more widely and confidently, simple expressions are preferred where input-parameters can be used to find the linear behaviour of these floor-elements.

As mentioned in the last paragraphs, the developed FE-model was not able to predict the behaviour of every PCSP-experiment, and no easy-to-use model is present. In the case of the Reinbouw project, the floors will be loaded by considerable shear forces as well. The effect of this load-combination on PCSPs is still unknown. Thus, it could be claimed that some important elements were not present in the currently-developed models. Without more developments focusing on the practical applicability of PCSPs, these floors are unable to be used more easily in practice.

2.2. Loading-behaviour usual floor-designs

When a common monolithic floor is loaded in bending, the Bernoulli-Euler beam theory can be applied. In this theory, two assumptions are present: plane sections remain straight, and that all beam-angles are small (Learn About Structures, 2020). This theory is still the method that is used most often to calculate the bending behaviour of beams. However, in some designs, these assumptions are not valid due to the non-straight plane sections. This is present in composite structures, like a mechanically connected timber floor-system or a concrete-steel composite floor.

In the case of mechanically connected timber beams as shown in Figure 2-6, a method is given in the Eurocode to calculate the effective stiffness of such a beam (NEN, 2011). Initially, a set of assumptions is given, that focus on the boundary conditions and material-restrictions. The bending stiffness is then calculated following the common method of summing the individual bending stiffness and the Steiner rule of each layer. However, a factor is added to the Steiner-part, which takes into account the relative slip between the layers, causing a reduction in the effective stiffness. This factor is dependent on the axial stiffness of the individual layer, the centre-to-centre distance between the steel connectors, the stiffness of these connectors and the span length. This factor could essentially be seen as the "composite factor" of these timber floor systems.

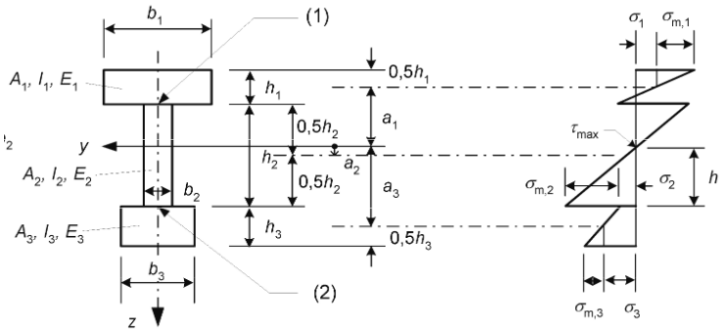

Figure 2-6: Cross-section of a mechanically connected beam, including qualitative stress-values

Regarding concrete-steel composite behaviour, the Eurocode also contains calculation methods for these composite structures (NEN, 2005). Behaviour is not the focus in these documents. However, some research has been done on the effect of potential slip and cracking in steel-concrete composite elements (Abspoel, 2018). These elements have a poured concrete top layer, which is connected to a steel element. Regarding slip, the influence can be neglected within certain boundaries. If slip cannot be neglected, an increase in deflection can be determined by a simple expression. In this case, a fully composite floor is assumed, except when specific boundaries are exceeded. In that case, an increase in deflection is assumed, referring to the presence of a partially composite structure.

Regarding the non-linear behaviour, the most well-known post-cracking behaviour is the tension tie model, which can be found in Figure 2-7. Simple formulas have been derived for this behaviour, that are dependent on the strengths and stiffnesses of concrete and reinforcement steel, as well as the relative amount of applied reinforcement. This theory is also applicable to a moment in a bending-beam, where curvature is used instead of strain. This model can be applied to most monolithic concrete elements.

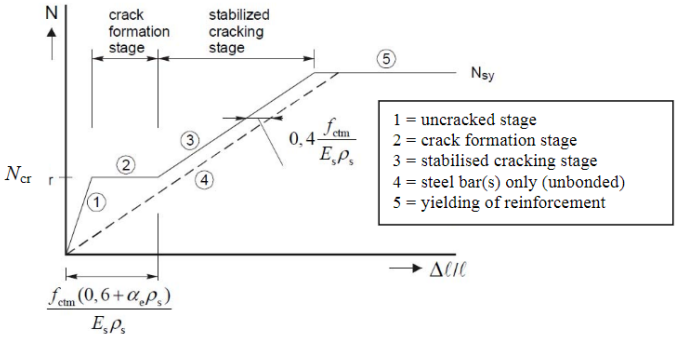

Figure 2-7: Tension stiffening behaviour simple RC beam

Even while the elements are monolithic, fibre reinforced concrete (FRC) cannot apply the graph from Figure 2-7, due to its significant different behaviour compared to conventional reinforced concrete. To solve this problem, much research has been conducted on the post-cracking response. For example, a tri-linear constitutive law was developed for this type of concrete. This law was required, in order to take into account both the tension-stiffening and -softening effects. A FEM-analysis was done on FRC and compared with the simulated curve from aforementioned model. This comparison showed good results for most designs (Soetens & Matthys, 2014), as is shown in Figure 2-8. This way of comparing the results between FE-model and experiment is a valid method to use in this research as well.

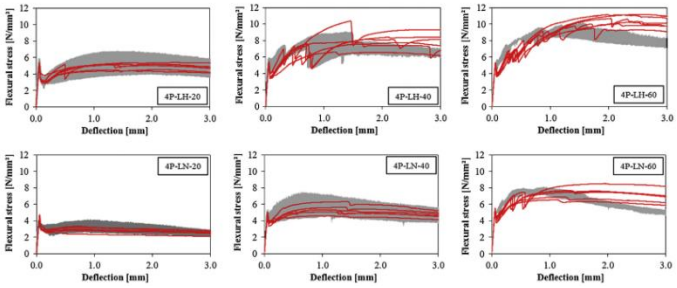

Figure 2-8: Comparison between numerically (red) & experimentally (grey) obtained flexural response of SFRC (Hellenberg Hubar et al., 2019)

In the case when the element is not monolithic, the Eurocode includes a strength-check for the friction layer between two layers of concrete that were poured at a different time. Next to parameters that are commonly used related to strength and reinforcement ratio, additional parameters regarding outward forces, perpendicular forces and roughness of the surface-layers are also present (Hellenberg Hubar et al., 2019). In general, the Eurocode only sets rules and requirements regarding strength, cracking & deflection. The behaviour of elements after cracking is not part of the calculation-procedure, and as such not specified.

If concrete-steel composite beams, as mentioned in the third paragraph of this section, are being used in a continuous form, cracking can occur in the concrete part of the beam due to negative moment at the supports. The reduction of moment due to this cracking will result in an increase of the deflection, which is expected with concrete cracking. Again, this increase can be calculated relatively easily by an expression. If a continuous beam is used within certain boundaries, an even simpler assumption can be used (Abspoel, 2018).

Apart from the abovementioned rules and regulations, most uncommon elements are tested or verified using experimental data. Many common floor-elements – flat slabs, conventional slabs, hollow core ribbed slabs etc. (Designing Buildings, 2019) – can be calculated using the procedure from Figure 2-7 as they are non-composite and poured monolithically, while the stiffness of simple composite beams can be verified using the formulas and assumptions in the last paragraph.

The FEA program DIANA has multiple predefined tension-softening and -stiffening models for its concrete crack model. These can be found in Figure 2-9. In this figure, models for fibre reinforced concrete are also included. Apart from tension models, compressive crushing models are also present. More generally, bond-slip models can be applied as well to include friction between different layers of materials.

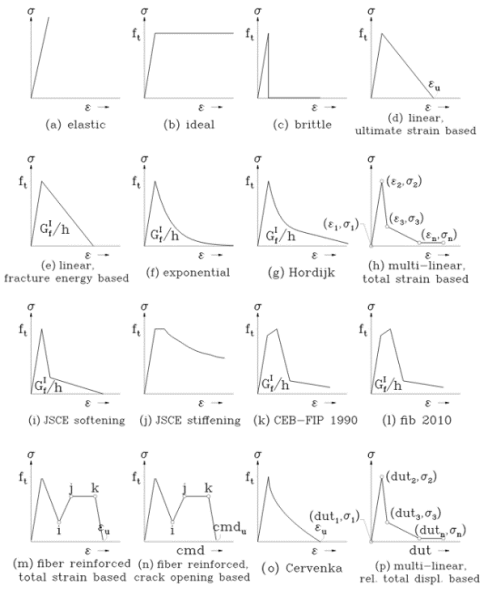

Figure 2-9: Predefined tension softening for Total Strain crack model

2.3. Unique aspects PCSPs

A PCSP floor varies from conventional floors in multiple ways. In order to analyse all the aspects that could make a difference in the behaviour, the PCSPs are being compared to the floors that are able to be calculated using the methods described in the last section. Finally, it is checked if any aspect is missed during this comparison.

Regarding the linear bending behaviour, the composite factor is the main unique parameter. This parameter is also present in other composite floors. However, compared to the timber and concrete-steel composite floors from Section 2.2, there are some clear differences. Firstly, the composite factor of both known behaviours are dependent on the interface between the different layers. The composite factor of PCSPs is mainly dependent on the entire layer between the concrete wythes. As mentioned before, the truss-connectors play an essential role here (Hopkins et al., 2017). As such, the composite behaviour of PCSPs is not comparable to these other composite floor- and beam-systems. This means that the known expressions from the Eurocode are very difficult to be used or edited so that they are applicable to a PCSP and their intermediate layer.

The non-linear behaviour is dependent on more features of PCSPs, and as such is discussed here more in detail. Firstly, the PCSP structure is non-monolithic. Due to this, the principle from Figure 2-7 cannot be used. Next to the concrete and reinforcement steel, shear connectors that protrude the concrete and insulation layers are also present.

Secondly, PCSPs also differ significantly from the common composite steel-concrete structure. It is said that the truss shear connectors have a linear behaviour, but that the global behaviour of PCSPs is still non-linear and ductile (Hamed, 2016). The steel-concrete composite structure mentioned in the last section will only crack in a continuous structure. However, as PCSPs also have a concrete bottom layer, cracking is expected to always occur (Yang, 2019).

Thirdly, PCSPs require an inefficient amount of truss connectors to gain full composite action (Hamed, 2016). As the behaviour between PCSPs and steel-concrete composite structures is significantly different, the same rules for ignoring slip cannot be used. Thus, in initial calculations, this slip cannot be ignored.

Lastly, as the individual layers do not possess very unique features, the predefined stiffness-models from DIANA can be used initially. However, the interaction between these layers could change the initial behaviour of these layers after they have cracked. This might result in the application of more advanced stiffness-models.

In summary, a bullet-list will be given to show all the unique elements of PCSPs:

- Top and bottom layer: concrete wythe
    - Partial or complete cracking of layer
    - Pull-out of truss shear connector
- Middle layer: insulation & truss connector
    - Lower stiffness
    - Lower resistance
- Top and bottom shear-surface
    - Effect of concrete cracking
    - Effect of insulation shearing
    - Shear surface
    - Shear connectors

In the next section, priority will be given to some of these aspects, based on conclusions made from research or expert opinions. The following researches on PCSPs are used for this analysis:

- Choi et al. (2015) present in-plane shear experiments of PCSPs with and without shear connectors. The variables in these experiments are related to the choice of insulation material and the dimensions of the shear connectors. The test lay-out is shown in Figure 2-10, where a vertical load was applied to the middle concrete element to create a direct shear force along the interfaces.

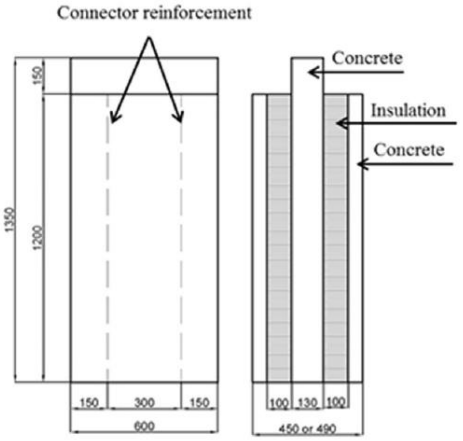

Figure 2-10: Shape & dimension push-out specimen

- Hopkins et al. (2017) tested four PCSPs on their creep behaviour in bending direction. FRP truss connectors were applied, and the structures were loaded for 150 to 250 days for different panels, as shown in Figure 2-11. While creep is not being included in this thesis, this paper did contain some statements about the behaviour of PCSPs that gave a clear priority to some features of these elements.

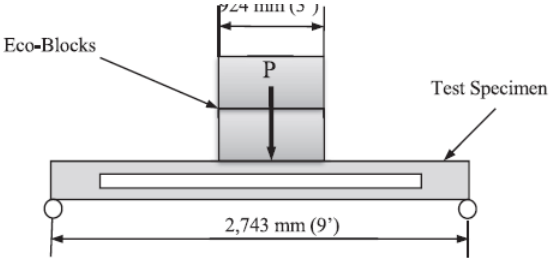

Figure 2-11: Creep loading schematic

- Hamed (2016) developed a theoretical model that is able to include the non-linearities of concrete and partial composite action. The research starts off with a summary of multiple experiments and researches that were performed on PCSPs. In one of these researches, it is claimed that the structural interaction with the insulation layer can be important under service- or post-peak loads (Yun et al., 2012). The model was initially compared to a high-order sandwich theory, which showed excellent agreements with the theoretical model. After this, both a parametric study and comparison to experimental bending tests were performed.
- Based on the theoretical model of Hamed, Huang (2019) developed FE-models of PCSPs. These models were compared to multiple experiments. Firstly, the model was compared to an experiment where 6 PCSPs were loaded by an airbag in the flexural direction (Bush & Stine, 1994). Two of these PCSPs were compared, together with two experiments from another research (Salmon et al., 1997). In most of the comparisons between FE-model and experiment, the results were good to excellent up until cracking, as shown in Figure 2-12.

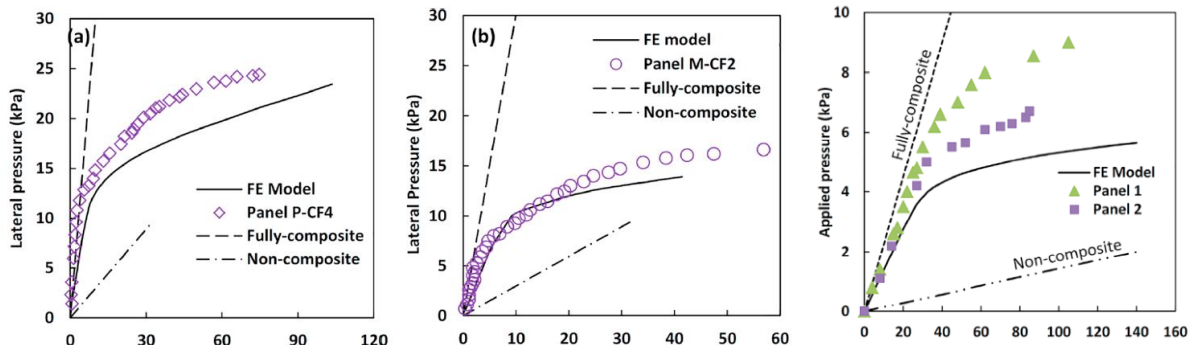

Figure 2-12: Comparisons between experiments and FE-model from Huang (2019)

2.4. Prioritising aspects for model-development PCSPs

Based on the aforementioned experiments and interviews, PCSP-features will be prioritised on significance. In the FE-model, this list will be the basis for development, where the most essential aspects are applied to the simple model first, in order to find an accurate model the quickest. Only the non-linear aspects are prioritised, as this is the most difficult aspect to predict and model.

Related to the concrete wythes, multiple statements have been made. Firstly, serviceability failures can often be caused by not accounting for concrete cracking and other non-linear long-term effects (Hopkins et al., 2017). Additionally, it is claimed that the "unique behaviour and stress redistributions that occurs after cracking [...] cannot be represented using simplified equivalent beam analysis, and should be carefully considered in the design and analysis of PCSPs" (Hamed, 2016). However, assuming a PCSP loaded to the point of cracking, it can be assumed that the bottom wythe will crack completely, imitating the behaviour of a simple reinforced concrete bar as mentioned in Section 2.2 (Yang, 2019). Lastly, pull-out of the shear connectors has occurred during shear-tests, but only during the post-peak deflection (Choi et al., 2015).

The insulation layer plays a much less important role when truss shear connectors are applied, as this layer will be much less effective and will also transfer significantly less stress (Hamed, 2016). In shear-experiments, the immediate loss of strength after the peak-strength is often accompanied by shear cracking of the insulation layer. Lastly, the choice of insulation also influences the post-peak behaviour in shear, as some insulation types fail more ductile than others (Choi et al., 2015).

Due to the complexity and many features of the shear surface and -connectors, many observations have been done related to this part of the structure. On top of the loss of strength during shear cracking of the insulation layer, bond face slip also occurs often after the peak strength-deformation was acquired in shear-experiments (Choi et al., 2015). It has also been mentioned that the global behaviour of the PCSPs heavily depends on the stiffness of the connectors (Hopkins et al., 2017). Additionally, the structural interaction between the insulation layer and concrete wythes can be an important factor under service or post-peak loads (Hamed, 2016).

A summary of the conclusions of these researches can be found in Table 2-1. For the most part, all papers agree on the importance of the different characteristics. However, it can be seen that the shear-experiments from Choi et al. (2015) consider insulation as an important element of the panel, while the researches on flexural experiments deem this element much less important. As the FE-model will be compared to a flexural test initially, the characteristics from flexural experiments will be used for the priority list in the development-phase. As such, the priority lies mostly on the concrete wythes, as the cracking-behaviour of PCSPs is very unique, and has not been able to be predicted well in FE-models so far. Additionally, the truss connectors seem to have a large effect on the general stiffness of the structure. Each element of PCSPs, including their characteristics, minimum and maximum values of used experiments, and importance to the global behaviour (based on the literature-study) are given in Table 2-2. A side-view of a PCSP is given in Figure 2-13, to visualise where the important aspects of these floors lie.

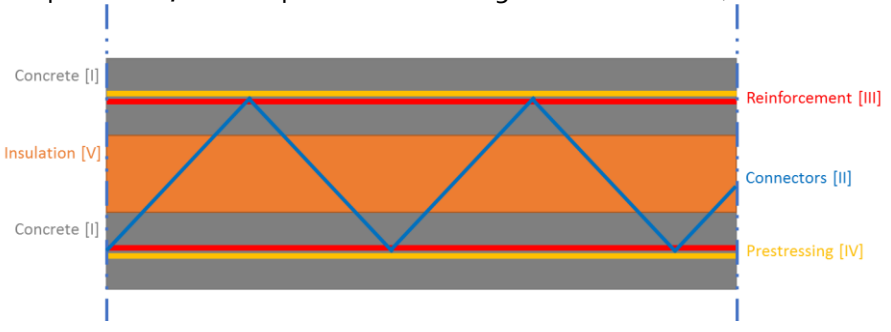

Figure 2-13: Side-view PCSP

Table 2-1: Summary of experiment-conclusions

Experiment	**Type of experiment**	**Concrete wythes**	**Connectors**	**Insulation**
Hopkins (2017)	Flexural	- Important to account for cracking	- Stiffness heavily depends on connectors	-
Hamed (2016)	Theoretical model: flexural	- Unique behaviour due to partially cracked top layer	- Interaction between layers can be important under post-peak loads	- Much less important role when connectors are applied
Huang (2019)	FE-model: flexural	- Was not able to fully predict post-cracking response	-	-
Choi (2015)	In-plane shear	- Ductility gained by pull-out	- Cause of peak-failure	- Choice of insulation important when no connectors are applied - Failure accompanied by loss of strength

Table 2-2: Parameter values and their importance

Element	**Parameter**	**Min. value in compared experiments**	**Max. value in compared experiments**	**Importance based on research**
Concrete wythe [I]				**++**
	Elastic modulus	30540 MPa	33550 MPa	++
	Thickness	60 mm	76 mm	++
	Compressive strength	30 MPa	38 MPa	0
	Tensile strength	2.89 MPa	3.7 MPa	++
Connectors [II]				**++**
	Elastic modulus	30200 MPa	200000 MPa	++
	Yield strength	401 MPa	424 MPa	0
Steel reinforcement [III]				**-**
	Elastic modulus	200 GPa	200 Gpa	-
	Yield strength	410 MPa	448 MPa	0
Steel prestressing [IV]				**0**
	Elastic modulus	200 GPa	200 GPa	-
	Yield strength	1644 MPa	1860 MPa	-
	Prestressing	1042 MPa	1080 MPa	+
Insulation [V]				**--**
	Elastic modulus	3.5 MPa	5 MPa	--
	Thickness	51 mm	100 mm	0
	Tensile strength	0.124 MPa	0.124 MPa	-

The importance of each of the aspects from PCSPs will be used to develop the FE-model in the next chapter. In order to gain a correctly-performing model as quickly as possible, the most important aspects are added first.

3. Finite Element Model

3.1. Development of the FE-model

Before the model-development can start in DIANA, some preparations have to be made. Firstly, a roadmap for development has to be produced, so that the model-development has a clear process that it can follow. This roadmap will not be very detailed, but is more of a mindset in how the model will be developed step-by-step. Secondly, an experiment from Section 2.4 has to be chosen to use as a comparison to fit the FE-model to.

Development roadmap

As one of the goals of this research is to gain a more detailed insight in which features have the greatest effect on the post-cracking behaviour, the FE-model will be built in multiple stages. It is also useful that the development process will be done in small steps, so that mistakes in the model can be found quickly. Additionally, computational time can be controlled, so that a very long computational time will not occur too suddenly.

In the development of the model, priority is given to the features that have been mentioned as most important in other research, as shown in

Table 2-2 in Section 2.4. However, in order to add these features, a base model must be made first. The initial plan of development is as follows:

1. Linear truss system with simplified concrete wythes
2. Add simplified physical non-linearity bottom concrete wythe
3. Add physical non-linearity truss connectors
4. Add physical non-linearity top concrete wythe
5. Add geometrical non-linearity
6. *Add linear insulation layer*
7. *Add normal physical non-linearity bottom concrete wythe*

The simplified bottom concrete wythe at point 2 refers to a simple line-element for the concrete, that cracks fully after the limit strength is reached. After this limit strength, the reinforcement resists the forces in the lower wythe. This simplified model is based on a discussion with Yang (2019) that is described in Section 2.4. Point 6 and 7 are optional additions, in the case of the model possessing insufficient accuracy.

Choice of experiment

There are multiple factors influencing the choice of the experiment. Firstly, a clear input is required in the research-paper, so that the input of DIANA is as specific as possible. Secondly, the output is preferably well-stated with large graphs and clear axes. On top of this, a description of what type of failure occurred during which phase is important. This can be used to check if the FE-model is following the experiment-results, both graph-wise and behaviour-wise. Lastly, to ensure that the experiment is also trustworthy, it is preferred that the same type of element has been tested multiple times. As can be seen in Figure 2-8, an experimental envelope can be visualised, to show the variation in the experiments themselves.

As mentioned in Section 2.4, Huang (2019) has already developed a FE-model that is able to predict the post-cracking behaviour in bending partially. However, it has only been compared to a small number of experiments, of which only one did follow the post-cracking behaviour very well. In the other comparisons, the model underestimated the stiffness considerably.

It has been decided to create a new FE-model in DIANA, where the model will be based on the research of Huang (2019). This model will be compared to experiments that Huang also used, to ensure that the FE-model was developed correctly (Bush & Stine, 1994) (Salmon et al., 1997). As panel M-CF2 from Bush and Stine (1994) possesses the most similar behaviour to the original FE-model (Huang & Hamed, 2019), this panel will be used to work through the plan of development to find the most essential features.

To give more insight in which features have more impact, the results of each intermediate model will be compared to each other and to the experiments. If the final model-version compares well to the experiment, it will be possible to test the robustness by comparing the model to more experiments. For example, other experiments from Bush & Stine (1994) or Salmon et al. (1997), or experiments with a different loading direction will be used to test the FE-model.

Experiment information

The characteristics and material properties of the M-CF2 panel are given in Table 3-1 (Huang & Hamed, 2019).

Table 3-1: Characteristics and material properties panel M-CF2

Parameter	Value	Parameter	Value
Amount of shear connector rows	2	**Steel truss connector angle**	51.81°
Height	4.88 m	**Steel truss connector diameter**	6.19 mm
Width	2.44 m	**Prestressing yielding strength**	1840 MPa
Thickness concrete wythes	76 mm	**Prestressing diameter**	9.5 mm
Thickness EPS	51 mm	**Prestressing compressive force**	384 kN
Elastic modulus steel	200 GPa	**Strands per concrete wythe**	5
Elastic modulus insulation	5 MPa	**Concrete crushing strength**	38 MPa
Steel yielding strength	410 MPa	**Concrete elastic modulus**	33.55 GPa
Steel reinforcement diameter	6.42 mm	**Concrete flexural strength**	2.89 MPa
Steel reinforcement spacing	152 mm		

The (non-linear) stress-strain relationships of the concrete and steel are also specified, which can be found in Figure 3-1. However, as the model will be rebuilt in another FEM program, the options from this program will be used initially. Both the insulation and the truss connectors are assumed to be linear elastic in the original FE-model (Huang & Hamed, 2019). As mentioned in the development roadmap, the truss connectors in the newly developed model will possess non-linearity.

$$\sigma_c = \begin{cases} f_{cm}\left[\dfrac{\frac{E_c}{E_{c1}}\frac{\varepsilon_c}{\varepsilon_{c1}} - \left(\frac{\varepsilon_c}{\varepsilon_{c1}}\right)^2}{1+\left(\frac{E_c}{E_{c1}}-2\right)\frac{\varepsilon_c}{\varepsilon_{c1}}}\right] & \text{for} \quad \varepsilon_{c,\lim} \leqslant \varepsilon_c \leqslant 0 \\ E_c\varepsilon_c & \text{for} \quad 0 < \varepsilon_c \leqslant \varepsilon_{cr} \\ e^{-0.8(\varepsilon_c-\varepsilon_{cr})\times 10^3}E_c\varepsilon_{cr} & \text{for} \quad \varepsilon_{cr} < \varepsilon_c \\ 0 & \text{for} \quad \text{otherwise} \end{cases} \qquad \sigma_s = \begin{cases} E_s\varepsilon_s & \text{for} \quad |\varepsilon_s| \leqslant \varepsilon_y \\ E_s\varepsilon_y & \text{for} \quad \varepsilon_y \leqslant \varepsilon_s \\ -E_s\varepsilon_y & \text{for} \quad \varepsilon_s \leqslant -\varepsilon_y \end{cases}$$

Figure 3-1: Stress-strain relationships of concrete (left) and steel (right) (Huang & Hamed, 2019)

Development-process

In this part, the development of the FE-model is described. As this is done in multiple steps where multiple models were developed, a summary of what in included in which models can be found in Table 3-2. The cross-section that is included in the FE-model is shown in Figure 3-2. Because the model is two-dimensional, the widths and areas are found as input in the model, and not possible to be viewed as shown in Figure 3-2.

Table 3-2: Summary model-process

Model	**Reinforcement & Prestressing**	**Bottom concrete wythe**	**Shear connectors**	**Top concrete wythe**	**Geometrical non-linearity**	**Insulation**
1	Indirectly applied	Truss Linear	Truss Linear	Truss Linear	Not applied	Not present
2	Indirectly applied	Truss Non-linear	Truss Linear	Truss Linear	Not applied	Not present
3	Indirectly applied	Truss Non-linear	Truss Non-linear	Truss Linear	Not applied	Not present
4	Indirectly applied	Truss Non-linear	Truss Non-linear	Sheet Non-linear	Not applied	Not present
5	Indirectly applied	Truss Non-linear	Truss Non-linear	Sheet Non-linear	Applied	Not present
6	Indirectly applied	Truss Non-linear	Truss Non-linear	Sheet Non-linear	Applied	Sheet Linear
7	Reinforcement truss Non-linear	Sheet Non-linear	Reinforcement truss Non-linear	Sheet Non-linear	Applied	Sheet Linear

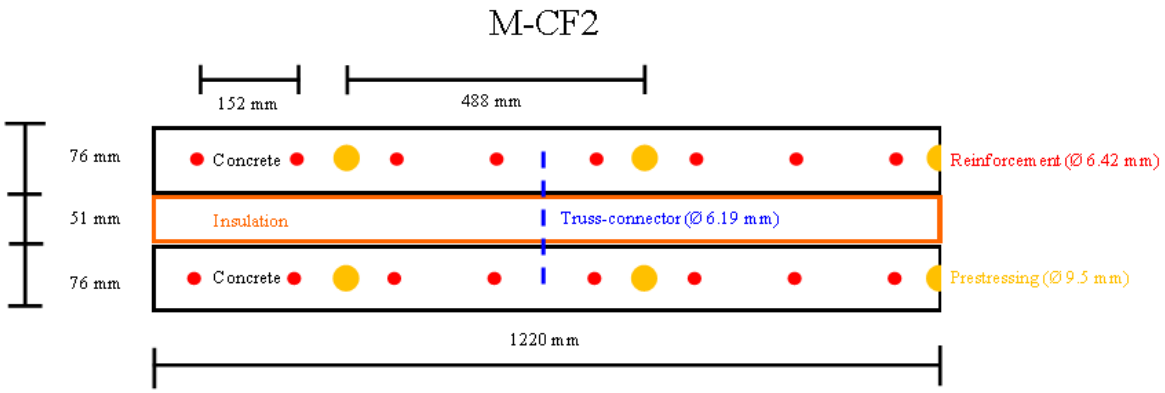

Figure 3-2: Cross-section FE-model M-CF2

As can been seen in the table, the reinforcement and prestressing is applied indirectly for the most part of the development process. This means that the additional and residual strength due to the steel were included in the characteristics of the concrete elements.

Apart from the input mentioned above, an effort has been made to make the other elements of the model as similar as possible. For example, the same element sizes were used for each version. Initially, element sizes of 38 mm were used without allowing many iterations per load step, in order to check

the correctness of the model without too much time spent on computation. These were later changed to 10 mm elements, in order to create a more realistic model. Additionally, in the non-linear versions, an effort was made to load the models until divergence of the model occurred. As such, multiple, smaller load-steps were taken.

Model versions

Version 1

The model is shown in Figure 3-3. This initial version is completely linear, where the white lines depict the concrete wythes, and the blue diagonal bars are the truss shear connectors. The input for stiffnesses have been acquired from Hamed (2019), which were 33550 MPa and 200000 MPa for concrete and steel respectively, as mentioned in Table 3-1.

The load is set at 18.3 N/mm, which is equal to half of the full distributed load applied on the structure. Additionally, the depth of the concrete is only taken as half of the original experiment, which is 1220 mm. The reasoning to take half of the structure, is to only have one set of truss shear connectors applied.

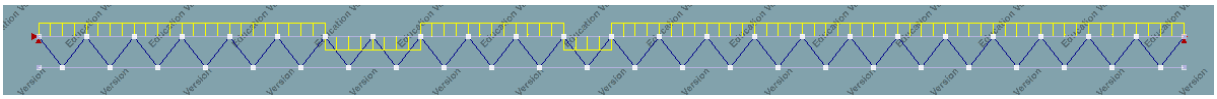

Figure 3-3: Model view of version 1 to 3

Version 2

In this version, the lower concrete wythe now possesses non-linearity. As mentioned before, this could be modelled as a simple beam, as this wythe will fully crack (Yang, 2019). This follows the behaviour of a simple tensile tie model. Thus, the model still looks identical to Figure 3-3.

The tensile model of the lower beam-element is set as a brittle behaviour, as the reinforcement and residue prestressing have less resistance than the tensile resistance of the concrete. Including the compressive prestressing, the total resistance of the concrete is set as 4.97 MPa. After cracking, the steel will still be able to resist 2.63 MPa.

Version 3

The change in this model consists of the addition of the non-linearity of the truss-shear connectors: the yield strength is set as 410 MPa.

Version 4

The upper concrete wythe is now also included as a non-linear element. However, as this wythe will partially crack, a simple line-element will not be able to follow a realistic behaviour. The new model can be found in Figure 3-4. The yellow sheet is the upper concrete wythe, while the lower concrete wythe is still modelled as a simple line.

However, the sheet elements possess the same characteristics as the lower beam element. A brittle behaviour, with tensile strength and residual strength set at 4.97 and 2.63 MPa respectively. This means that the reinforcement is not applied individually in the model.

According to the analysis from Section 2.4, the versions after this version should have little to no effect on the behaviour.

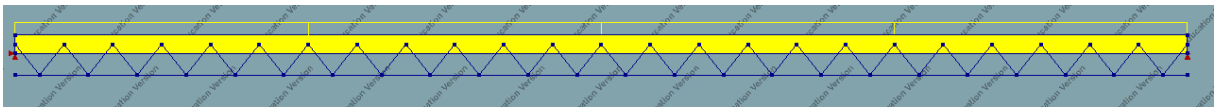

Figure 3-4: Model view for version 4 and 5

Version 5

The only change in this version is that geometrical non-linearity has been added.

Version 6

The new lay-out of the model can be found in Figure 3-5. In this version, the insulation is added. As this material has a very low stiffness – 5 MPa – it is considered linear elastic for computational purposes.

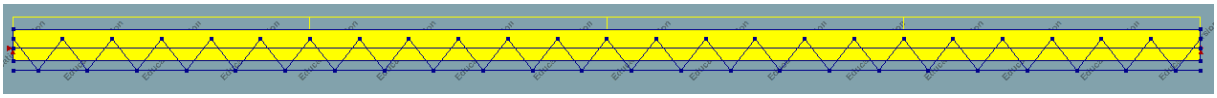

Figure 3-5: Model view for version 6

Version 7

In the last version of this model which can be seen in Figure 3-6, multiple changes have been made to make the behaviour more realistic. This was due to the model still showing a heavy underestimation in the stiffness. Firstly, the lower concrete wythe has also been modelled with non-linear sheet elements. Secondly, the truss connectors are now modelled as reinforcement trusses, causing a more realistic behaviour as more nodes per element are possible. Thirdly, the reinforcement and prestressing steel has been added independently as reinforcement trusses, and the concrete now only contains its own characteristics. This also means that the prestressing is added as a load instead of an additional concrete strength. Due to this, the concrete is able to follow the CEB-FIP Model Code 1990, with a fracture energy of 0.112 N/mm (Ulfkjær & Brincker, 1995). The reinforcement steel has a yield strength of 410 MPa, while the prestressing steel has a strength of 1840 MPa and a prestress of 1080 MPa.

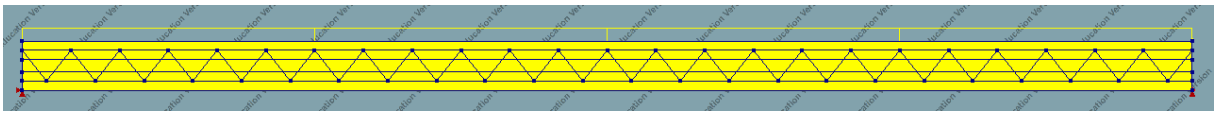

Figure 3-6: Model view for version 7

Results

As mentioned before, all models were initially tested with larger elements and a small amount of maximum iterations. Afterwards, smaller elements were used, and the amount of maximum iterations were increased. For the (partially) linear models, results are limited to the point where any linear element exceeds their strength. This way, only realistic results from the models are shown. The model-results for version 1 to 6 can be found in Figure 3-7. Version 1 and 2 limit their results due to the stress in the truss connectors exceeding their strength. Version 3 is limited by the point where the bottom edge of the top wythe would start cracking. All other versions are fully non-linear, which means that they are loaded until no convergence can be found. It is noteworthy that version 1 to 6 all follow the same behaviour, where specifically no visible change can be found in the non-linear part between version 4 to 6. Load-displacement results for model version 6 and 7 can be found in Figure 3-8. In this figure, the experiment-results are also shown. Version 7 shows a significant positive change, increasing both the stiffness and resistance. This causes the model to be much more accurate in predicting the non-linear behaviour of this PCSP-design.

In order to gain more insight in the actual behaviour, the FE-model will be analysed more thoroughly based on six points in the loading-process. In Figure 3-8, these points are shown by red crosses. Both models V6 and V7 will be shown at similar levels of deflection, in order to have some level of comparison between the versions. The displacements for each of these visualisations, together with the applied load at that load-step and what this point visualises, are given in Table 3-3.

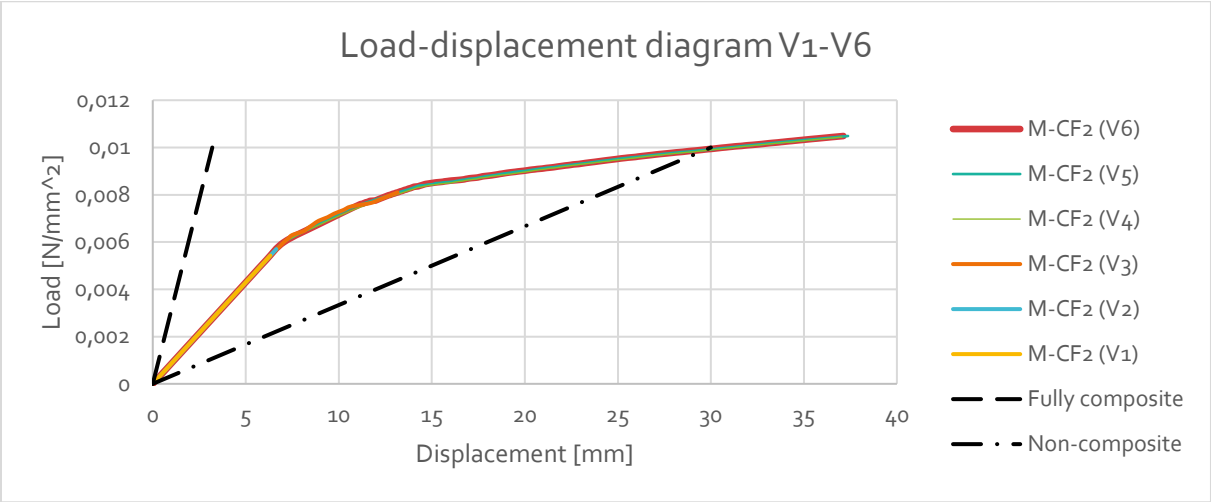

Figure 3-7: Load-displacement diagram of model version 1 to 6

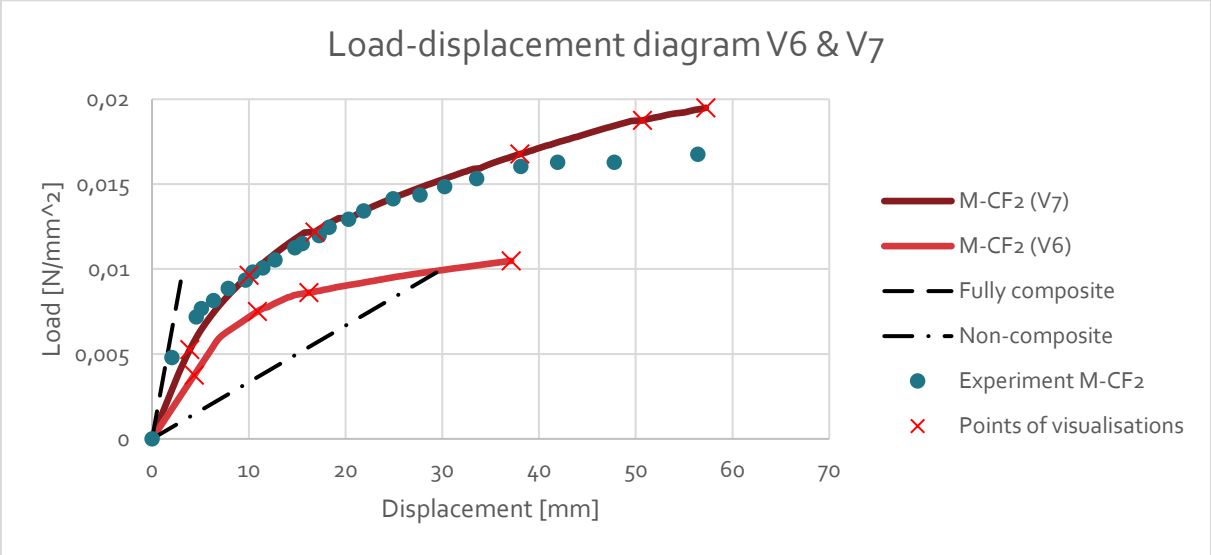

Figure 3-8: Load-displacement diagram of model version 6 and 7

Table 3-3: Description of result-visualisations

Image	**Deflection V6**	**Load V6**	**Deflection V7**	**Load V7**	**Visualised**
1	4.36 mm	0.0038 N/mm^2	3.90 mm	0.0053 N/mm^2	Linear behaviour
2	10.88 mm	0.0075 N/mm^2	10.01 mm	0.0096 N/mm^2	Initial non-linear behaviour
3	16.19 mm	0.0086 N/mm^2	16.82 mm	0.0122 N/mm^2	First big crack V7
4	37.13 mm	0.0105 N/mm^2	38.02 mm	0.0168 N/mm^2	Failure V6
5			50.67 mm	0.0188 N/mm^2	Clear crack propagation V7
6			57.24 mm	0.0195 N/mm^2	Failure V7

First, the detailed results from model version 6 will be analysed. In Figure 3-9, the plastic strains of the four steps in model version 6 are shown. Throughout the loading of the model, the plasticity of the truss-connectors is activated, starting at the edges and slowly moving to the mid-span. However, the connectors close to the mid-span never reach their elastic limit. It is noteworthy that the truss-connectors at the edges yield very early during loading, even while the global structure still acts relatively linear.

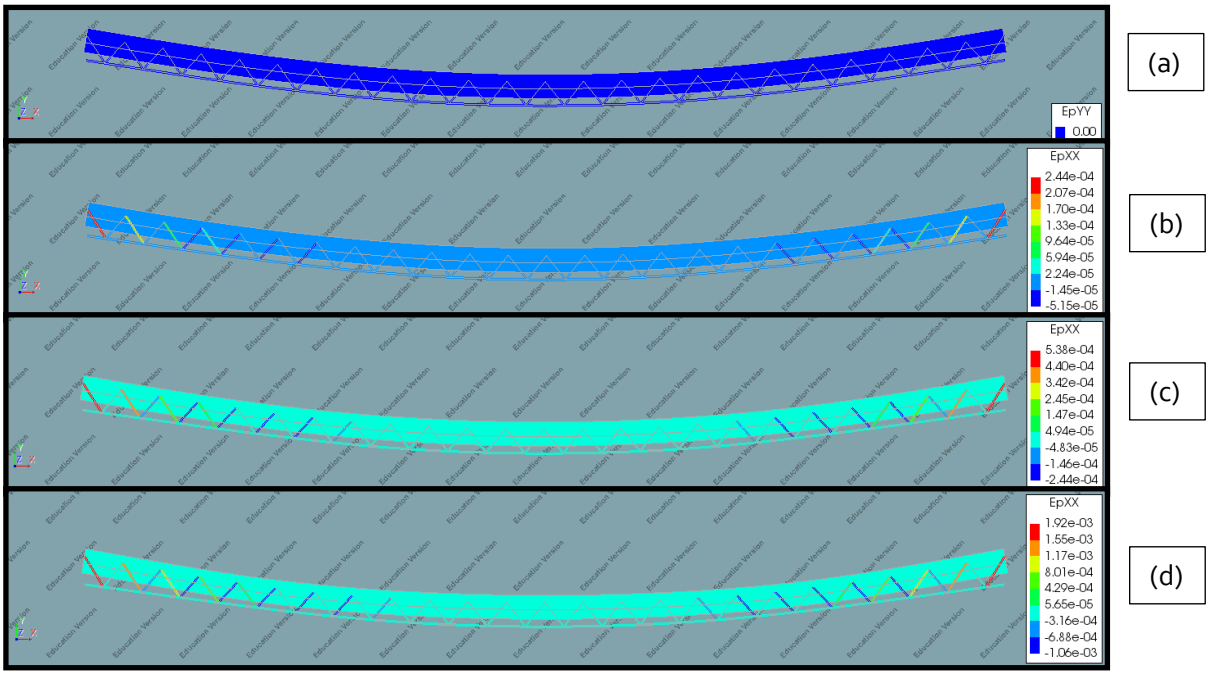

Figure 3-9(a)-(d): Plastic strain of model version 6

In Figure 3-10, the stress of the truss-reinforcement is shown. While the yield strength of the reinforcement is set at 410 MPa, some results show stresses slightly higher than this limit. This has to do with calculation-errors that occur in DIANA. Just before failure in Figure 3-10-d, almost all truss-connectors are stressed to a high degree, with the exception of the middle two connectors, which have close to no stress. The reason for this is that no longitudinal shear occurs in the mid-span of a bending beam. From this figure, it seems that the truss-connectors yield, but do not cause immediate failure.

In Figure 3-11, the concrete stresses are shown. In this figure, the boundaries of the contour plot are fixed between zero stress and the limit strength of the prestressed concrete. This shows the clear cracking that spreads through the lower wythe, due to the reduction of the stresses that occur at midspan in the lower concrete wythe. In Figure 3-11-b, it is also clear that cracking occurs next to the truss connectors first. Lastly, it can be seen that the top concrete wythe is also being loaded in tension at the end of the loading process, taking over some of the lost strength of the lower wythe. The full lower concrete is cracked, causing a much lower strength throughout the entire lower concrete wythe. The residual strength in the lower concrete wythe is from the reinforcement and prestressing only.

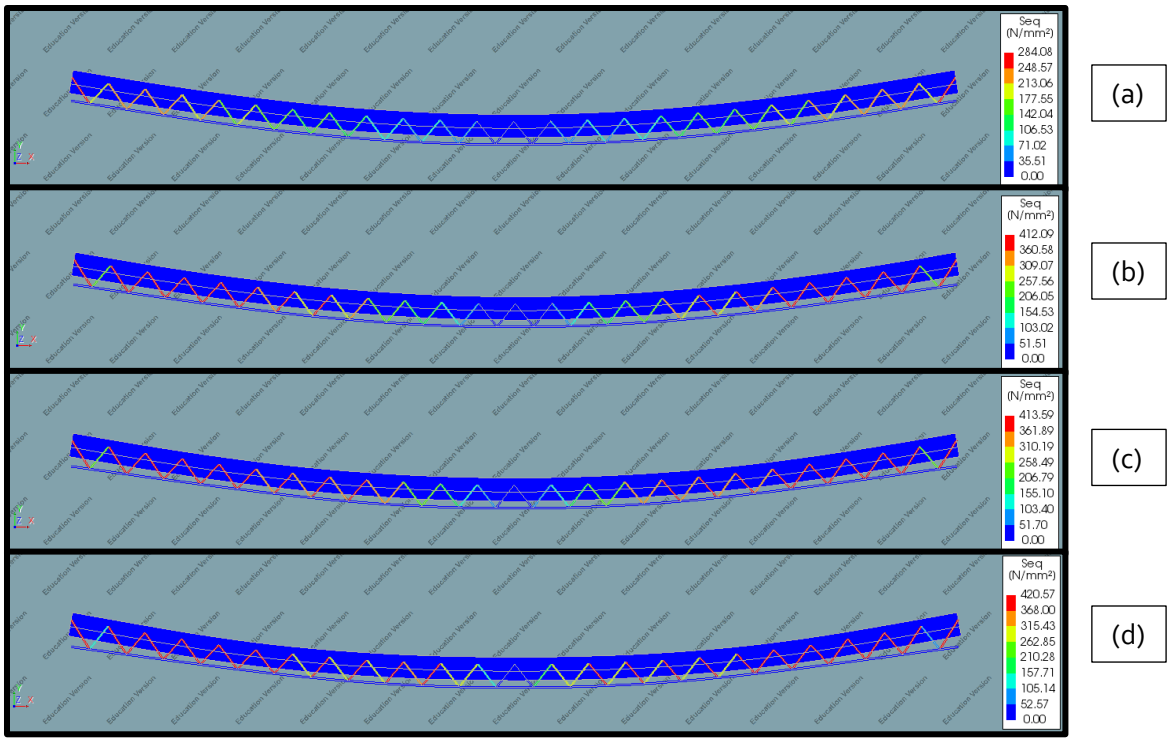

Figure 3-10(a)-(d): Steel stress in model version 6

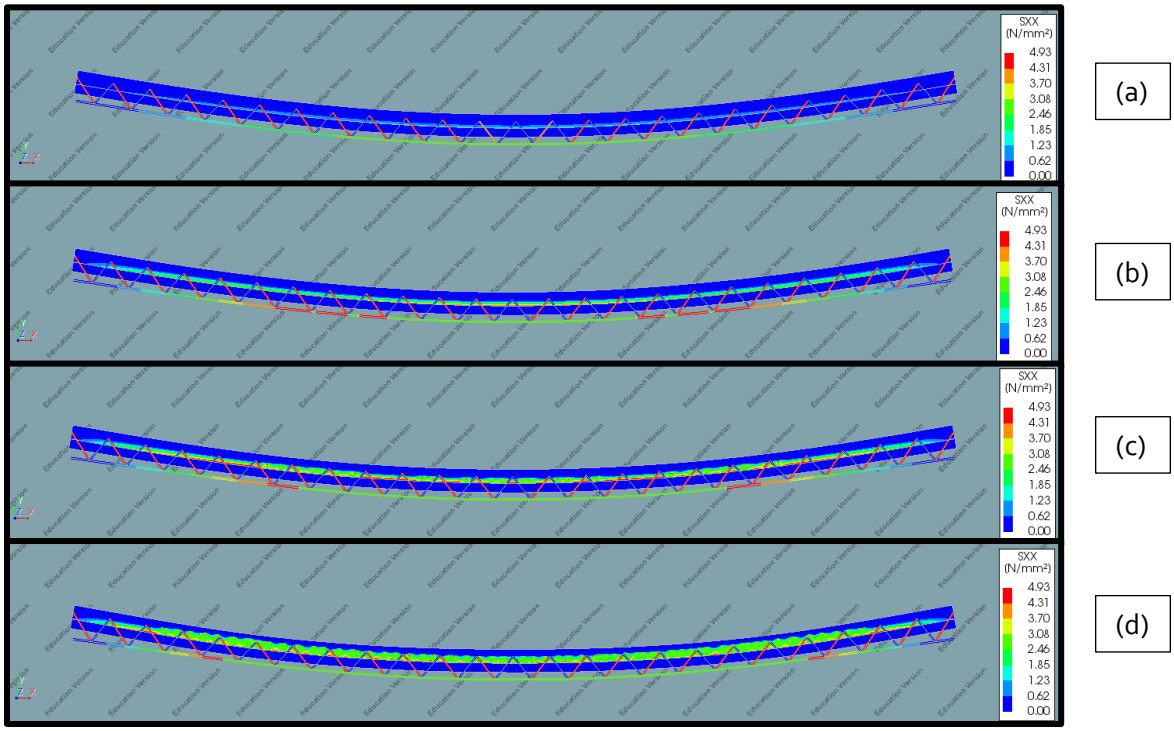

Figure 3-11(a)-(d): Concrete stress of model version 6

Figure 3-12 shows the concrete cracking. In this figure, only three images are shown as the first step from Table 3-3 does not contain any cracking. Initially, cracking only occurs in the lowest concrete wythe. In the later phases, cracking in the top wythe is focused mostly in the midspan and at a quarter from each edge. Just before failure, cracks are present throughout almost the entire span of the top wythe. However, the magnitude of the cracks is the largest at a quarter length from the supports. At midspan, the cracks are relatively small. When looking at the cracking behaviour before failure, it shows that the protruding cracks are the largest at a quarter length. Because of this, it can be assumed that failure will occur in this part of the structure.

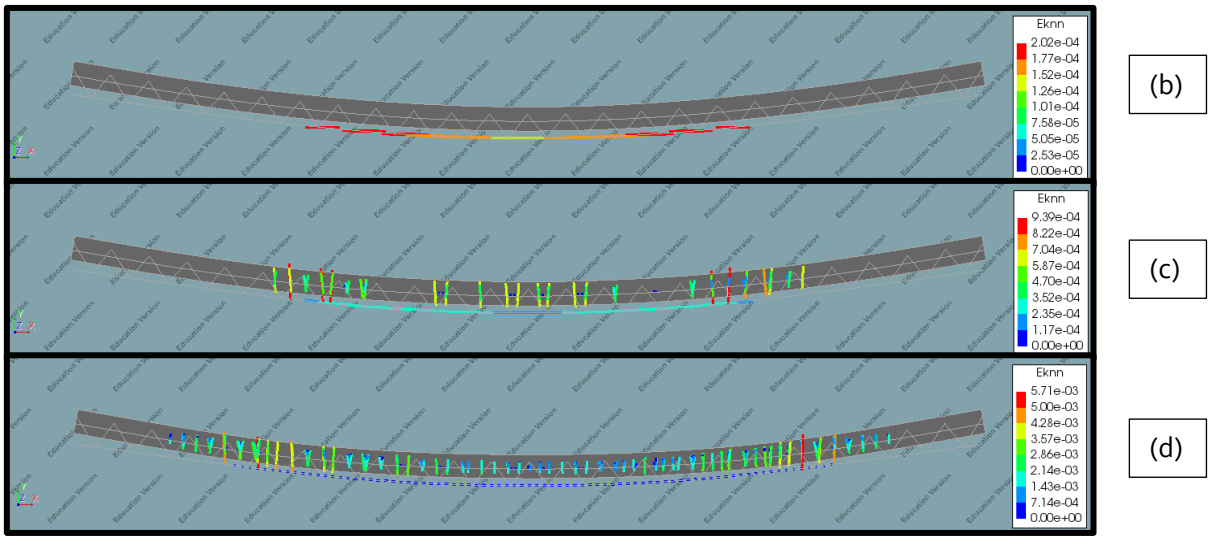

Figure 3-12(a)-(c): Concrete cracking of model version 6

From now on, the results from the final model version 7 are analysed. Figure 3-13 shows the plastic strains of the reinforcement and truss connectors. It is worth mentioning that the truss connectors already show slight plasticity at the edges, even before the global behaviour is non-linear. Additionally, the truss-connectors only show plasticity through the depth of the insulation. The highest increase in plastic strains is found between Figure 3-13-c and d. While the load does not increase considerably, the displacement at midspan is more than doubled. It seems the global displacement of the structure is related to the plastic strains. Lastly, plasticity is present through almost the same amount of truss connectors compared to version 6. Just before failure, the longitudinal reinforcement still does not yield. Even after initial large cracking, the steel is still able to resist the residual force elastically, preventing a brittle failure.

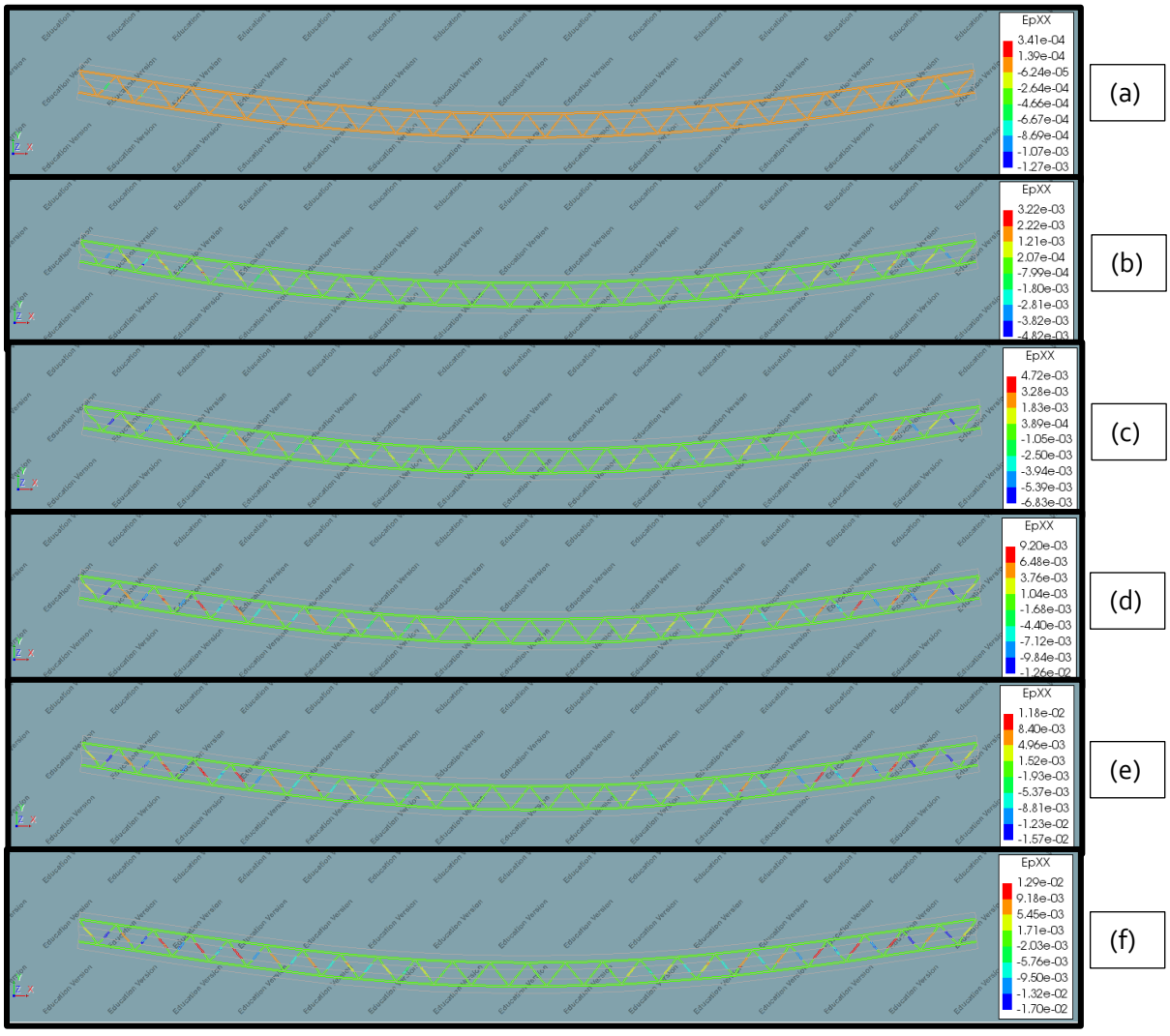

Figure 3-13(a)-(f): Plastic strain of model version 7

In Figure 3-14, the concrete stress is visualised, where the limits of the contour plots are between zero stress and the tensile strength of concrete. Due to the applied prestressing, the initial image shows close to no tension, even in the lower parts of the lower wythe. When clear non-linearity has occurred in the load-displacement diagram, it seems the edge of the bottom wythe has reached its limit strength slightly in the second image. In Figure 3-14-c, two clear cracks are visible due to the reduction in concrete stress at those points. In the load-displacement diagram in Figure 3-8, the cracks are also visible by a sudden horizontal line, visualising an instant increase in deflection. These horizontal lines occur every time a large crack appears in the lower wythe. Accompanying the large cracks in the bottom wythe, multiple smaller cracks occur in the top wythe. Just before the failure of the structure, these small cracks have spread almost entirely through half of the floor. Additionally, the concrete cracks penetrate almost entirely through the lower wythe. It is possible that the occurrence of this causes failure, as the steel is not able to resist the tension forces anymore.

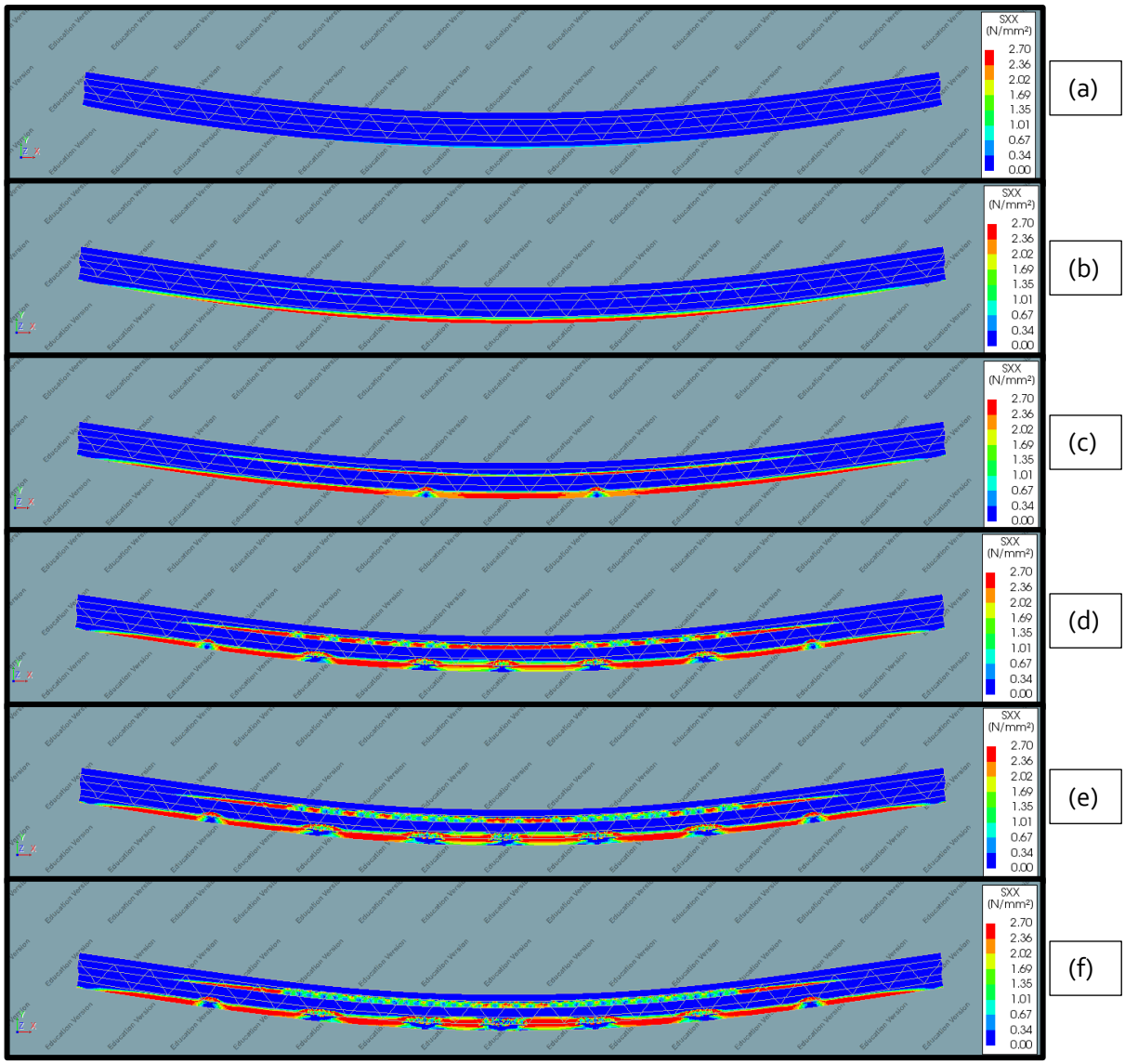

Figure 3-14(a)-(f): Concrete stress in model version 7

Figure 3-15 shows the concrete cracking throughout the loading of the floor. As the linear visualisation does not contain any cracking, only five images are shown. In Figure 3-15-b, only very small cracking occurs, spread across most of the span. It is notable that the cracking increases significantly at each point where the truss-connectors are connected to the lower reinforcement. Additionally, all large cracks that are present in the following images also occur next to the truss-connector connection. While the middle crack is not the first crack that occurs, it is the largest crack just before failure. As was also visible in Figure 3-14, the cracks in the top layer are much smaller than the cracks in the lower wythe. Just before failure, the middle crack in the lower wythe increases significantly, visualising a possible point of failure there.

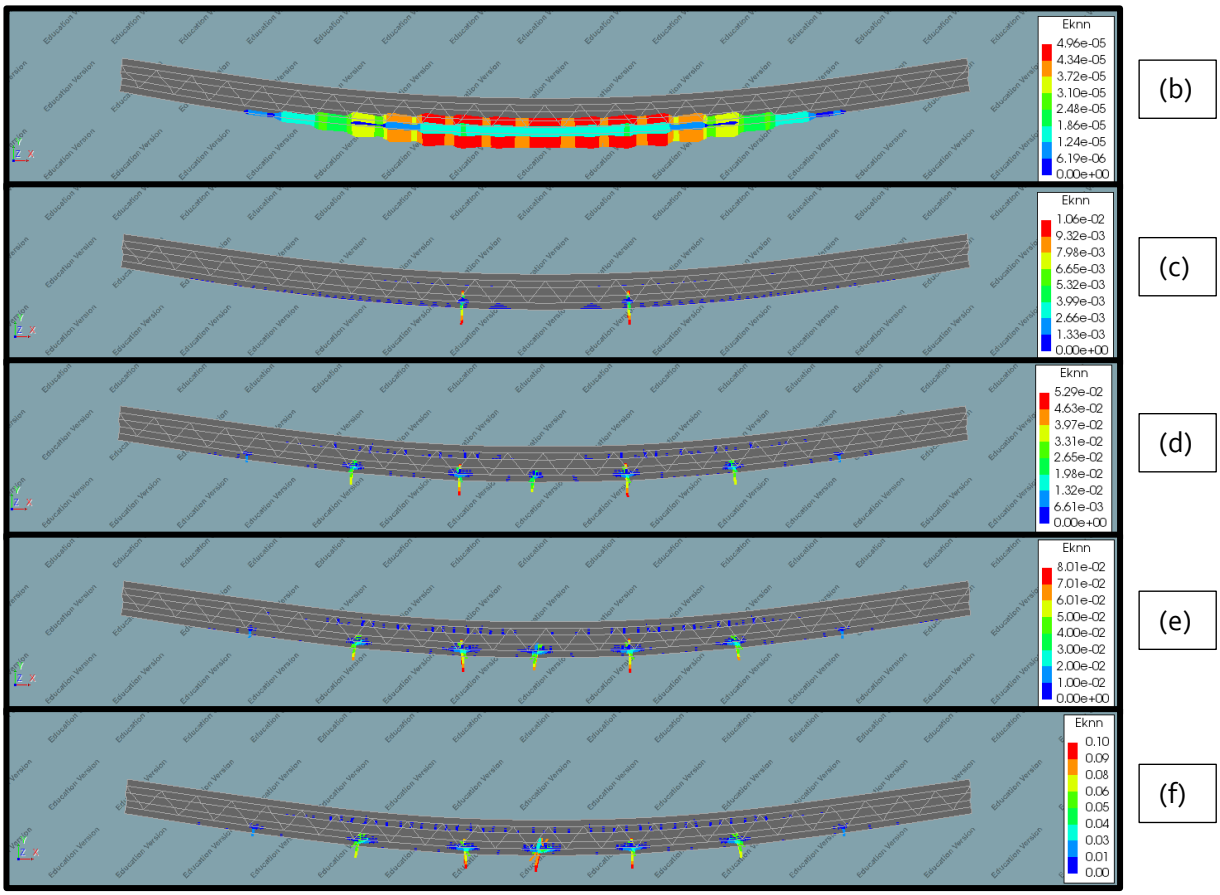

Figure 3-15(b-f): Concrete cracking in model version 7

Discussion

When comparing version 6 and 7 of the FE-model, some similarities and differences can be found. Firstly, the truss connectors start yielding around the same magnitude of deflection. Additionally, cracking in the lower wythe starts next to the truss-connectors. However, in version 6, the cracking behaviour of the lower wythe is significantly different from version 7. Version 6 only shows equally large cracks over the entire cracking area, while version 7 clearly shows concentrated cracks at certain points of the span. Next to this, the top wythe shows much more cracking in version 6. This could be related to the bottom-wythe model of version 6 being less stiff in general. As was realised at a later stage of the research, the simplified lower concrete wythe did not possess its full resistance, as some steel reinforcement was not accounted for. Lastly, version 7 requires much more computational time than version 6, resulting in a computational time of 90 minutes instead of 15 minutes.

Comparing the results from the FE-model to the experimental results, the graph in Figure 3-8 shows that version 7 has an excellent comparison to the experiment. On top of this, the description of the experiment-results mention that classical flexural cracking occurred in the tension concrete wythe (Bush & Stine, 1994), which is also partly present in Figure 3-14 and Figure 3-15. Crushing of concrete was not included in the FE-model, but it was manually checked if the limit strength was reached. As shown in Figure 3-16, this was not the case. However, the experiment only mentions yielding and buckling in the truss connectors after a sufficient load (0.014 MPa), while yielding in the model occurs almost immediately after loading. Before failure, more truss-connectors have yielded in the model than was the case in the experiment. Still, no buckling occurred, as imperfections like these are not included in the FE-model. Additionally, bond-slip is not included in the model, resulting in less computational time but what might cause a less-accurate model. Another computational-time-saving element is the application of a 2D-model instead of 3D. Although some aspects in the third direction cannot be modelled fully correct, "when shear connectors are applied through the height of the panel only, the deflection of the PCSP obtained using [an] 3D model becomes very close to the response obtained using 2D model" (Huang & Hamed, 2019).

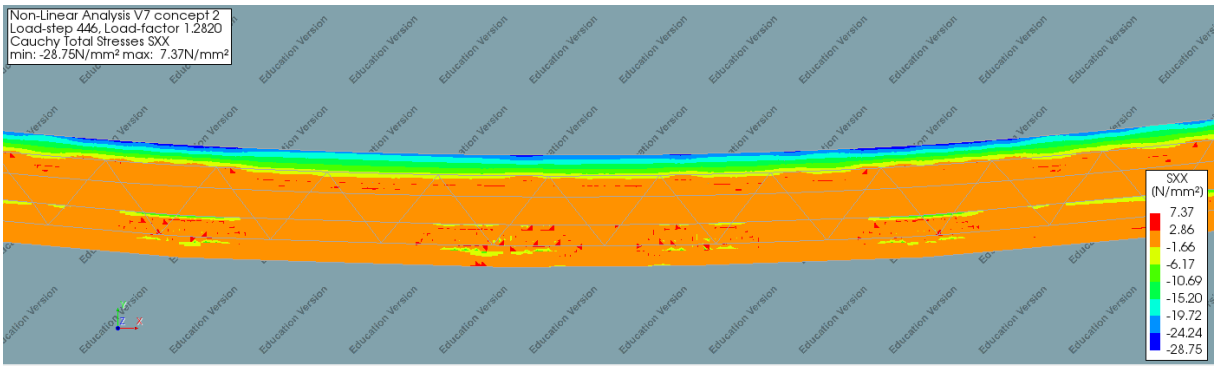

Figure 3-16: Crushing strength check M-CF2

Findings

Still, when looking at the global results, it seems that the predictions of the FE-model are well in line with the experiment. While this is a solid initial confirmation, the FE-model needs to be checked by more experiments to have a more solid foundation for setting up rules of thumb. Characteristics of the panels needs to be varied, to ensure that the FE-model can predict a broad spectrum of experiments. Next to the varying of material-characteristics, a shear-experiment will also be compared to the FE-model, to check if another form of loading can also be predicted correctly.

3.2. Checking other experiments to the FE-model

After the initial model with essential non-linearities is set up, it must be checked if the model also follows the behaviour of other experiments of PCSPs. Due to time- and information-constraints, the main method of comparison is by load-displacement diagrams.

Other bending elements

Firstly, an experiment from the same research as M-CF2 will be compared to the FE-model, called M-CF3 (Bush & Stine, 1994). The only difference between these two experiments is that M-CF3 contains three truss-connectors instead of two. In order to develop the FE-model, model version 7 from Section 3.1 is taken from M-CF2 and the depth of the sheets are edited to the new area that one truss-connector needs to resist. The new cross-section that is input into DIANA is shown in Figure 3-17.

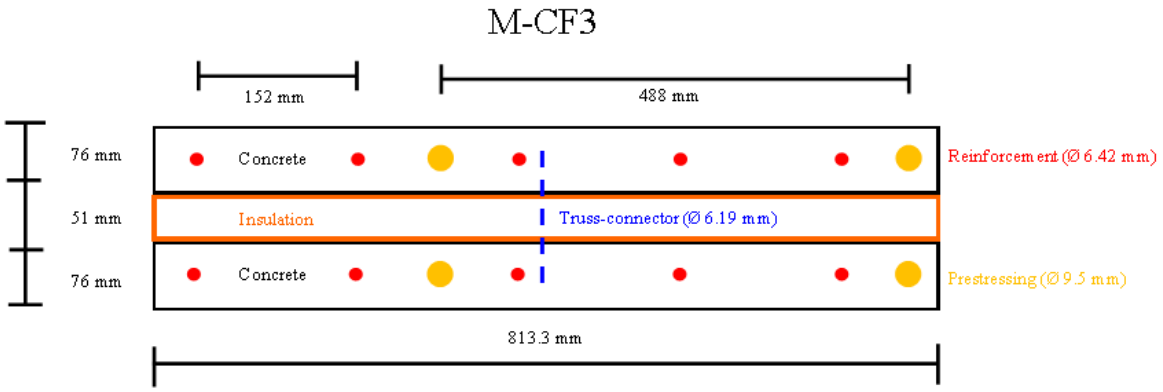

Figure 3-17: Cross-section FE-model M-CF3

The results of this new comparison between model and experiment is shown in Figure 3-18. This figure shows that the model predicts the behaviour perfectly, with a small difference in the initial linear response. It is noteworthy that in this experiment, the panel behaves stiffer than a fully composite floor, which should not be possible. The model is unable to find a solution after an applied load of around 0.019 N/mm², which is around 90% of the maximum load. The displacement has a larger discrepancy, as the FE-model (45 mm) is only able to displace around 60% of the experiment-displacement (75 mm). Because the model is loaded in a load-controlled experiment, it is unsure if the model is able to resist a similar displacement as the experiment at a lower load level. However, as the experiment-graph is almost horizontal, it can be assumed the model is not far off from the experiment-results.

In order to gain an initial insight of the effect of certain parameters, the FE-models of both M-CF2 and M-CF3 are shown in Figure 3-19. It can be clearly seen that the increase of truss connectors result in a substantial increase in stiffness through the entire load-displacement diagram. However, both models still possess the same limit strength. This is logical, as truss-connectors do not necessarily increase the tensile resistance of the lower concrete wythe, which is the weakest link in this structure.

The results of the FE-model of M-CF3 just before failure is shown in Figure 3-20. This shown a similar type of behaviour as panel M-CF2, which follows the stated failure mode of the research (Bush & Stine, 1994).

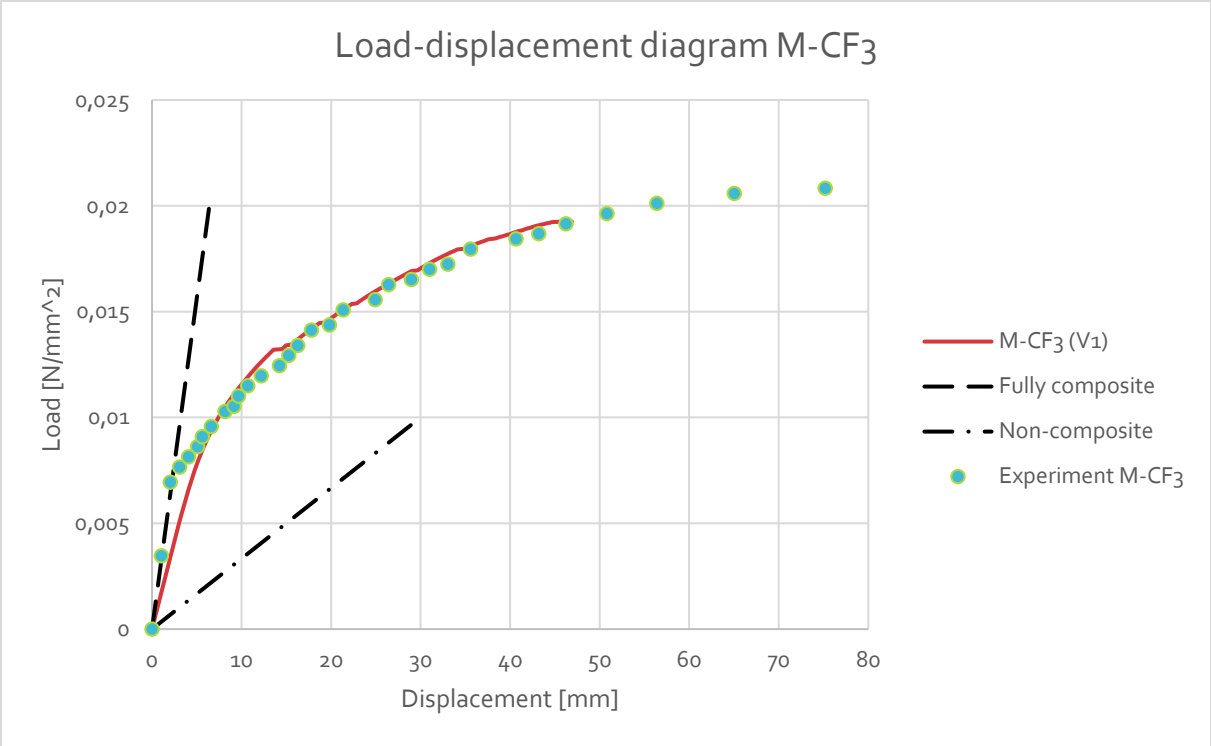

Figure 3-18: Load-displacement comparison FE-model (orange) and experiment (green) M-CF3

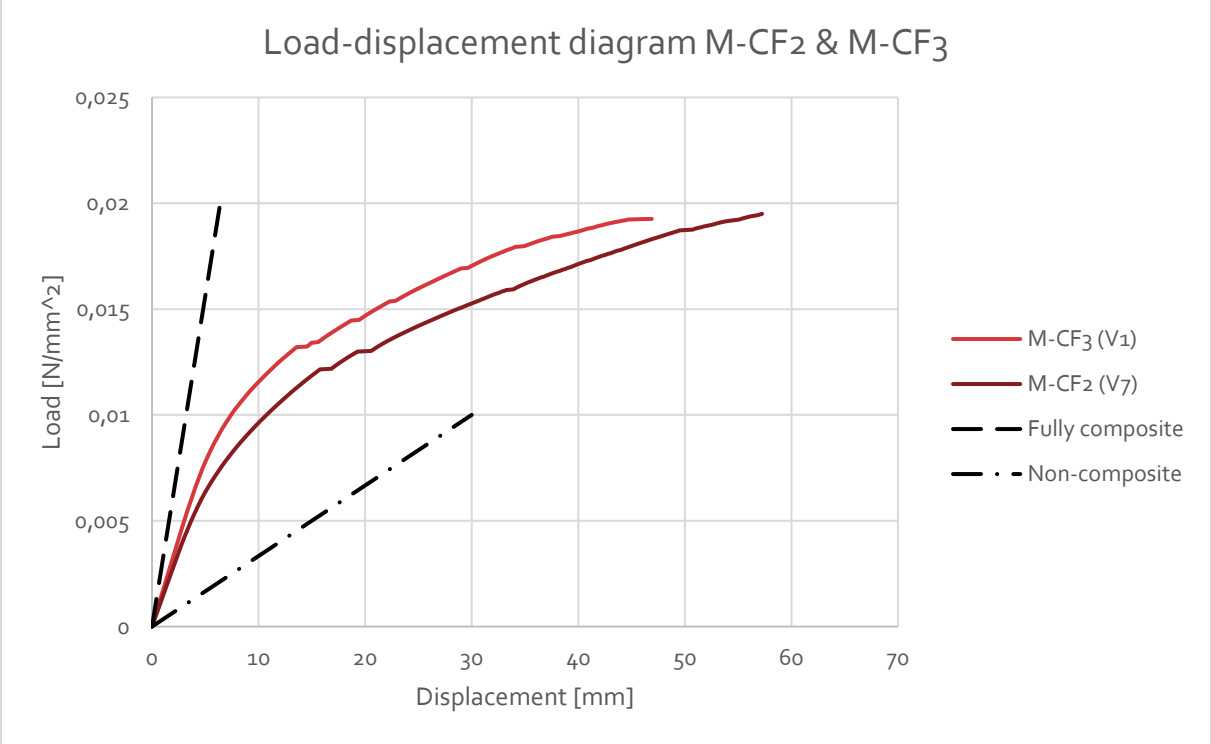

Figure 3-19: Load-displacement comparison model M-CF2 (brown) and M-CF3 (orange)

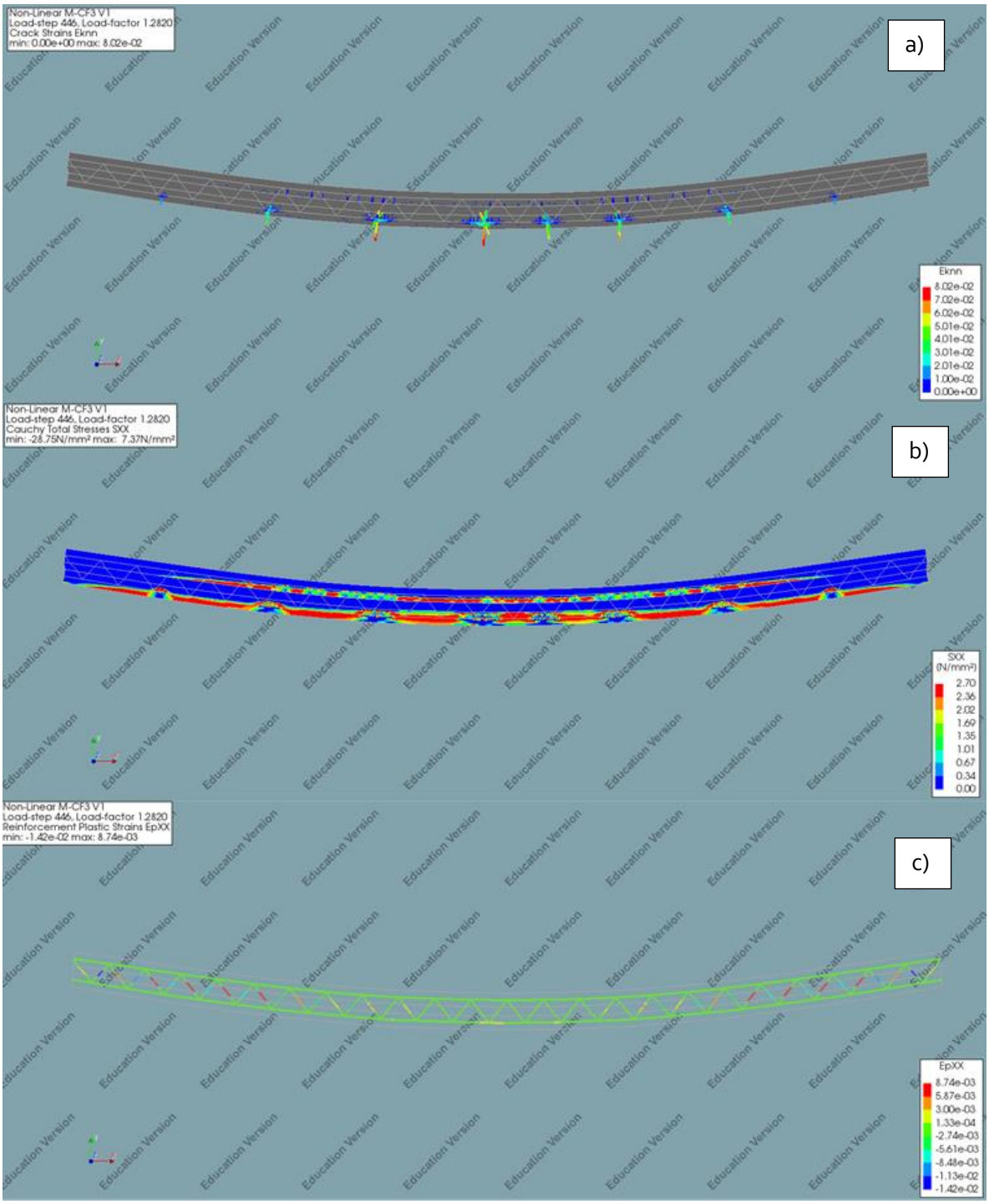

Figure 3-20(a-c): Behaviour FE-model just before failure M-CF3: concrete cracking (top), concrete stress (middle) and plastic strains reinforcement (bottom)

Additionally, another flexural experiment from a different research was compared to the FE-model. Salmon et al (1997) tested four panels with both steel and FRP connectors in a flexural test, where PCSPs were loaded by a distributed load using neoprene airbags. Panel 1 and 2, containing FRP connectors, have been modelled in DIANA. Both of these panels have identical characteristics and dimensions. The information of this element can be found in Table 3-4. At the edges until one-third of the length on both sides, the shear connectors are doubled to a total of 6 truss connectors. Only the middle third of the span consists of only three truss connectors. Cross-sections of the input in DIANA is shown in Figure 3-21. An image of the FE-model can be found in Figure 3-22. The upper image shows the general lay-out of the model, while the lower image shows the mesh lay-out in a close-up.

Table 3-4: Characteristics of panel 1 and 2 from Salmon et al.

Parameter	Value	Parameter	Value
Amount of truss connector rows	3*	**FRP truss connector diameter**	9.5 mm
Height element	9140 mm	**FRP truss connector strength**	401 MPa
Width element	2440 mm	**FRP truss connector angle**	50°
Thickness concrete wythes	63.5 mm	**Prestressing diameter**	9.5 mm
Thickness EPS	76.2 mm	**Prestressing yielding strength**	1688 MPa
Elastic modulus steel	200 GPa	**Prestressing compressive force**	369 kN
Elastic modulus FRP	48330 MPa	**Strands per concrete wythe**	5
Elastic modulus insulation	5 MPa	**Concrete crushing strength**	34 MPa
Steel reinforcement diameter	5.7 mm	**Concrete elastic modulus**	30540 MPa
Steel reinforcement spacing	152 mm	**Concrete flexural strength**	3.7 MPa
Steel yielding strength	448 MPa		

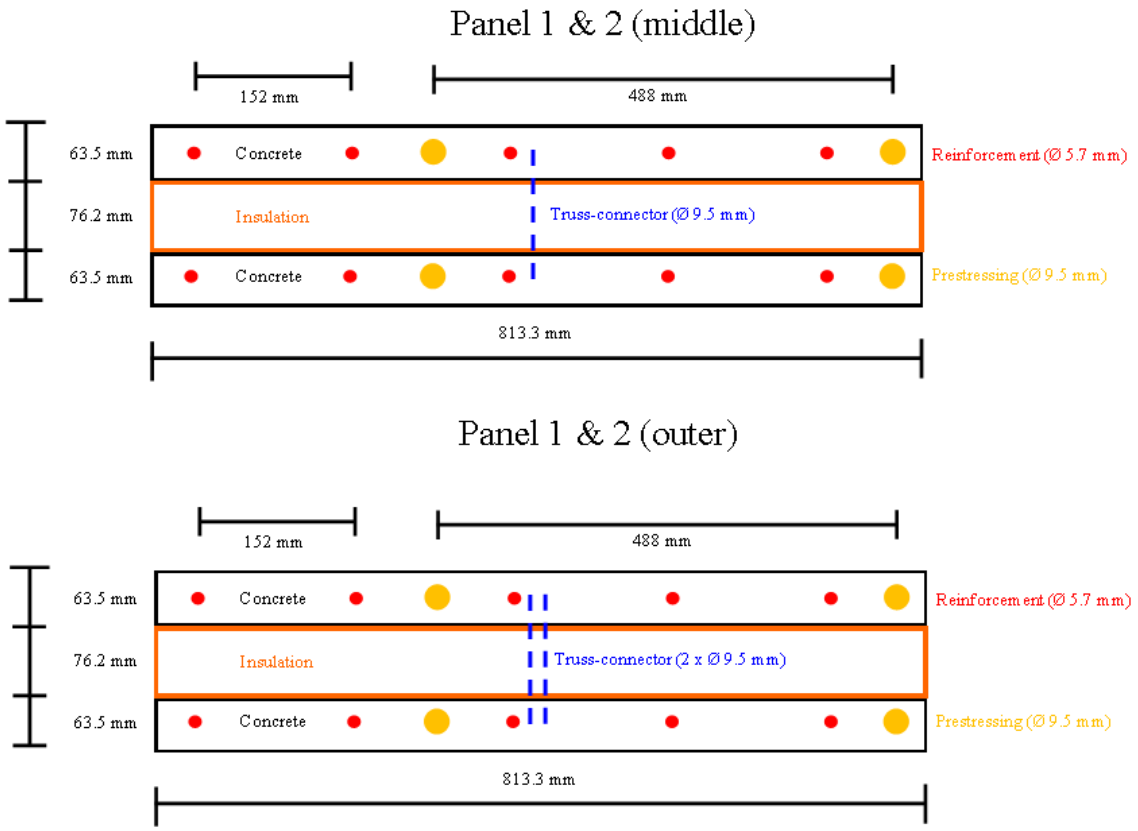

Figure 3-21: Cross-sections FE-model Panel 1 and 2 of both the middle area (top) and outer areas (bottom)

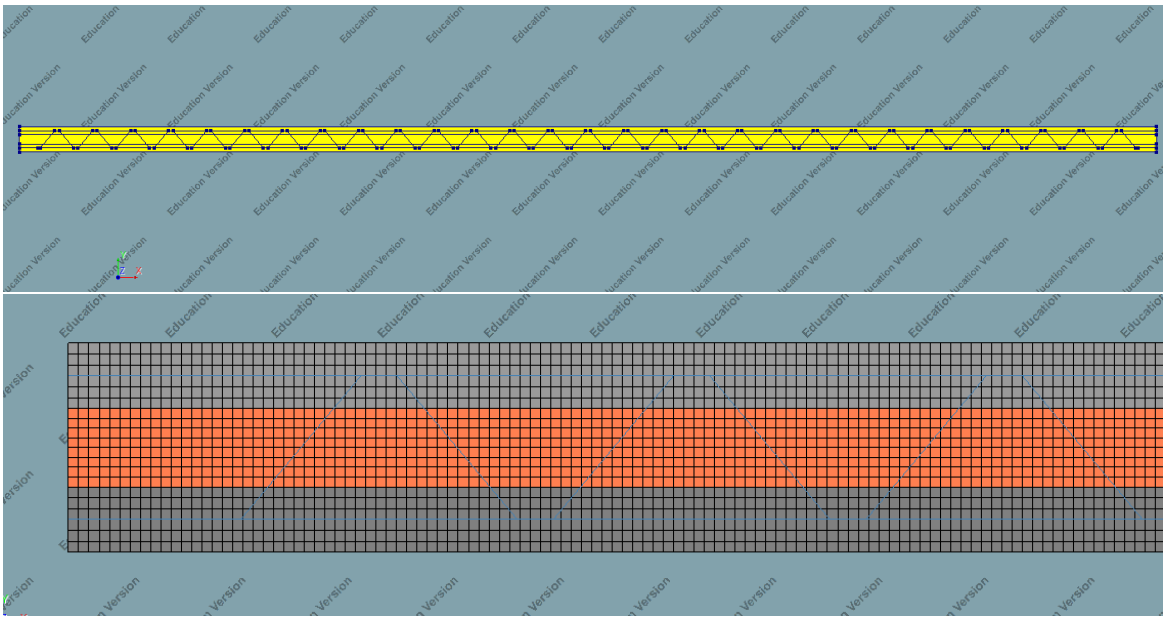

Figure 3-22: FE-model of panel 1 and 2 from Salmon et al. (1997)

The results of this comparison can be found in Figure 3-23. As the crushing limit of concrete is not included, it has been manually checked if this is reached. This can be seen in Figure 3-24, showing that the limit is not reached. The results of the models just before failure can be found in Figure 3-25. From these figures, it can be seen that the bottom wythe is fully cracked at midspan. Additionally, the bottom reinforcement has not reached its plastic limit yet.

The graph shows a perfect comparison to the linear behaviour of panel 1. The stiffness in the non-linear part of this panel is underestimated. However, the developed FE-model of Huang (2019) also had difficulties with predicting the behaviour of these experiments, as can be seen on the right figure in Figure 2-12. Both FE-models show a very similar behaviour to each other. It could be argued that some elements from the experiment were not considered or miscalculated, causing additional stiffness in the experiments in comparison to the FE-models. This variation can also be caused by experimental imperfection (Huang & Hamed, 2019). In an effort to make the FE-model more stiff, the truss-connectors were modelled as beam-elements instead of trusses. However, this did not change the result, as was also confirmed by another research (Huang & Hamed, 2019).

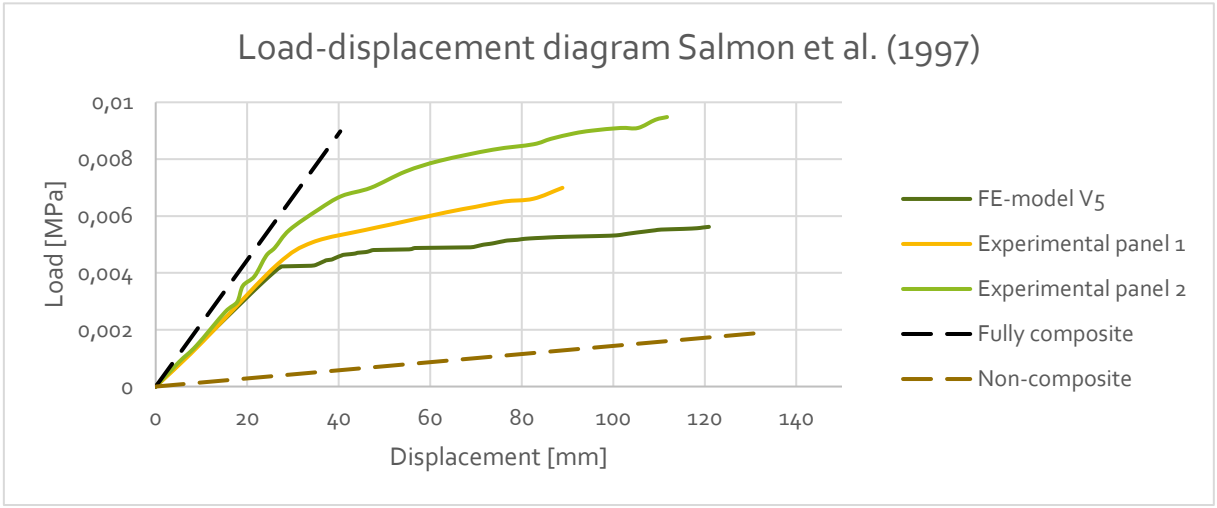

Figure 3-23: Load-displacement diagram of experimental & FE-models from Salmon et al. (1997)

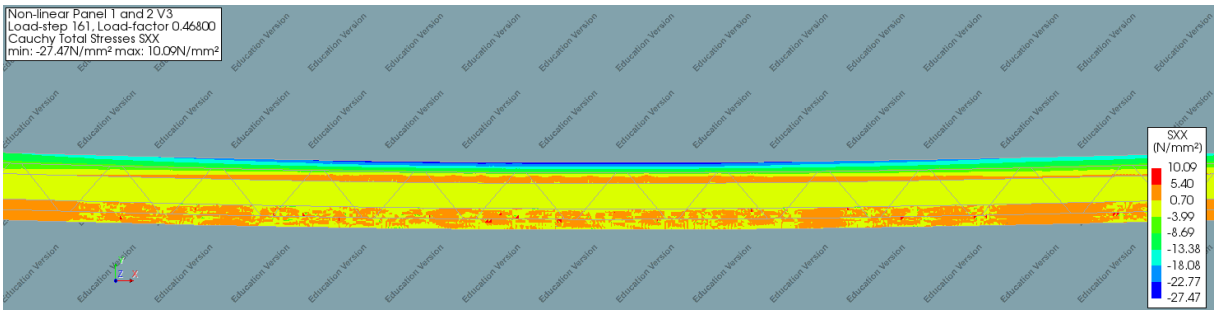

Figure 3-24: Crushing strength check panel 1 & 2

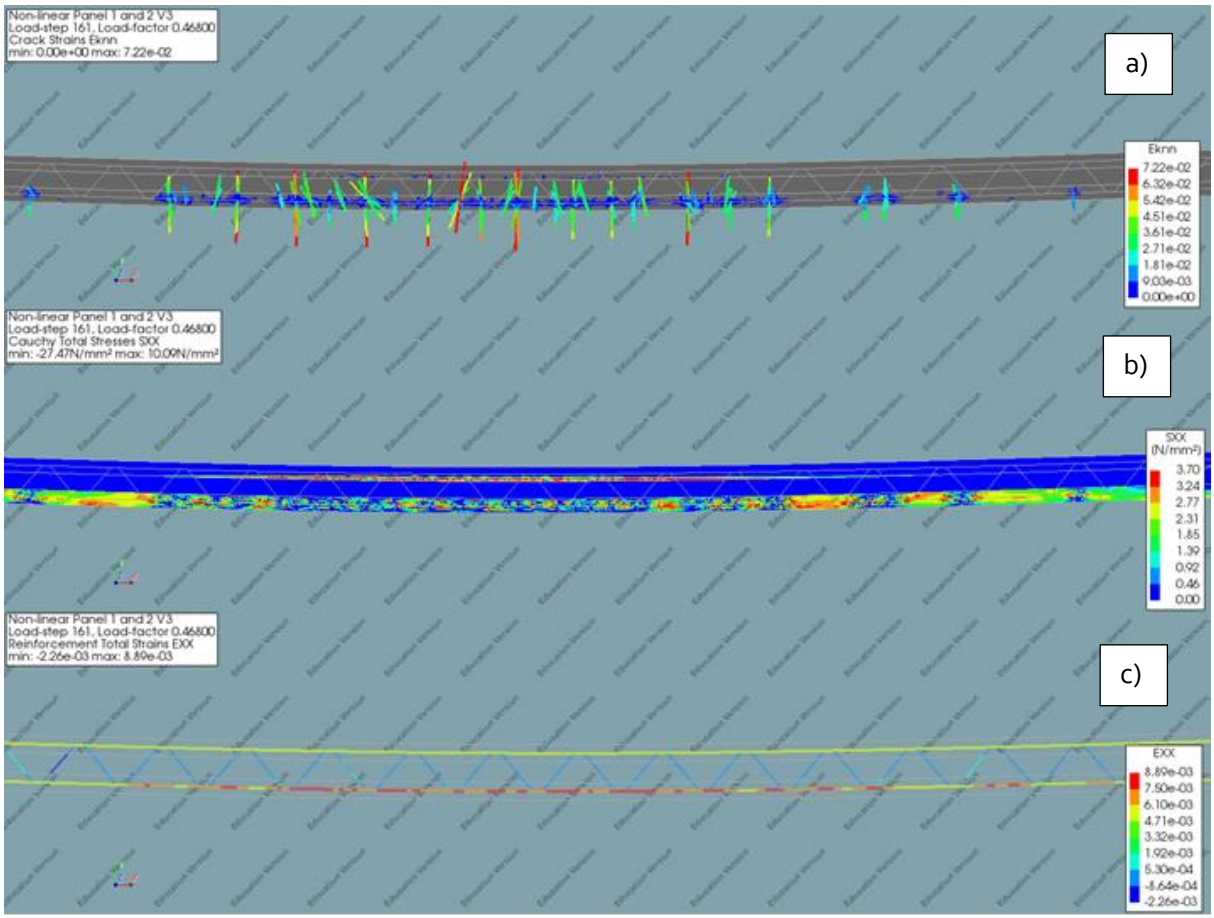

Figure 3-25(a-c): Panel 1 & 2 in its final loading stage: concrete cracking, concrete stress and steel strains

PCSPs loaded in shear

Choi et al (2015) tested multiple panels with different parameters on in-plane shear. These panels were loaded in the system shown in Figure 3-26. The inner concrete wythe is loaded by a pressure from the top, while the structure is supported at the bottom of the outer concrete wythes. To test the functionality of all FE-considerations from earlier paragraphs in an in-plane shear-experiment, an FE-model has been developed to compare to such an experiment. The experiment that was chosen was panel EPS-A30 from Choi et al. (2015).

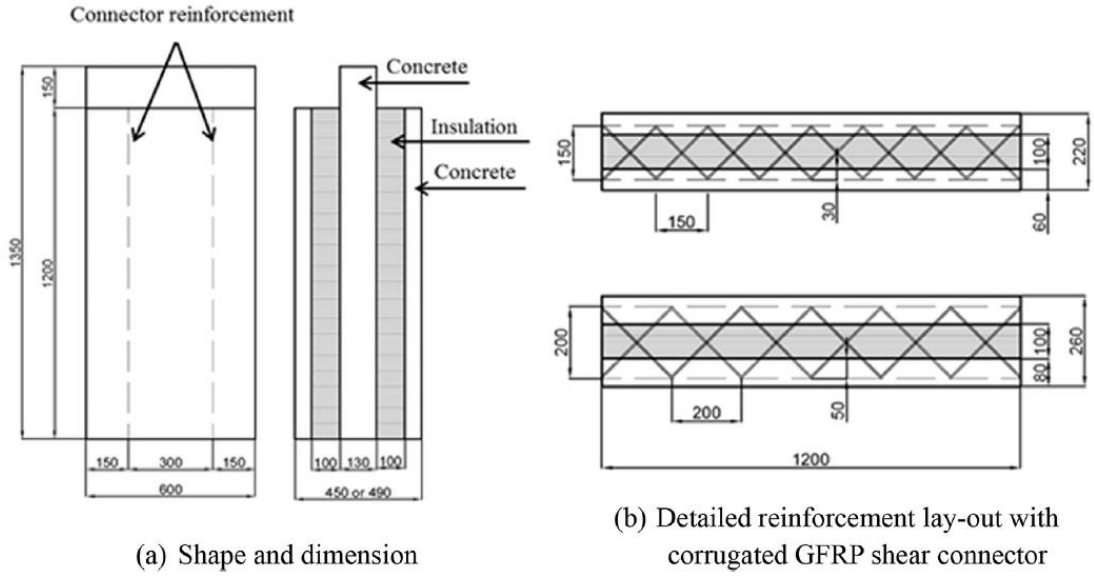

Figure 3-26: Test specimen for in-plane push-out experiment (Choi et al., 2015)

All relevant parameter-information can be found in Table 3-5. Because this research did not compare the experimental results to a model, not all stiffness-characteristics are given in the report. To still be able to compare the FE-model and experimental results, practical values for these characteristics have been estimated on basis of literature. These values are shown in the table in italic (Northwest Foam Products inc., n.d.) (Eurocodeapplied.com, n.d.) (Qiu et al., 2018). As it was expected that longitudinal reinforcement did not have an influence on the behaviour, these elements were not included in the initial model in order to save computing time. While experimenting with the model, it was clear that non-linearity for insulation-material was required to acquire more sensible results.

Table 3-5: Characteristics of panel EPS-A30 from Choi et al. (2015)

Parameter	Value	Parameter	Value
Amount of truss connector rows	2*	**GFRP truss connector cross-section area**	50 mm²
Height	1200 mm	**GFRP truss connector strength**	424 MPa
Width	600 mm	**GFRP truss connector angle**	45°
Thickness outer concrete wythes	60 mm	**GFRP elastic modulus**	*30200 MPa*
Thickness inner concrete wythe	130 mm	**Concrete crushing strength**	30 MPa
Thickness EPS layers	100 mm	**Concrete tensile strength**	2.9 MPa
Insulation elastic modulus	*3.5 MPa*	**Concrete elastic modulus**	*32837 MPa*
Insulation tensile strength	*0.124 MPa*		

An image of the FE-model can be found in Figure 3-27. The left image shows the general lay-out of the model, while the right image shows the mesh lay-out in a close-up.

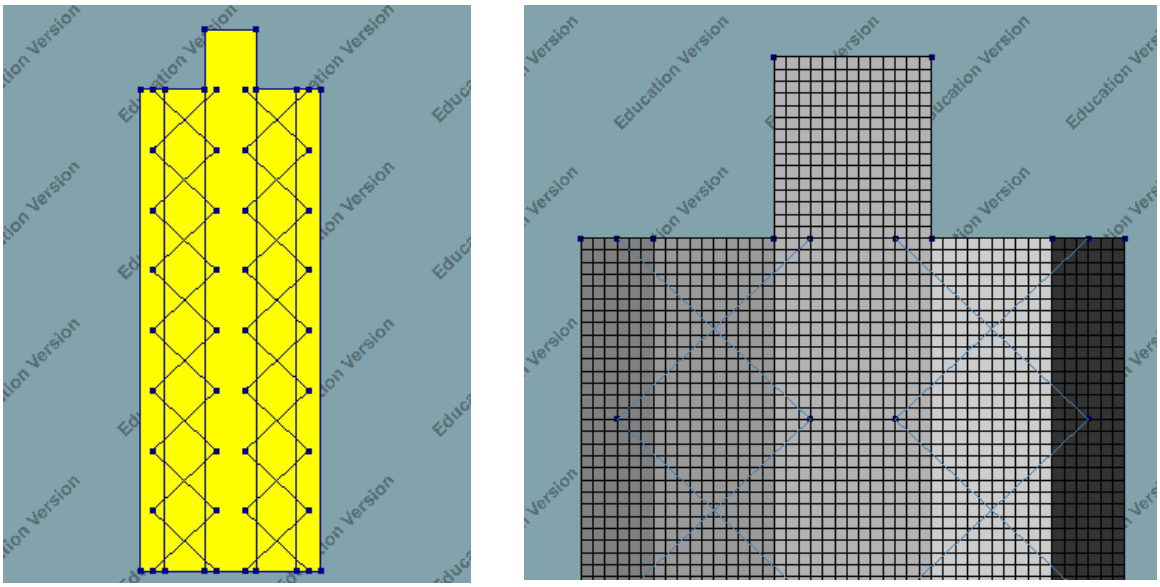

Figure 3-27: FE-model of panel EPS-A30 from Choi et al. (2015)

The results from the experiment and FE-model can be found in Figure 3-28. Here, it can be seen that the FE-model shows very different results than the experiment. A more detailed description of failure in the experiment can be found in Figure 3-29. Although the FE-model is much more brittle, it does show a similar behaviour pattern when compared to this figure. The large decrease in strength is accompanied by the failure of the truss connectors, as can also be seen in Figure 3-30. The second large reduction comes from the bond strength between the insulation and concrete being exceeded, as is shown in Figure 3-31. This also follows the experimental behaviour, where the initial decrease of strength due to the failure of the truss connectors is followed by the shearing of the insulation layer.

There are various uncertainties that could cause the large stiffness- and resistance-differences between the FE-model and experiment. Firstly, The stiffness of the concrete, insulation and GFRP-connectors have all been gained from literature not related to the paper. If the stiffness of the GFRP-connectors in the experiment is lower than the one used in the FE-model, the initial linear response would be much less stiff. However, the maximum shear strength is not influenced by this stiffness. As the strength is specifically mentioned in the experimental paper, this input cannot be edited. Additionally, some aspects like bond-slip between layers or pull-out of connectors is not included in the model. While an effort has been made to include these in the model, they caused the models to be dysfunctional. These aspects might cause a different flow of forces, which might cause lower stiffnesses or earlier failures. In order to understand the large difference of linear behaviour between experiment and model, more research has to be done on finite element shear-models.

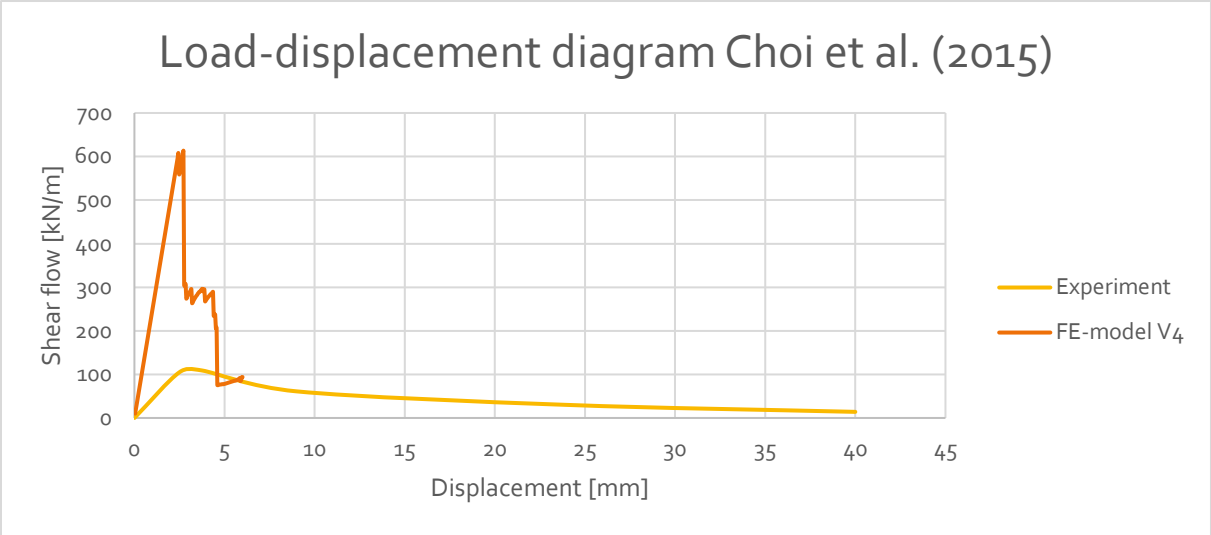

Figure 3-28: Load-displacement diagram of experimental & FE-models from Choi et al. (2015)

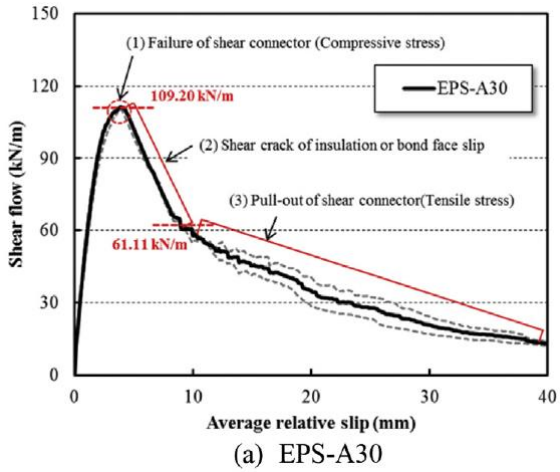

(a) EPS-A30

Figure 3-29: Detailed load-displacement diagram of experiment from Choi et al. (2015)

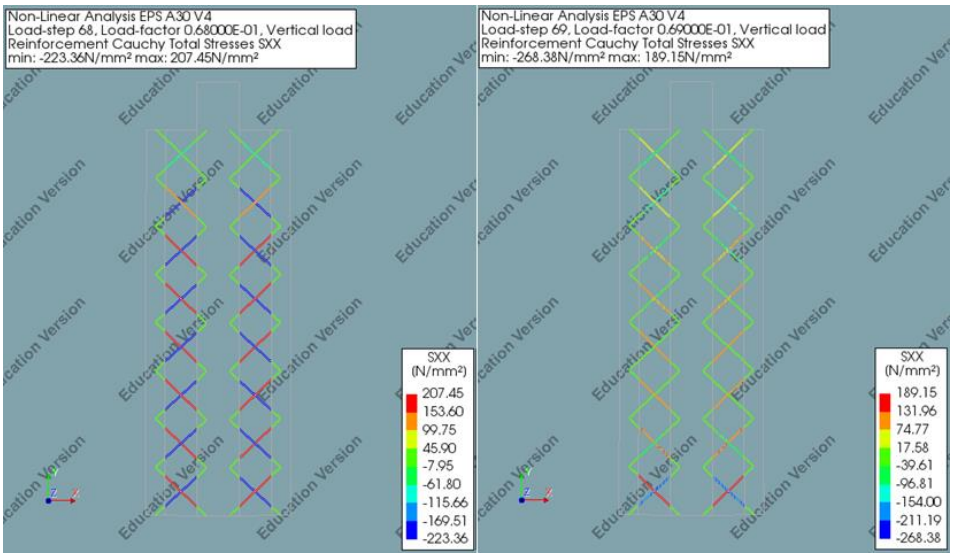

Figure 3-30: Steel stresses just before and after the first large decrease in strength

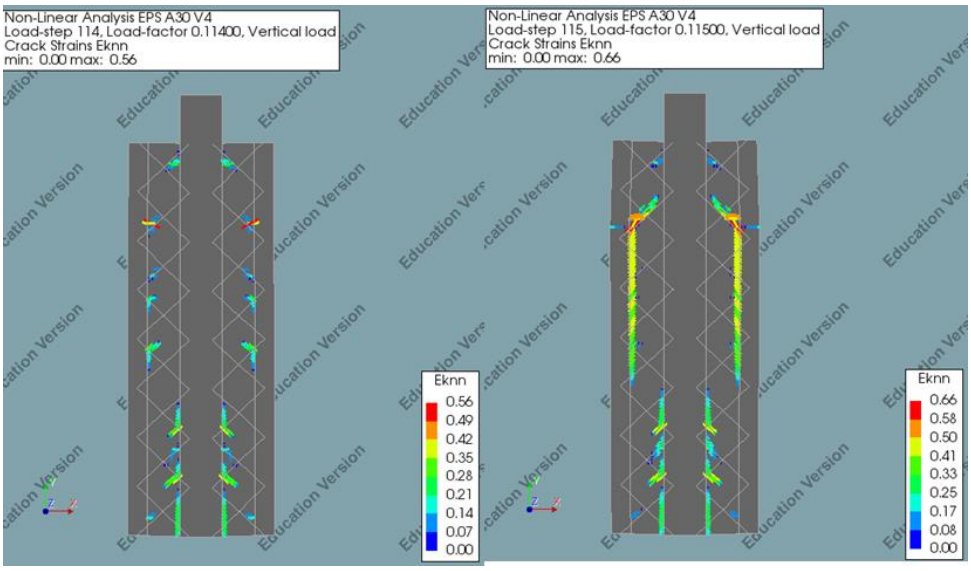

Figure 3-31: Crack strains before and after second large reduction in strength

Discussion

In all bending experiments, the linear part showed close to perfect results. In one of the three comparisons, the discrepancy between the FE-model and experiment becomes relatively large in the non-linear part of the comparison. In general, the linear parts seem to be estimated better than the non-linear parts. This might be related to experimental variation (Huang & Hamed, 2019), where stiffnesses and strengths of materials in the same type of panels are different. While only the stiffness is important in the linear part, the strength also influences the load-displacement diagram in its non-linear stage. This gives the possibility for more variation in the results.

In the case of the shear experiment, no clear similarities could be found. The differences between model and experiment are far too large to be caused by experimental variation. In the development of the shear-model in DIANA, many different aspects were added and modified in an effort to make the behaviour more similar to the experiment. However, as none of these methods work, it would seem that the shear-behaviour of PCSPs requires more in-depth research in order to function properly.

Findings

As the results from the bending FE-models are consistently correct, these will be mainly used to gain more insight into the interaction and behaviour of the three layers in a PCSP-structure. For the shear-experiment, too much elements are uncertain, and due to time-constraints, it is decided to not include this aspect further in this research.

In the next section, DIANA will be used to analyse the behaviour of PCSPs more thoroughly. This will be split into a linear part and a non-linear part, in order to see what kind of behaviour always occurs, and how this changes with non-linearity.

3.3. Gained insights from the FE-model

Before expressions will be set up for the behaviour of the PCSPs, the FE-model from this chapter will be used to gain more insight into the detailed behaviour of the PCSPs. Different features of the PCSP will be analysed, in order to verify certain behaviours along the full span of the PCSP structure.

Linear

Without truss-connectors, the cooperation between both concrete wythes is fully dependent on the insulation-layer in-between. In the analysis-model, the load is applied on the top layer, while the floor is supported on its lower edges, as shown in Figure 3-32. From this model, some unique behaviours were visible.

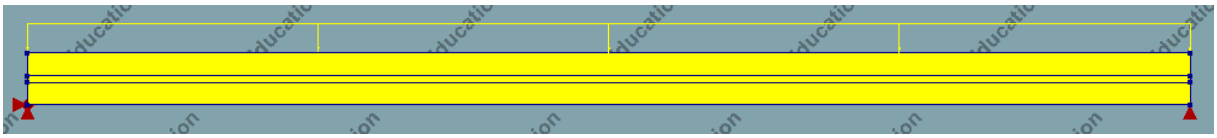

Figure 3-32: Lay-out of the analysis-model

Firstly, the assumption that plane sections remain straight is invalid in these calculations. As is seen in Figure 3-33, the insulation layer causes a shift between both concrete wythes. This is also visible when looking at the shear strains, where a relatively high shear strain can be found in the insulation layer, both without and with truss connectors, as is shown in Figure 3-34 and Figure 3-35 respectively. However, the shear strain in the intermediate layer is one hundred times smaller when truss connectors with large diameters are applied. It could be assumed that the PCSP functions as a fully composite floor in this case. The shear strains result in shear stresses in the insulation, which transport these forces to the upper and bottom concrete wythes, resulting in cooperation between the layers.

From the contour plots shown in Figure 3-34 and Figure 3-35, the shear strain pattern along the beam is the same for both models. This is logical, as the strains are proportional to the beam-angle along the length, which can be calculated by relatively simple construction mechanics. As such, it can be assumed that the shear strain pattern along the span length will always stay the same in each PCSP-floor. This is useful when developing the simplified calculation model.

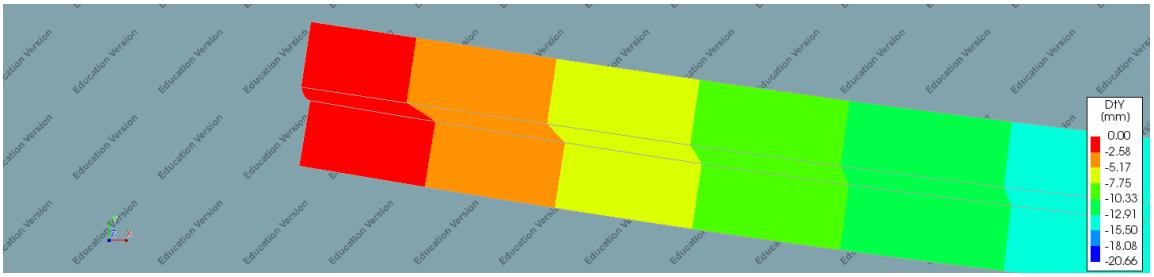

Figure 3-33: Shift between concrete wythes

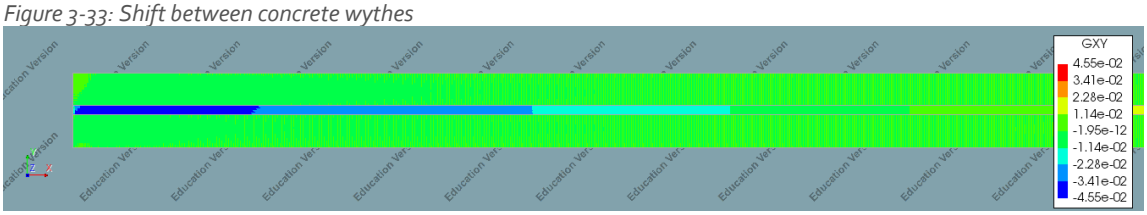

Figure 3-34: Shear strains without truss connectors

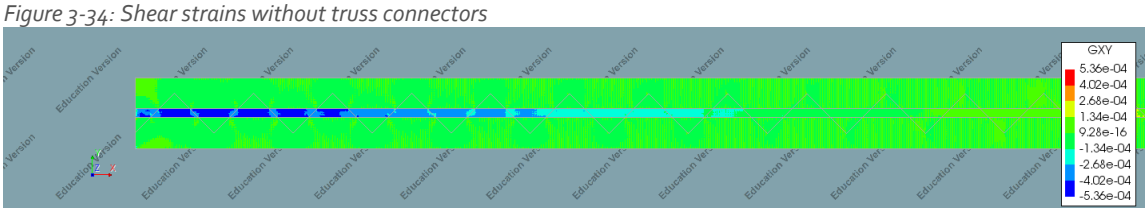

Figure 3-35: Shear strains with truss connectors

Another feature that was note-worthy, was when the intermediate layer-stiffness got increased. Even when the intermediate layer only possesses a stiffness that is $\frac{1}{62}$ of the concrete stiffness (500 N/mm²), an almost entirely fully composite element is acquired, as shown in Figure 3-36 and Figure 3-37. The first figure shows a floor with the stiffer intermediate layer, which is still much weaker than the surrounding concrete. The second figure shows the deflection of a fully concrete floor. It seems that the stiffness of a solid concrete layer is not required to acquire an almost-fully composite structure.

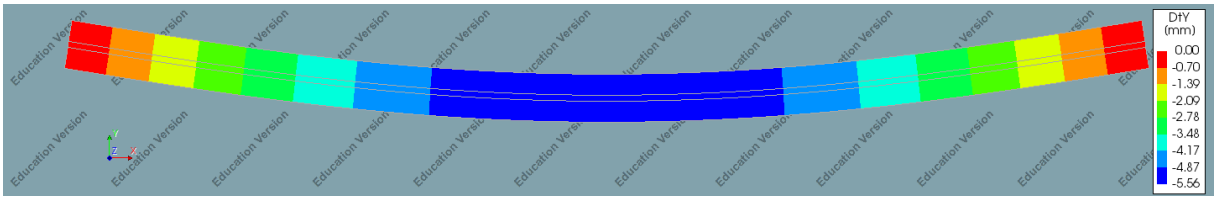

Figure 3-36: PCSP with stiffer intermediate layer

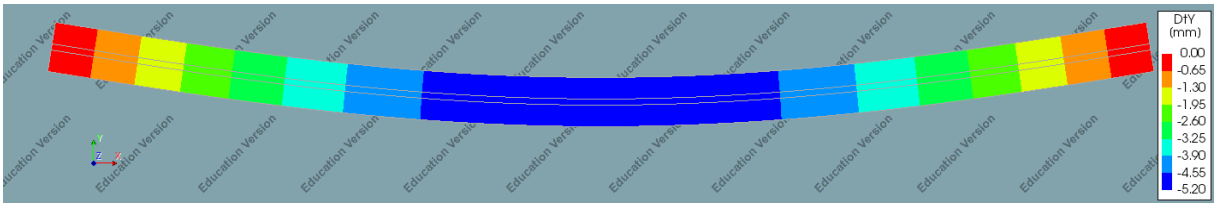

Figure 3-37: A solid concrete floor

Additionally, it became clear that the upper concrete wythe does not follow the same deflection as the lower wythe. Firstly, the normal stresses in the span-direction are shown in Figure 3-38, showing that the bending stresses in the top wythe occur in a much later state than in the lower wythe. When checking the curvature of both concrete layers, this behaviour is also clear. As shown in Figure 3-40, the upper concrete layer does not curve as much as the lower layer. Only in the middle half of the span, both layers curve in a similar way. When applying an extremely high amount of truss connectors, this deviation seems to disappear. However, it can be seen that the stresses increase in steps, due to the forces being transported by mainly the truss connectors. This is visible in Figure 3-39.

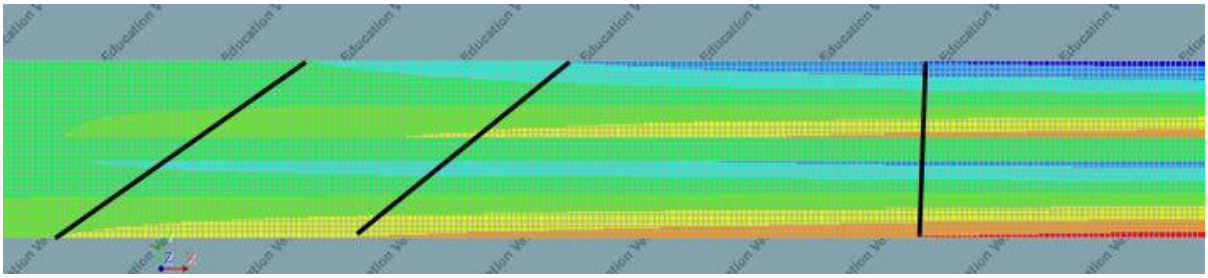

Figure 3-38: Bending stress differences between top and bottom concrete wythe

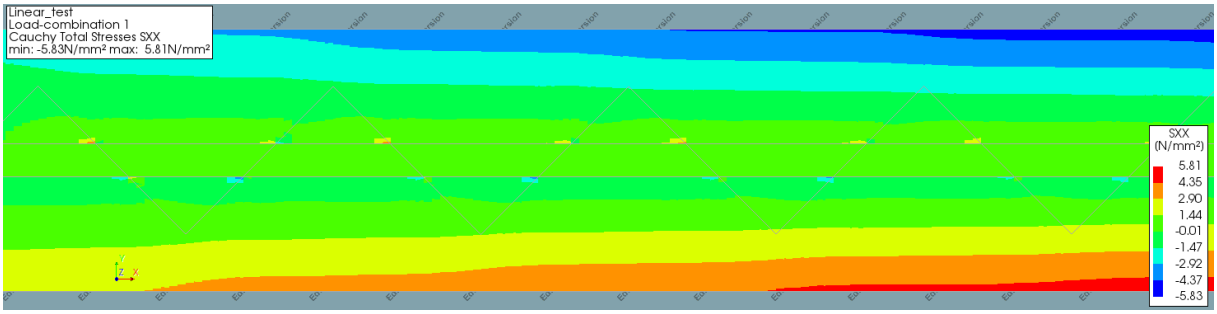

Figure 3-39: Increase of bending stresses due to connection truss connectors

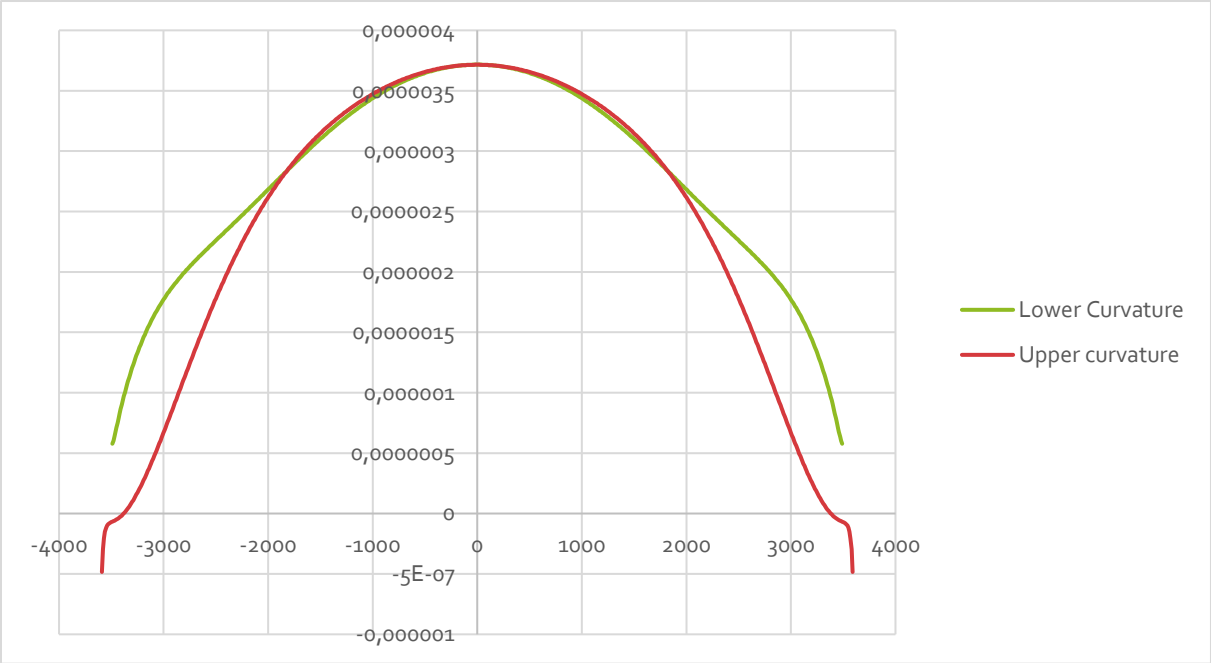

Figure 3-40: Graph showing curvature of both the lower and upper concrete wythe

Lastly, in Figure 3-41, the vertical strain at the edge of the floor is shown. The sudden increase in strain in the insulation hints towards the upper wythe not bending as much as the lower wythe. Although present at a much lower level, the same behaviour is present when applying an extreme high amount of truss connectors, as shown in Figure 3-42.

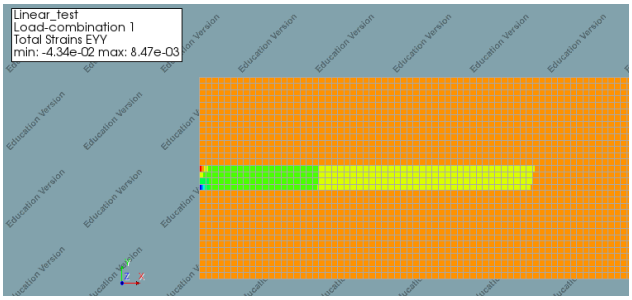

Figure 3-41: Increase of insulation strains at floor-edge – without truss connectors

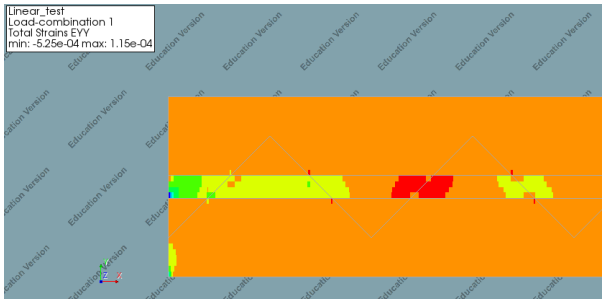

Figure 3-42: Increase of insulation strains at floor edge - with truss connectors

Non-linear

The behaviours discussed at the start of this section are relatively straight-forward in the case of a linear model. However, when non-linearity is applied, a multitude of difficulties arise when trying to analyse simple behaviours of the structure. These elements will be discussed here.

Firstly, the cracking of concrete has a large effect on the general behaviour of the structure. Similarly to the tensile tie model, cracking reduces the bending stiffness of the PCSP. However, in the case of a PCSP, this reduction works differently than in the case of a solid reinforced bending beam. Because only one reinforcement bar is present along the thickness of the wythe, the wythe essentially acts more as a tensile tie than a bending beam. Additionally, the reduced stiffness of this wythe means that the proportion between the truss-stiffness and wythe-stiffness is increased. These types of changes in the different proportions of the structure cause a higher composite action, but a lower "potential" stiffness in the case of a fully composite structure. The rate of actual stiffness-changes due to concrete cracking in PCSPs has not been analysed yet. Due to the shift of the centre-line of the PCSP that is caused by cracking, it is also more difficult to calculate the composite factor.

Next to the concrete, the plasticity of the truss-connectors is also an important factor to the general behaviour and level of composite action of the structure. As mentioned before, the strain of the intermediate layer is dependent on the angle of the beam. As such, this means that the highest stresses occur at the edges of the beams. This can also be seen in Figure 3-13 from Section 3.1, where the truss-connectors at the edges show plasticity very early in the loading-scheme. In Figure 3-43, a graph of the truss-stresses can be found along the length of the beam. Although the angle of the beam varies over the entire span, the stresses are almost identical, with the exception of the two trusses closest to midspan. While the angle – and as such the shear strain – increases, the reaction force stays the same. This means that the effective stiffness of the steel trusses is reduced along the span of the beam when a certain level of load is applied. As this reduces the stiffness of the intermediate layer at the edges, the composite action is reduced. It is expected that this behaviour is the initial cause for non-linearity in PCSPs. However, the rate of reduction of composite-action due to this plastic behaviour is still unknown at the moment.

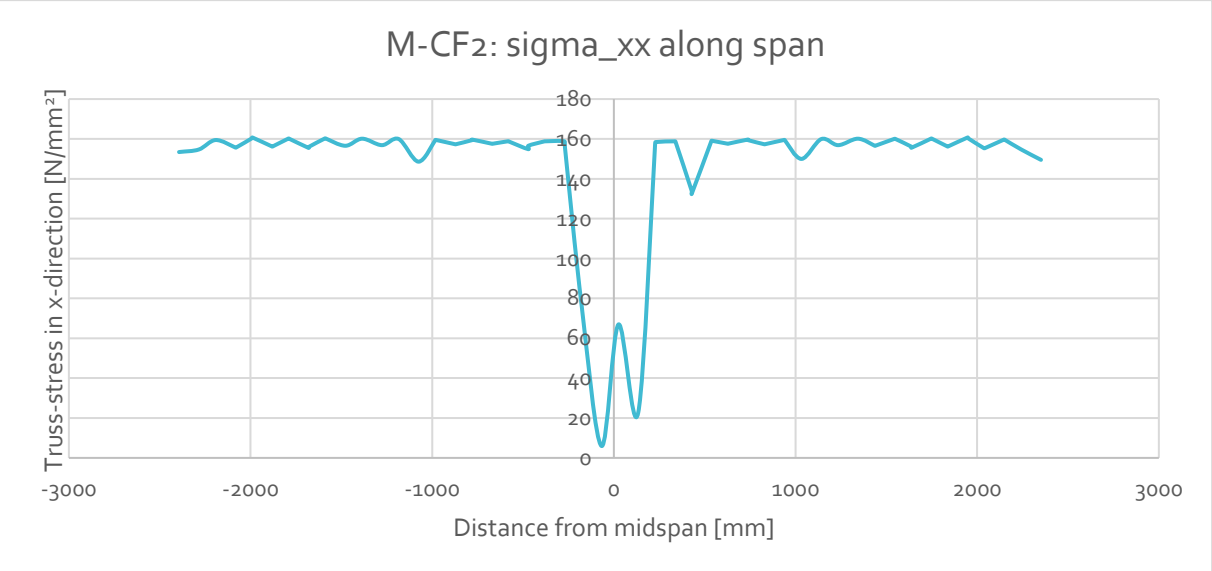

Figure 3-43: Truss-connector stresses along the span of the beam

3.4. Parameter-study of FE-model

In order to get a general idea how different parameters influence the composite factor, a set of results are gathered from the FE-model. For linear calculations of PCSPs, the essential parameter is the so-called composite factor. This composite factor shows the level of cooperation between the different layers. The formula for this factor is as follows:

$$CF = \frac{w_{real} - w_{non}}{w_{full} - w_{non}}$$

Where:

w_{real}: The deflection of the actual PCSP (gained from a model or experiment, see Figure 3-44c)

w_{non}: The deflection, assuming all layers behave independently of each other (see Figure 3-44b)

w_{full}: The deflection, assuming all layers behave as one unit (see Figure 3-44a)

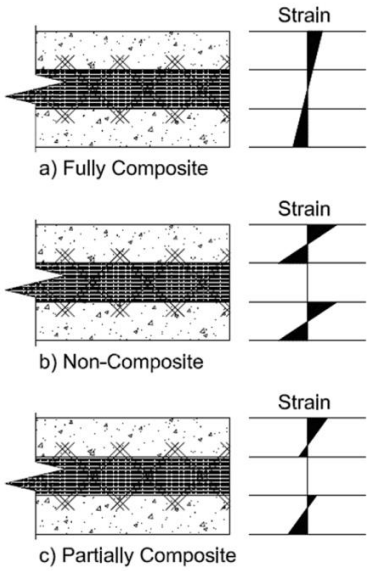

Figure 3-44: Different types of composite action (Salmon et al., 1997)

Initially, models are tested without use of truss-connectors. Three main parameters have been varied in DIANA to check the change of composite factor:

- Span length: 4000 – 7200 mm (in steps of 800 mm)
- Concrete thickness: 60 – 140 mm (in steps of 20 mm)
- Insulation thickness: 40 – 80 mm (in steps of 10 mm)

The variations of these parameters are based on practical values that have been found in experiments, combined with the preferred PCSP-design of the Reinbouw project of Lievense | WSP. Different combinations have been modelled, in order to find both the individual effects of these parameters and the dependence of these parameters on each other. As mentioned before, in order to prevent the two concrete wythes to behave differently from each other, tyings have been applied at the edges of the structure, that keep the deflection of both wythes the same.

In Figure 3-45 and Figure 3-46, the composite factor is plotted over the varied span length and concrete thickness respectively. In both graphs, the parameter that is not varied along the x-axis, is visualised with multiple lines in each graph. From these figures, it is clear that an increase of span will result in an increase of the composite action. This increase seems to be non-linear, as the composite effect increase is reduced at higher spans. Additionally, it can be concluded that an increase in concrete thickness decreases the composite factor. This change also seems to be non-linear. Observing the differences between each lines in the same graph, it seems like both of these parameters behave independently on each other, where the increase of one parameter does not increase the effect on the composite factor on the other parameter.

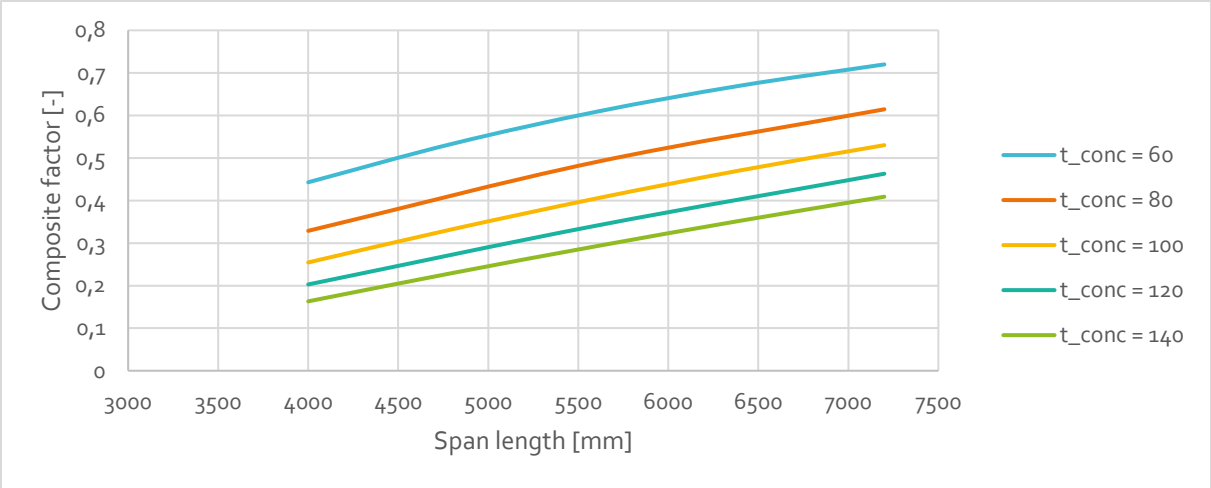

Figure 3-45: Composite factor varied over the span length

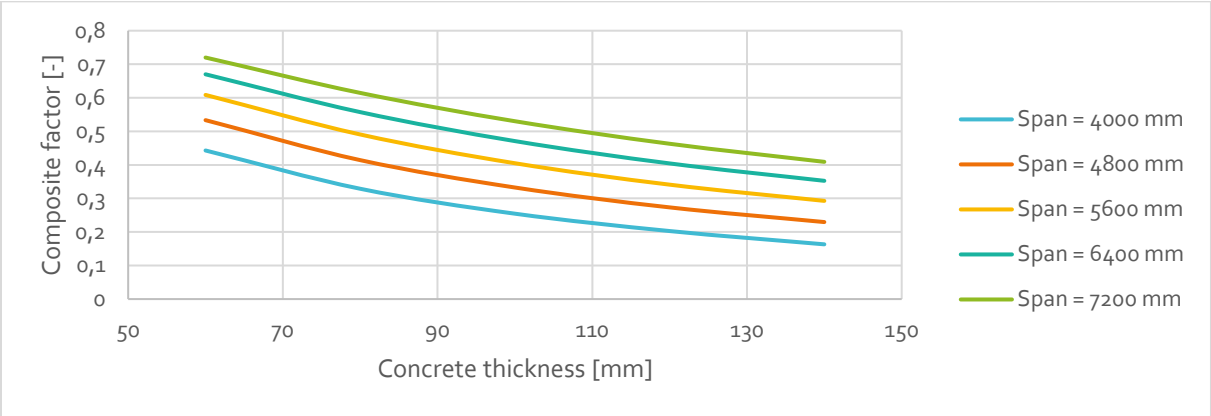

Figure 3-46: Composite factor varied over the concrete thickness

Figure 3-47 shows the effect of the insulation on the composite action. In a similar fashion as the last two figures, the multiple lines show different parameters that are not varied along the x-axis. In this case, these are combinations of span length and concrete thickness. In general, the insulation causes a decrease in composite factor. When checking the different graph-lines, it can also be observed that designs with a higher concrete thickness result in a higher effect of the insulation on the composite factor. When using concrete thicknesses of 60 mm, a decrease of only 0.02 composite factor is observed. In the case of 140 mm thickness, this increases to a 0.07 reduction when changing the insulation from 40 to 80 mm. These results show that the effect of insulation on the composite factor is dependent on concrete thickness. This is not unexpected, as the interaction between the intermediate and concrete layer form the basis for the level of composite action.

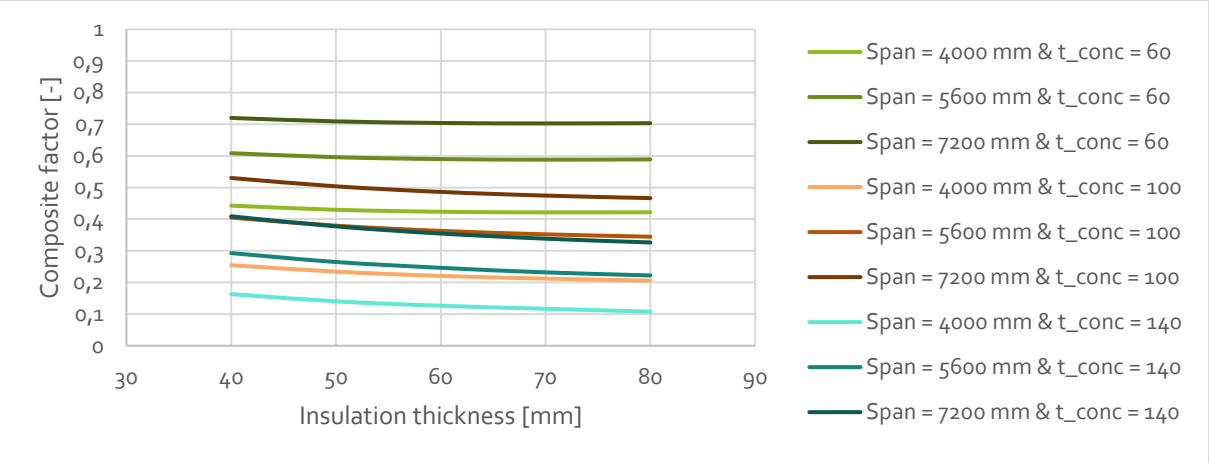

Figure 3-47: Composite factor varied over the insulation thickness

When truss-connectors are applied, the floor-design from Hamed (2018) has been replicated and the results from his model were compared. These showed a perfect comparison, as shown in Figure 3-48.

From these results, it can already be seen that a fully composite structure is very difficult to acquire. The steep increase in composite-action with thinner diameter-bars is the important part, as this is the area when floors will be designed in for the most part. As such, three different designs from Figure 3-47 have been modelled with the application of truss-connectors, and can be found in Figure 3-49. Here, a clear difference in this part of the behaviour can be found, even when the model without truss-connectors shown relatively similar results. It seems that the varied parameters have an influence on the rate of increase of composite action. The mathematical model that is developed in the next paragraph will try to calculate this influence.

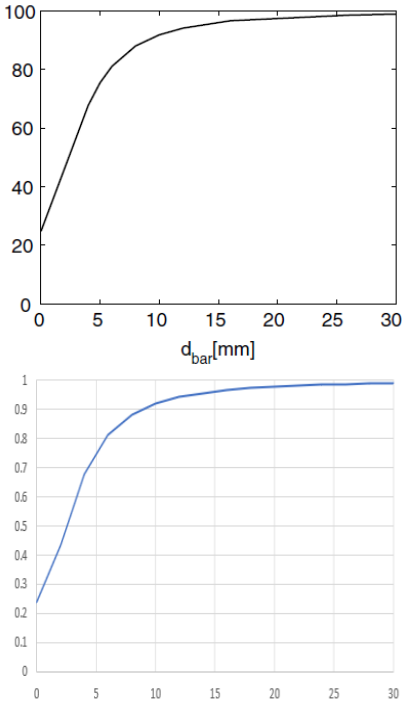

Figure 3-48: Effect of truss connectors, from both Hamed (2018) and the DIANA-model

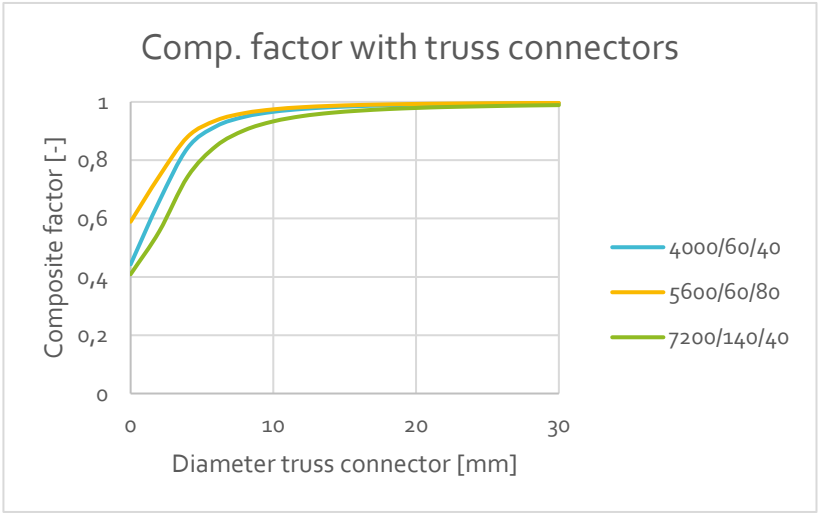

Figure 3-49: Composite factor when truss connectors are applied (Span/concrete thickness/insulation thickness)

Findings

For the linear analysis, it seems that most behaviours are relatively clear and simple. One of the only behaviours that is more difficult to predict is the compression of the insulation layers at the edges, as this causes a difference between the behaviour in both concrete wythes. For the non-linear analysis, a lot of the simple behaviours that can be assumed or estimated in the linear analysis are not valid anymore. As such, it is very difficult to predict this behaviour with a simplified model, without any foundation to build this complicated model on.

For the development of a simple prediction model, it is decided to only focus on the linear aspect of the floors. The reasoning for this is that the non-linear part is only a small fraction of the total resistance of the structure. Additionally, the non-linear part causes the development of the prediction model to be significantly more difficult. The only feature that is hard to predict for the linear model is the compression of the insulation at the edges. As such, the FE-model will make use of tyings to prevent this type of displacement, so that the analytical prediction model does not have to take this into account when comparing this model to the FE-model.

With regards to the parameter study, it can be seen that the concrete thickness and span length influence the composite behaviour the most when truss connectors are not applied. Increasing the concrete thickness of the PCSPs from 60 to 140 mm would decrease the composite factor for a value of around 0.28. Increasing the span length from 4000 to 8000 mm would increase the composite factor for around 0.31. The effect of increasing the insulation thickness from 40 to 80 mm depends on the concrete thickness, where the reduction of the composite factor is 0.02 and 0.06 for a concrete thickness of 60 and 140 mm respectively. When truss-connectors are applied, most PCSP-designs will possess a composite factor of above 0.95 when 12 mm diameter bars are being used every 800 mm. However, when concrete wythes with a thickness of 140 mm or higher are being used, the increase in composite-action due to the application of trusses decreases significantly. When 140 mm wythes are used instead of 60 mm, the composite factor is reduced from 0.96 to 0.91.

4. Analytical prediction model

In this chapter, an easy-to-use analytical model is developed. Firstly, the theoretical background that is used to develop this analytical model is explained. In this section, the calculation-method of the analytical model is also explained, where assumptions and the most important calculations are the main focus. Afterwards, the results of the comparison between the analytical and linear FE-model are shown. A view of the analytical model can be found in Appendix o.

4.1. Theoretical background of analytical model

Multiple different methods have been used to find a working analytical model to predict the behaviour of PCSPs. Although some methods were not showing correct results, the insights and thought-processes behind these methods were important for the development of the model. This development-process and the final version of the analytical model are explained here.

In order to be able to make a simplified calculation of PCSPs, the structure must be simplified into a mechanics-model. The initial mechanics model is shown in Figure 4-1, and makes use of the following considerations:

- Both concrete wythes are pure bending beams:
  - No axial displacement is present ($EA = \infty$)
  - No shear displacement is present ($G_c = \infty$)
- Intermediate layer does not compress in vertical direction
  - Meaning that both concrete floors bend identical (parallel/symmetrical model)

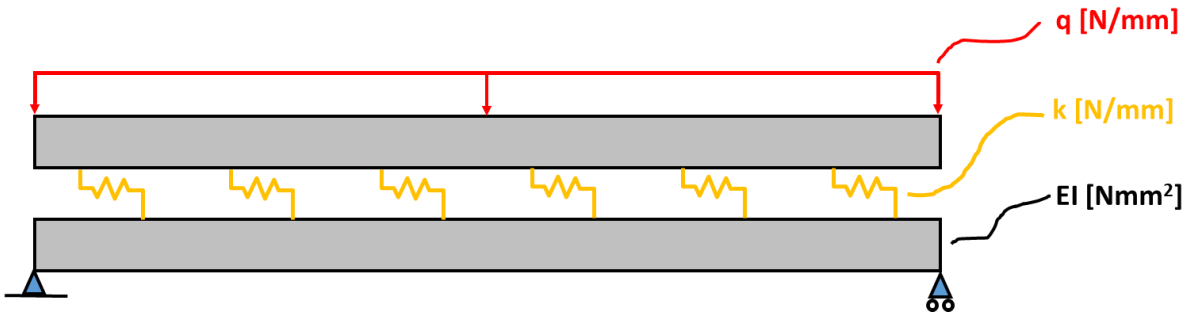

Figure 4-1: Initial mechanical model PCSP

In this model, the intermediate layer is replaced by horizontal springs, that are put between the two concrete wythes. In the initial model, it is assumed that these springs have a reactionary bending moment on both concrete wythes. To work further with this model, the strains and stiffnesses of the intermediate layer needs to be calculated.

When calculating the strains of the intermediate layer, a non-composite floor is initially assumed and loaded by a distributed load as shown in Figure 4-2. All layers are not connected to each other in any way, causing an identical beam-angle over all layers in the entire span. When zooming in at the edge, this beam angle can be used to find the difference in axial displacement between the different layers. In Figure 4-2, the distance between the top concrete wythe and insulation layer at location x is calculated as follows:

$$\Delta u_{x,t,max}(x) = \frac{1}{2}(t_c + t_i) * \varphi(x) \quad (1)$$

Where:
$\Delta u_{x,t,max}(x)$: Distance between top concrete- and insulation-layer at location x [mm]

t_c: Thickness of concrete layer [mm]

t_i: Thickness of insulation layer [mm]

$\varphi(x)$: Beam angle at location x [rad]

Now that the difference in axial displacement is determined, a situation is now assumed where the intermediate layer is fully connected to the concrete wythe. A visualisation is shown in Figure 4-3. In all sensible designs for PCSPs, the intermediate layer will possess a significantly lower shear stiffness compared to the concrete wythes. Thus, it is assumed that all shear strain caused by this difference in axial displacement is present in the intermediate layer. This results is the following calculation for the shear strain of the intermediate layer:

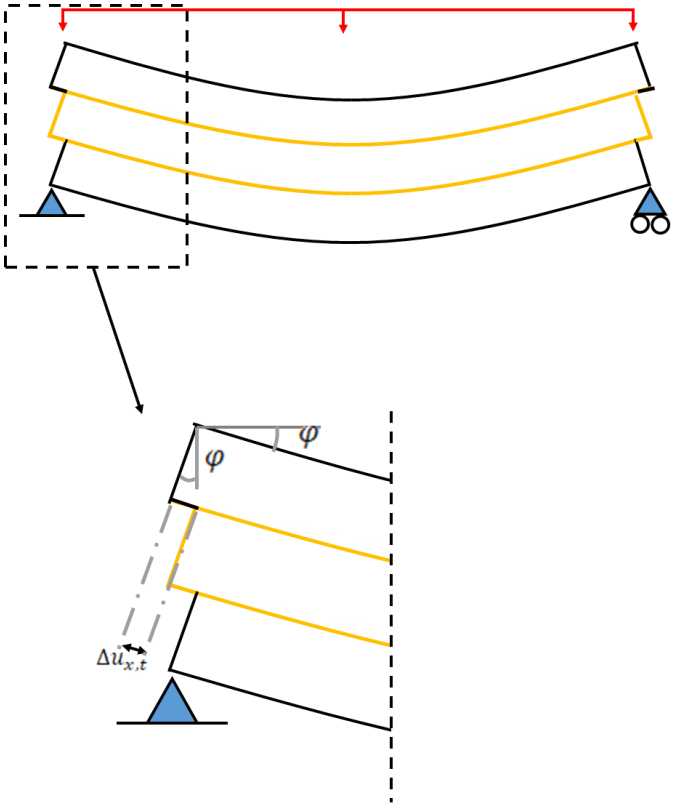

Figure 4-2: Initial non-composite assumption and determination of difference of axial displacement

$$\gamma_{xy}(x) = \frac{\Delta u_{x,t}(x)}{\frac{1}{2}t_i} = \frac{t_i + t_c}{t_i} * \varphi(x) \quad (2)$$

Where:
$\gamma_{xy}(x)$: Shear strain of interm. layer [-]

Only half of the insulation-thickness is used, as $\Delta u_{x,t}$ only includes the top concrete wythe.

Now, the response for this intermediate layer must be calculated. In the case where no truss-connectors would be applied, the calculation would be very straight-forward:

$$G_{inter} = \frac{E_{ins}}{2(1+\nu)} \quad (3)$$

Where:
G_{inter}: Shear modulus of the intermediate layer [N/mm²]

E_{ins}: Elastic modulus of the insulation-layer [N/mm²]

ν: Poisson ratio of the material [-]

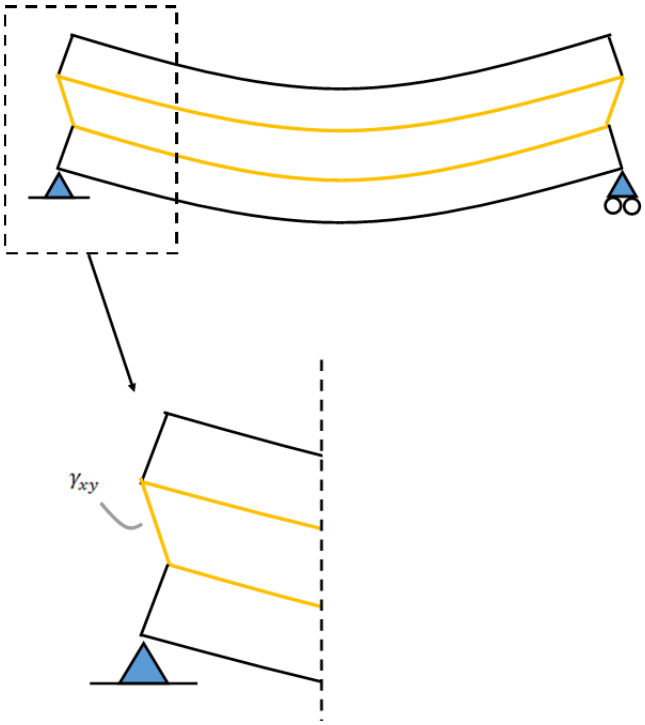

Figure 4-3: Partially-composite behaviour of PCSPs and determination of shear strain intermediate layer

However, as truss-connectors are always applied when PCSPs are load-bearing, an additional calculation has to be done to determine the total stiffness of the intermediate layer.

In this calculation, the stiffness of the truss-connectors are translated into an increased stiffness of the intermediate layer. A visualisation showing this translation is given in Figure 4-4. Some parts of the truss-connectors are not activated due to the difference in axial displacement, as these truss-connectors are present in the concrete part of the PCSP. In the figure, these parts are visualised by the blue striped line. The solid red line shows the part of the truss-connectors that do increase the stiffness of this intermediate layer. Only this red part has to be included in the model, and will be used to calculate the fictitious stiffness of the intermediate layer.

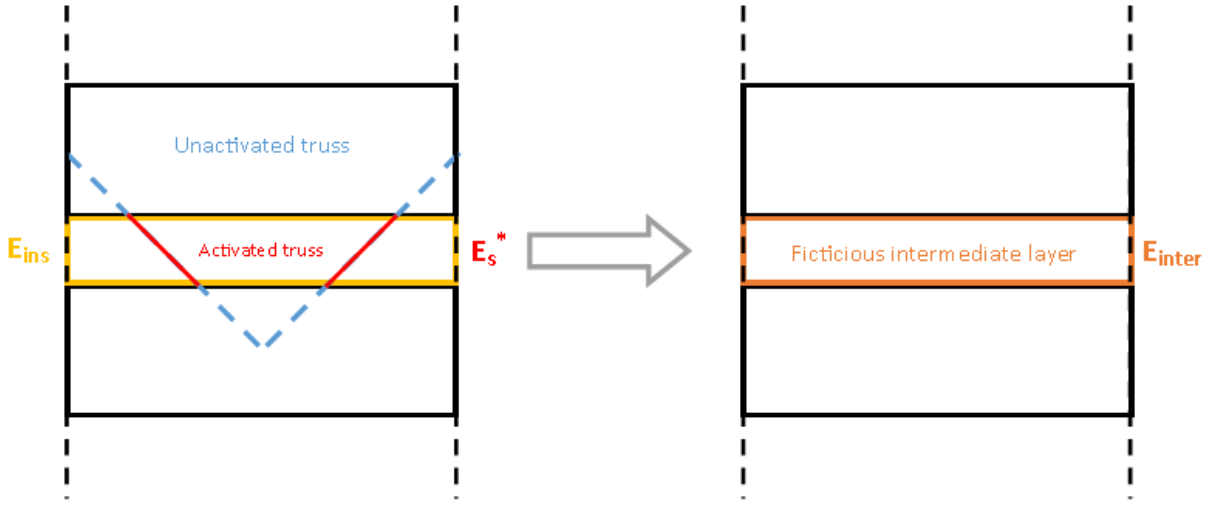

Figure 4-4: Translation of truss-connectors to increased intermediate layer-stiffness

For this calculation, some assumptions are made. Firstly, it is assumed that the truss-connectors are always applied from and to the centre-line of the concrete wythes. Additionally, the angle in which the truss-connectors are applied is fixed at 45°. Lastly, the angle of the truss-connectors is not taken into account when calculating the stiffness of these elements. These assumptions are done to not add too much variables to the analytical model. As such, the calculation of the intermediate layer-stiffness is done as follows:

$$A_s = \frac{1}{4} * d_s^2 * \pi \tag{4}$$

$$EA_s^* = E_s * A_s * \left(\frac{t_i}{t_i + t_c}\right) \tag{5}$$

Where:
$\boldsymbol{A_s}$: Cross-sectional area of truss-connector [mm²]

$\boldsymbol{d_s}$: Diameter of truss-connector [mm]

$\boldsymbol{EA_s^*}$: Fictitious axial stiffness of truss-connector [N]

$\boldsymbol{E_s}$: Elastic modulus of truss-connector [N/mm²]

For these calculations, the centre-to-centre distance of the truss-connectors is assumed to be equal to the width of the floor. As such, the cross-sectional area of the truss-connectors must be spread over this entire width:

$$E_s^* = \frac{EA_s^*}{t_i * b} \tag{6}$$

Where:
$\boldsymbol{E_s^*}$: Fictitious elastic modulus of truss-connector [N/mm²]

$\boldsymbol{b}$: Centre-to-centre distance of truss-connectors [mm]

From this calculation, the two stiffnesses can be summed and finally calculated to the elastic shear stiffness:

$$E_{inter} = E_{ins} + E_s^* \tag{7}$$

$$G_{inter} = \frac{E_{inter}}{2(1+\nu)} \tag{8}$$

Where:
$\boldsymbol{E_{inter}}$: Elastic modulus of intermediate layer [N/mm²]

Now that the shear strain and stiffness are known from Equation (2) and (8) respectively, the reaction force over the span length can be determined:

$$n_{xy}(x) = \gamma_{xy}(x) * G_{inter} * b = \frac{(t_i + t_c)}{t_i} * G_{inter} * \varphi(x) * b \tag{9}$$

Where:
$\boldsymbol{n_{xy}(x)}$: Shear force of intermediate layer at location x [N/mm]

For the initial analytical model, it was assumed that the reaction force at the concrete edge caused a reactionary bending moment in the concrete wythes, adding up to the total bending stiffness. This is also visualised in Figure 4-5. As such, the additional composite bending moment in the concrete wythes is equal to:

$$\Delta m_{comp} = n_{xy} * \frac{1}{2} t_c \tag{10}$$

$\boldsymbol{\Delta m_{comp}}$: Additional moment in concrete wythe due to composite-effect [Nmm]

Now, equations can be set up to be used in an analytical model in Maple. Given this model, an Ordinary Differential Equation (ODE) can be set-up and solved to find a displacement field. The equations and ODE are as follows:

Kinematic equations:

$$\varphi = -\frac{dw}{dx} \qquad \kappa = \frac{d\varphi}{dx}$$

Constitutive equation:

$$M = EI * \kappa$$

Equilibrium equations:

$$\frac{dV}{dx} = -q \qquad \frac{dM}{dx} = V - k_{eff} * \varphi$$

ODE:

$$EI\frac{d^4w}{dx^4} - k_{eff}\frac{d^2w}{dx^2} = q$$

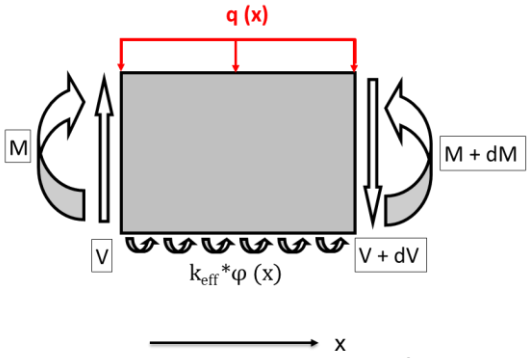

Figure 4-5: Small-element determination of initial model

Where:
$\boldsymbol{\varphi}$: Beam angle at location x [-]

$\boldsymbol{w}$: Beam deflection at location x [mm]

$\boldsymbol{\kappa}$: Beam curvature at location x [mm^{-1}]

$\boldsymbol{M}$: Moment in individual concrete wythe at location x [Nmm]

$\boldsymbol{EI}$: Rotational stiffness of individual concrete wythe [Nmm^2]

$\boldsymbol{V}$: Shear force in individual concrete wythe at location x [N]

$\boldsymbol{q}$: Distributed load over beam [N/mm]

$$k_{eff} = G_{inter} * b * \left(\frac{t_i + t_c}{t_i}\right) * \frac{1}{2} t_c$$

$\boldsymbol{k_{eff}}$: Effective stiffness of the intermediate layer [N]

This model has been put into calculation-software Maple, in order to find the displacement field, and compare the results to FE-models. Initially, some results without truss connectors seemed promising. However, the application of truss-connectors resulted in the analytical model to heavily over-estimate the stiffness of the PCSP, to the point where these models were much stiffer than a fully composite floor. When checking the applied forces on the concrete wythes, it seemed that the additional axial forces would cause the wythes to significantly compress in the axial direction. As such, it can be assumed that the axial displacement needs to be accounted for in the analytical model.

The updated mechanical model is shown in Figure 4-6. The same considerations as the initial model hold, although now axial displacements of the individual wythes is included. On top of this change, it was considered that it was easier to work with the reaction-force from the intermediate layer if it was modelled as a force instead of a bending moment.

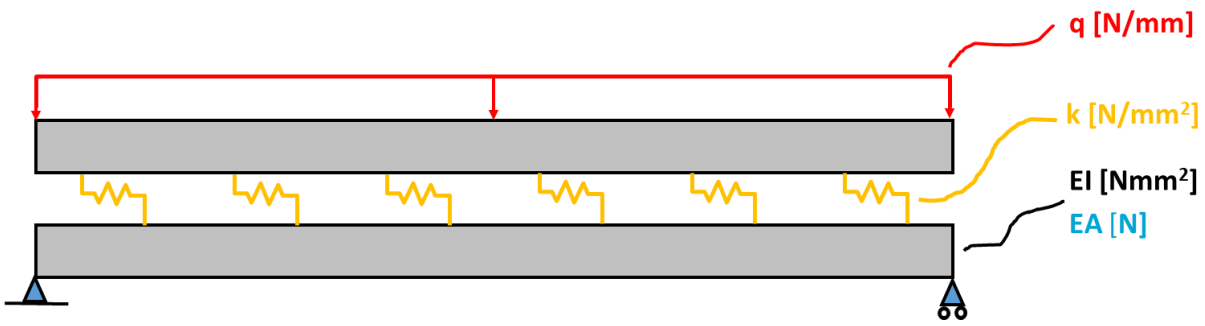

Figure 4-6: Updated mechanical model, including axial compression

This change of the mechanical model also changes the method of calculating the shear strain in the intermediate layer. The axial displacement of the individual concrete wythes reduces the total difference of the axial displacement between the concrete wythes and the intermediate layer. An adjusted version of Figure 4-2 is given in Figure 4-7. For visualisation purposes, the intermediate layer is not connected to the concrete wythe. In reality, the intermediate layer is connected to the edge of the concrete, and is the cause for the forces that cause an axial displacement in the individual concrete wythes $u_{x,t}$ and $u_{x,b}$. As such, the actual difference of the axial displacement between the layers can be calculated as follows:

$$\Delta u_{x,t,act} = \Delta u_{x,t,max} - u_{x,t} \tag{11}$$

Where:

$\Delta \boldsymbol{u}_{x,t,act}$: Actual difference of axial displacement between top concrete wythe and intermediate layer [mm]

$\boldsymbol{u}_{x,t}$: Axial displacement of the top concrete wythe due to the response of the intermediate layer [mm]

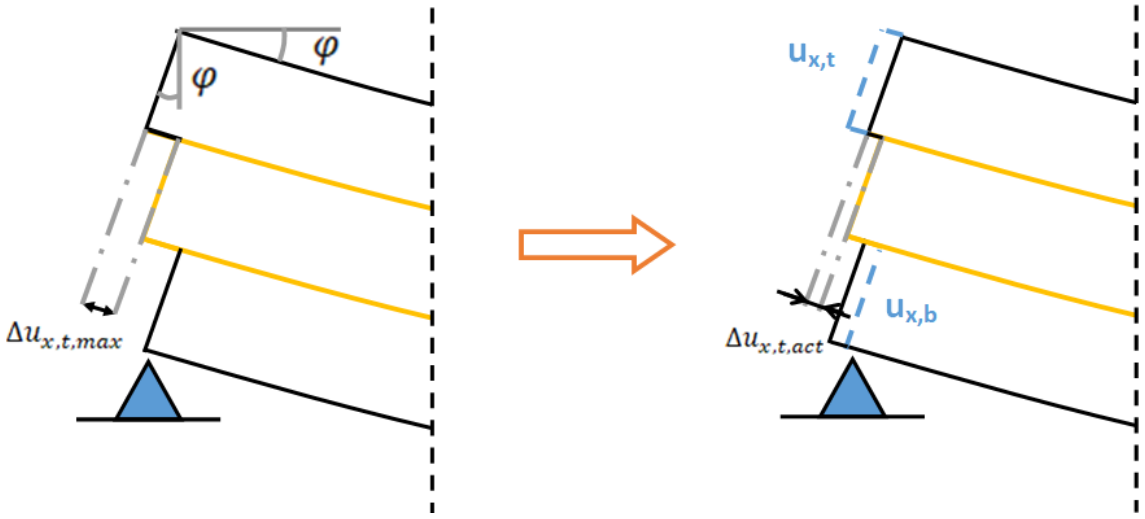

Figure 4-7: Change in determination of difference of axial displacement, by adding axial displacement of individual concrete wythes

The magnitude of the axial displacement in the individual concrete wythes depends on the stiffness of the intermediate layer. Different methods were developed to include this behaviour in a Maple model, but none were successful. When the reduction-effect was included in the equations, this caused the solution of the ODE to contain imaginary numbers. As such, it was decided to change the approach from ODEs and Maple to an analytical model developed in Microsoft Excel.

In the developed Excel-model, a calculation-process is followed to determine the composite factor of the PCSP-design set as input. This process, only including the most important calculation-steps, is shown in Figure 4-8. Although some values are based on estimations from structural mechanics called "forget-me-nots" or via other simplified methods, the determination of the actual difference between the axial displacement is relatively complicated. Both the simplified and complicated equations will be explained.

Before the different calculation-methods can be explained, some global assumptions and considerations have to be mentioned. Firstly, the analytical model in Excel is developed as a deflection-controlled model. This means that the assumed deflection of the PCSP is fixed for the entire calculation, while the additional response due to the intermediate layer is calculated afterwards. Additionally, even though the PCSP-structure is only partially-composite, it is assumed that the floor possesses a constant bending stiffness over the entire length. With this assumption, the forget-me-nots can be used to calculate certain parameters with simple expressions.

Initial input

In order for the model to function, some input is required from the user. This input covers the dimensions and stiffnesses of all applied materials. On top of this, the applied load is also required to set an initial assumed deflection in the model.

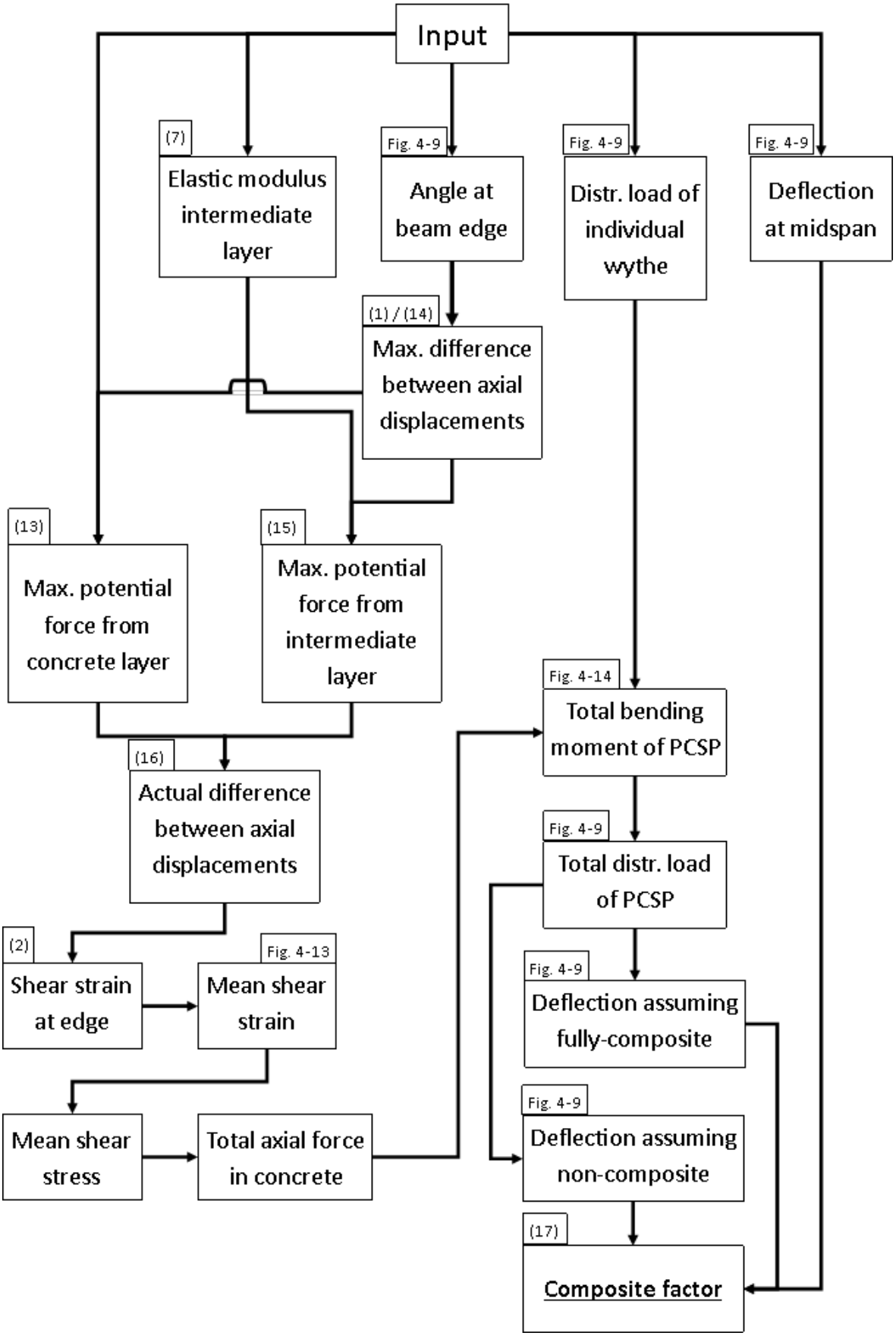

Figure 4-8: Flow-chart for calculation composite factor

Starting values

To start off the calculation, an initial deflection at midspan is assumed based on the load, as well as the deflection-values for a fully- and non-composite structure of the same dimensions, as calculated with Figure 4-9. Initially, a composite factor of 0.5 is assumed, taking the mean of both deflections. This deflection at mid-span is then used to calculate the other two starting values using forget-me-nots: the distributed load for one concrete wythe and the angle at the edge of the beam. The distributed load at the edge is used to determine the bending moment-part of the individual concrete beams. The angle at the edge of the beam is used to calculate the maximum potential difference between the axial displacements between the layers. This is the parameter that will be used in the next part.

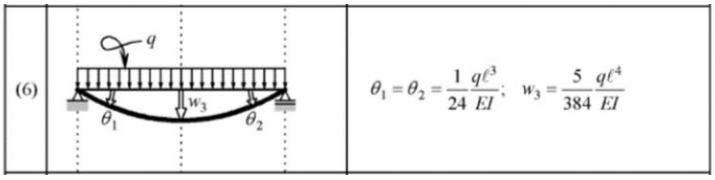

Figure 4-9: Forget-me-nots for a simply supported beam with a distributed load

Difference between axial displacements

Based on the beam-angle at the edge, the maximum potential difference between axial displacements between layers can be determined, as shown in Figure 4-2. However, as axial displacement of the individual concrete wythes is included in this calculation, the actual difference is lower than this maximum value. The method for calculating this value is explained in this part.

Essentially, two extremes can be calculated:

- When the entire difference in axial displacement is accounted for in the intermediate layer ($G_{inter} \ll E_c$)
- When the entire difference in axial displacement is accounted for in the concrete layer ($G_{inter} \gg E_c$)

These situations are also visualised in Figure 4-10. In both extreme situations, the maximum potential difference $\Delta u_{x,t,max}$ is equal to the value measures in each extreme situation.

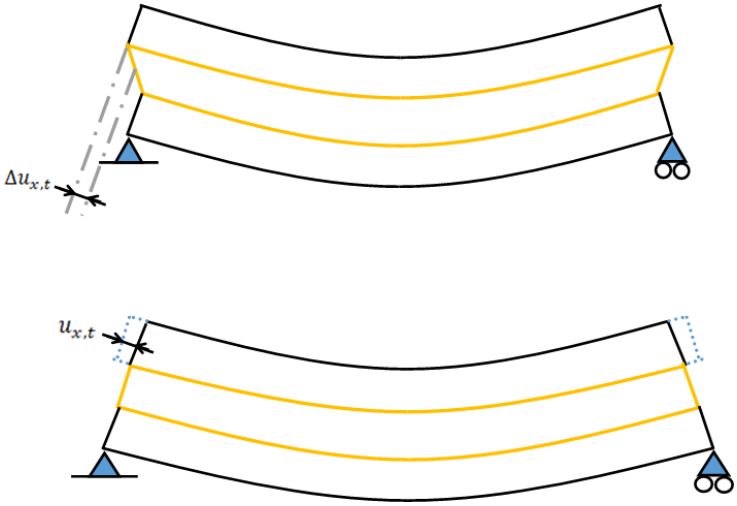

Figure 4-10: The two extremes in calculating the actual difference in axial displacement between the PCSP-layers

In reality, the answer lies somewhere in-between, where the difference in axial displacement is accounted for by both layers partially. However, these extremes can be used to calculate the actual difference in axial displacement. When, for example, the situation is assumed where the axial displacement is fully accounted for in the intermediate layer, it can be said that the concrete layer is not strained at all. If no strain occurs, the resulting axial force in those elements is zero. The same can be said for the other way around. At the same time, if it is assumed that the intermediate layer fully accounts for the strain, this full strain can be used to calculate the maximum response of the intermediate layer due to the difference in axial displacement. A graph showing this calculation method is shown in Figure 4-11.

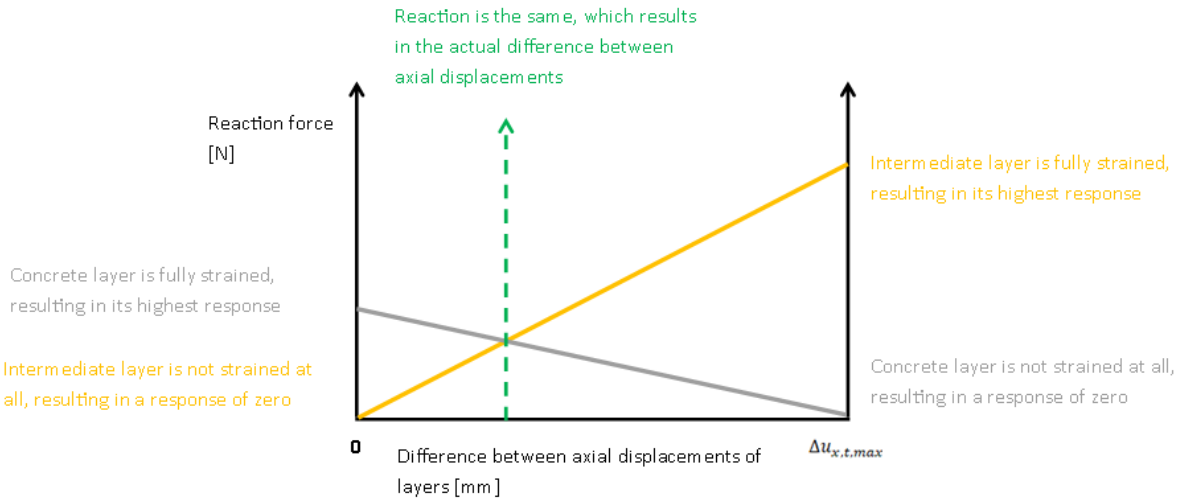

Figure 4-11: Explanation of the calculation-method of the actual difference between axial displacements

Now that the method of finding the actual difference between axial displacements is found, these extreme values must be calculated.

For the determination of these extreme values, some estimations are done. These estimations are based on the previously-developed Maple- and FE-model, that were still useful with the goal to find estimations based on given parameters. Throughout this calculation, it is also assumed that the response from the intermediate layer is immediately loaded onto the centre-line of the concrete wythe, as shown in Figure 4-12. As such, the response from the intermediate layer results solely in an axial displacement.

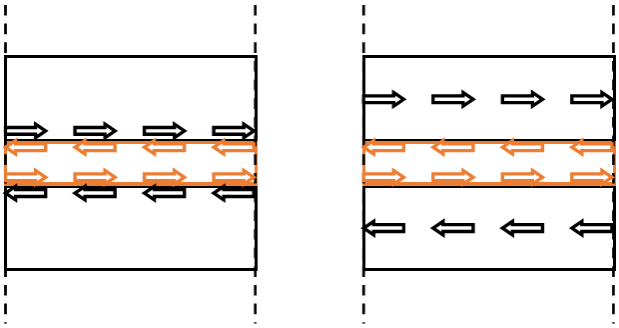

Figure 4-12: Realistic interaction between intermediate layer and concrete (left) and assumed behaviour (right)

For the calculation of the maximum response of the concrete layer, the following valid estimate was found in Maple between the axial displacement at the outer edge and the strain at mid-span:

$$\varepsilon_m \approx 3 * \frac{u_{x,edge}}{l} \tag{12}$$

Where:

$\boldsymbol{\varepsilon_m}$: Axial strain of concrete wythe at midspan [-]

$\boldsymbol{u_{x,edge}}$: Axial displacement of concrete wythe at edge [mm]

$\boldsymbol{l}$: Span length of beam [mm]

As the axial displacement at the edge is the variable of this calculation, and the strain at midspan is useful to find the total maximum response of the concrete layer, this is a perfect equation to use for this calculation. As such, the total maximum response from the concrete layer is as follows:

$$N_{c,max} = 3 * \frac{\Delta u_{x,t,max}}{l} * E_c * b * t_c \tag{13}$$

$$\Delta u_{x,t,max} = \frac{t_c + t_i}{2} * \varphi \tag{14}$$

Where:

$\boldsymbol{N_{c,max}}$: Maximum possible axial response from the concrete wythe [N]

$\boldsymbol{\Delta u_{x,t,max}}$: Maximum difference in axial displacement between the bottom edge of the concrete layer and the top edge of the intermediate layer [mm]

$\boldsymbol{E_c}$: Elastic modulus of concrete layer [N/mm²]

When calculating the maximum response of the intermediate layer, a similar estimate was found using the FE-model in DIANA. When plotting the shear strain of the intermediate layer over the span length as shown in Figure 4-13, it can be seen that the strain is not behaving linear over the span length. As an intermediate solution, the mean has been calculated over the full span, which is equal to 0.57 of the value at the edge of the beam. As such, the total maximum response from the intermediate layer is as follows:

$$N_{inter,max} = 0.57 * G_{inter} * \frac{\Delta u_{x,t,max}}{\frac{1}{2} t_i} * b * \frac{l}{2} \tag{15}$$

Where:

$\boldsymbol{N_{inter,max}}$: Maximum possible shear response from the intermediate layer [N]

$\boldsymbol{G_{inter}}$: is the elastic shear stiffness of the intermediate layer and calculated following Equation 4 to 8 [N/mm²]

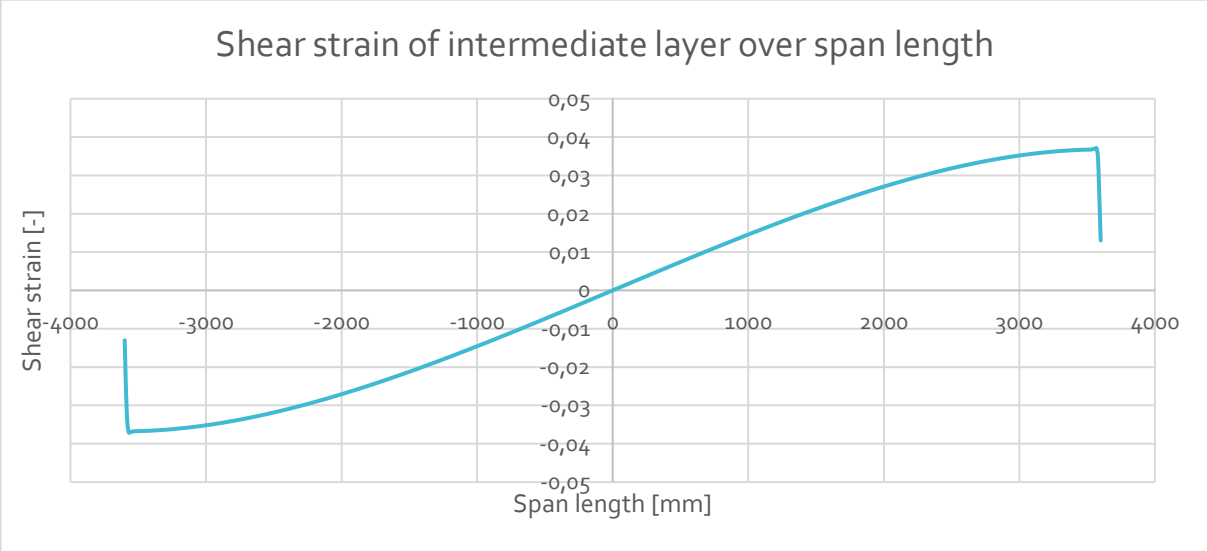

Figure 4-13: Shear strain of the intermediate layer over the span length of a FE-model

Finally, in order to find the actual difference between the axial displacements of the PCSP-layers, the following equation can be solved, to find the value which is shown with the green line in Figure 4-11:

$$\Delta u_{x,t,act} = \frac{N_{c,max}}{N_{c,max} + N_{inter,max}} * \Delta u_{x,t,max} \tag{16}$$

Where:

$\boldsymbol{\Delta u_{x,t,act}}$: Actual difference of axial displacements of concrete wythe and intermediate layer [mm]

Finding the total axial force

Now that the actual difference of axial displacements at the edge is found, the next step is to find the total axial force that is present in the concrete wythes. The shear-strain at the edge is calculated by dividing $\Delta u_{x,t,act}$ over the thickness of the intermediate layer as shown in Equation 2. Then, the assumption from Figure 4-13 is used to find the mean shear-strain over the entire length of the beam. From here, the stress and the total axial force can easily be calculated using Equation 15 and simple mechanics-rules.

Determining the total bending moment and composite factor

Combining the individual bending moments from the initial steps of the calculation, together with the couple of axial forces from the wythes as shown in Figure 4-14, the total bending moment can be determined.

Using the equation $M = \frac{1}{8}ql$, this bending moment can be translated back into a distributed load. This distributed load is then again used to find the mid-span deflection for a fully-composite and non-composite assumption using the forget-me-nots from Figure 4-9. The initially assumed deflection is compared to these values to find the composite factor as follows:

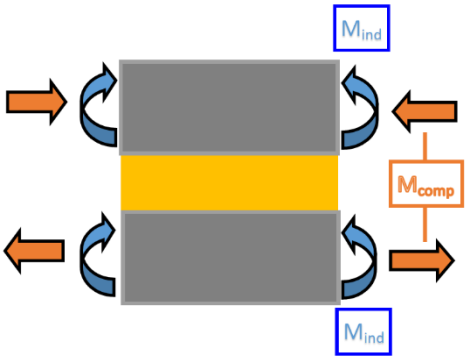

Figure 4-14: Schematisation showing combination of individual moments and composite moment

$$CF = \frac{w_{as} - w_{non}}{w_{full} - w_{non}} \tag{17}$$

Where:

$\boldsymbol{CF}$: Composite factor of the designed PCSP [-]

$\boldsymbol{w_{as}}$: Assumed deflection at mid-span at the start of the calculation [mm]

$\boldsymbol{w_{non}}$: Deflection at mid-span assuming a non-composite structure, loaded by the newly-calculated distributed load [mm]

$\boldsymbol{w_{full}}$: Deflection at mid-span assuming a fully-composite structure, loaded by the newly-calculated distributed load [mm]

4.2. Comparison-results between analytical- and FE-model

With the calculation-steps mentioned above, the behaviour can be correctly calculated. All comparisons have shown almost perfect results. In Figure 4-15, comparisons between many different designs without truss-connectors can be found. In all of these comparisons, the maximum error between the mathematical- and FE-model is only a composite factor-difference of 0.02. When truss connectors are applied, the mathematical model from Excel still shows a perfect comparison with the FE-model as shown in Figure 4-16. The different designs compared in this figure are the same as Figure 3-49, which each show a clear different behaviour per design. As the analytical model is able to fully predict the linear behaviour of PCSPs, this Excel-file is edited and cleaned up, so that practical use is easier. This updated model can be found and is explained in Appendix 0.

Because the analytical model perfectly follows the behaviour of the linear FE-model, the conclusions about the influence of certain parameters on the composite factor at the end of Section 3.4 are also still valid here to the exact same extent. However, the knowledge-requirements for this analytical model are much lower than in the case of the FE-model. As such, this model can be used very broadly by people without much in-depth knowledge about the behaviours of these types of floors. On top of this, results from this model are acquired much quicker. Even in the case of a linear FE-model, a calculation still takes some seconds to fully finish. The analytical Excel model immediately shows you the results.

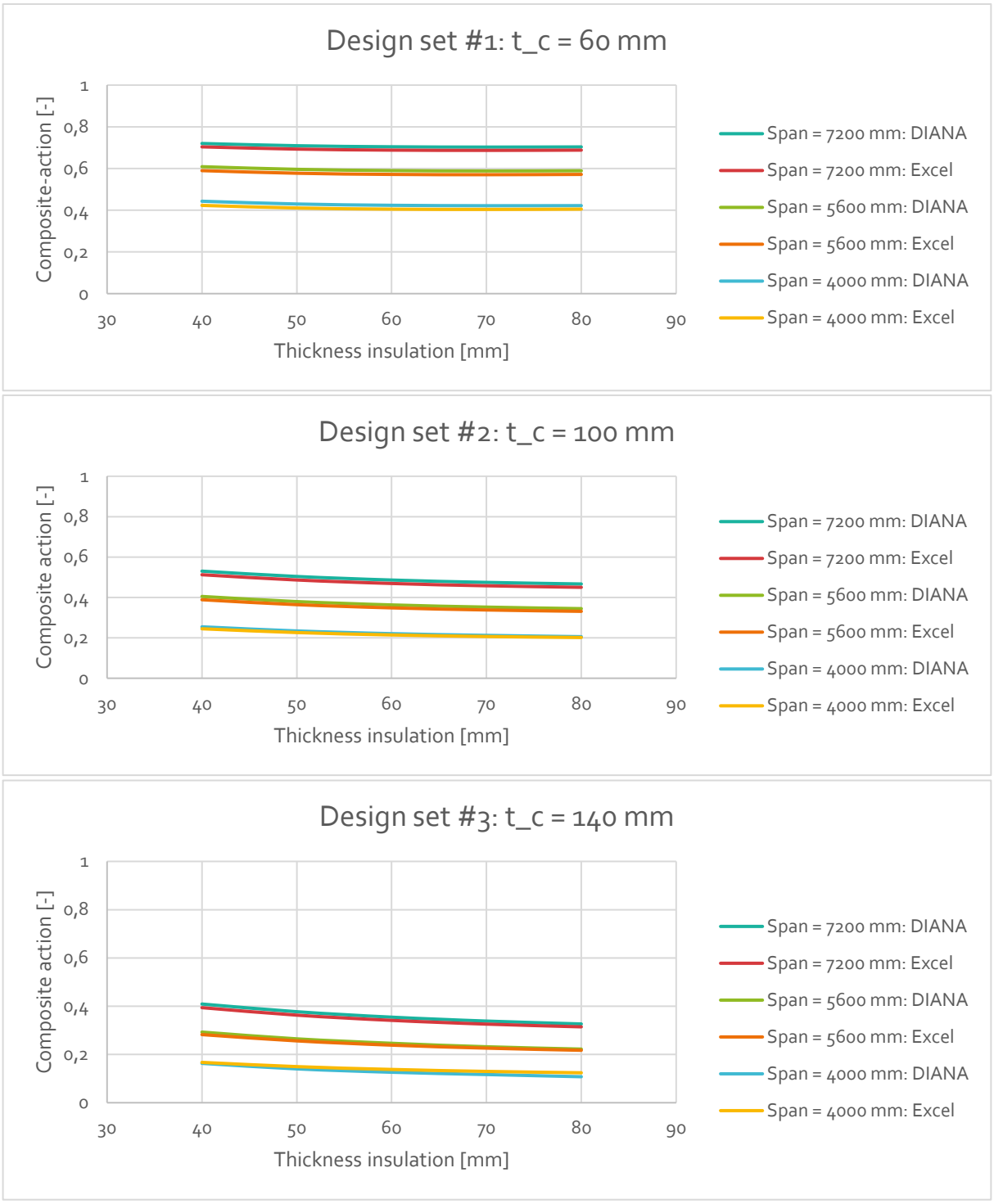

Figure 4-15: Comparison between mathematical- and FE-model: no trusses

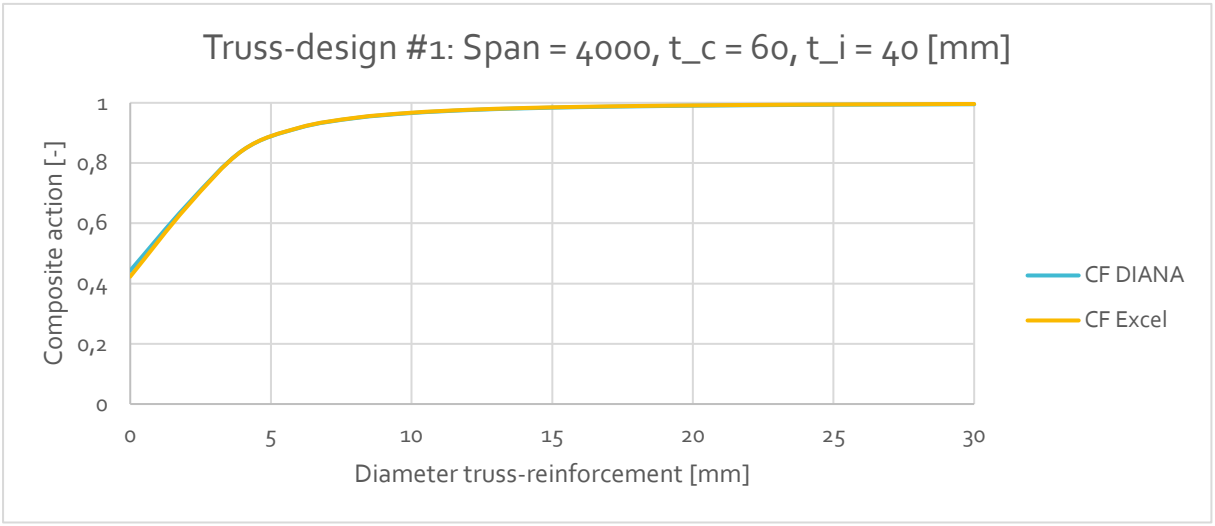

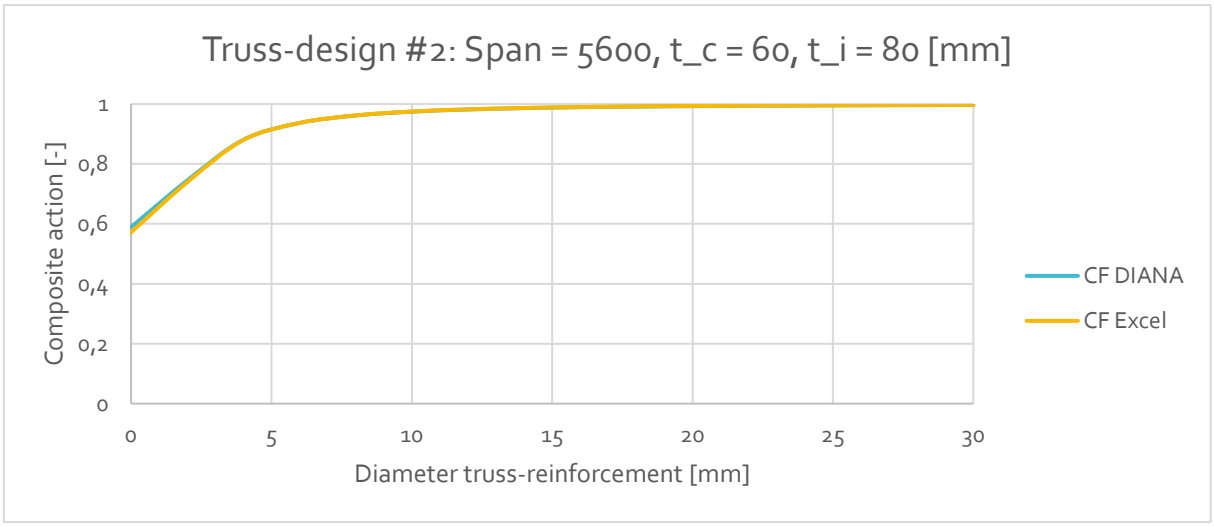

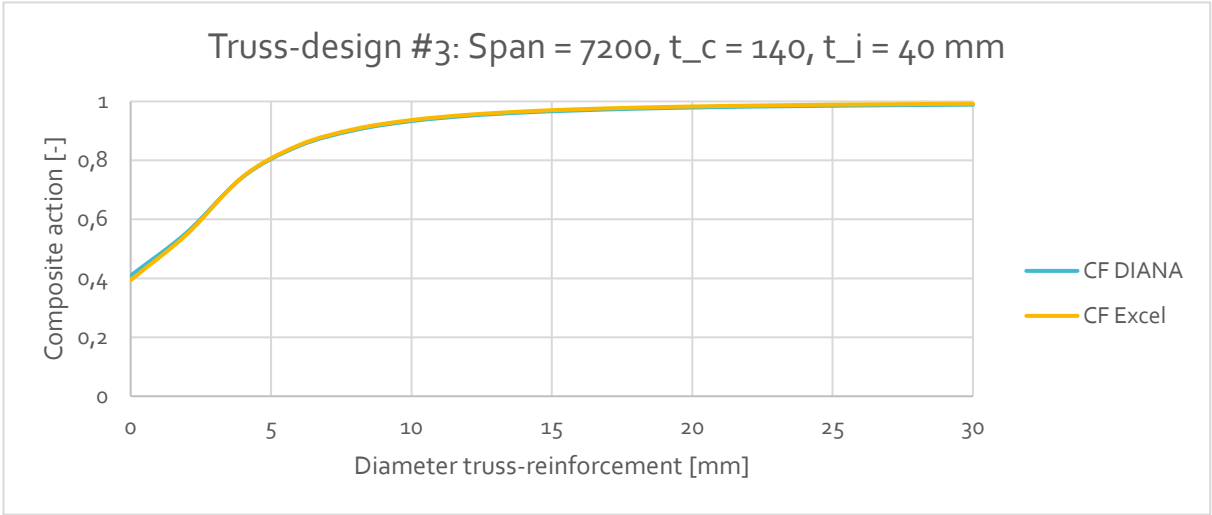

Figure 4-16: Comparison between mathematical- and FE-model: trusses

4.3. Discussion on influence of main input-parameters

As mentioned in Section 4.2, as the FE-model and analytical model behave almost identical, the insights gained from the FE-model are also applicable to the analytical model: Increasing the concrete thickness of the PCSPs from 60 to 140 mm would decrease the composite factor for a value of around 0.28. Increasing the span length from 4000 to 8000 mm would increase the composite factor for around 0.31. The effect of increasing the insulation thickness from 40 to 80 mm depends on the concrete thickness, where the reduction of the composite factor is 0.02 and 0.06 for a concrete thickness of 60 and 140 mm respectively. When truss-connectors are applied, most PCSP-designs will possess a composite factor of above 0.95 when 12 mm diameter bars are being used every 800 mm. However, when concrete wythes with a thickness of 140 mm or higher are being used, the increase in composite-action due to the application of trusses decreases significantly, causing a decrease in composite factor from 0.96 to 0.91 compared to when 140 mm and 60 mm wythes are used respectively.

Next to the composite factor, additional output is given by the analytical model in the form of stresses. The influence of the main parameters on these stresses has been analysed. A fixed design was developed of which the values can be found in Figure 4-17, where the following parameters were varied:

- Concrete thickness: 60 mm – 140 mm
- Span length: 4000 mm – 8000 mm
- Diameter truss-connector: 0 mm – 30 mm

CALCULATION-INPUT

Span length:	5600	mm	Truss diameter:	4	mm
Width (c.t.c.):	800	mm	Truss stiffness:	200000	N/mm^2
Concrete thickness:	100	mm			
Insulation thickness:	40	mm	Applied load:	10	N/mm
Concrete stiffness:	31000	N/mm^2			
Insulation stiffness:	5	N/mm^2			

Figure 4-17: Fixed design for parameter-study of analytical model

This means that if the concrete thickness is varied from 60 to 140 mm, the span length and truss-diameter are fixed at 5600 mm and 4 mm respectively. For each of these varied parameters, three different outputs are visualised:

- The concrete stress at the bottom edge of the lower concrete wythe;
- The concrete stress at the bottom edge of the upper concrete wythe;
- The truss-connector stress at the edge of the beam.`

The results when the concrete thickness is varied can be found in Figure 4-18. Because increasing the concrete thickness also increases the bending stiffness of the individual wythes, the stress of the bottom edge of the lower concrete wythe is reduced as seen in Figure 4-18a. As is known from previous insights, increasing the concrete thickness lowers the composite factor. This is also present in Figure 4-18b, where the stress from the bottom edge of the upper wythe changes sign, resulting in a tension-stress in this wythe. With high composite factors, the entire upper wythe would be in compression. When analysing Figure 4-18c, it can be seen that the stress in the truss-connectors is reduced linearly. This is related to the reduction of the composite factor: if the cooperation between both concrete layers is reduced, less loads are required to be transferred by the truss-connectors to the individual wythes.

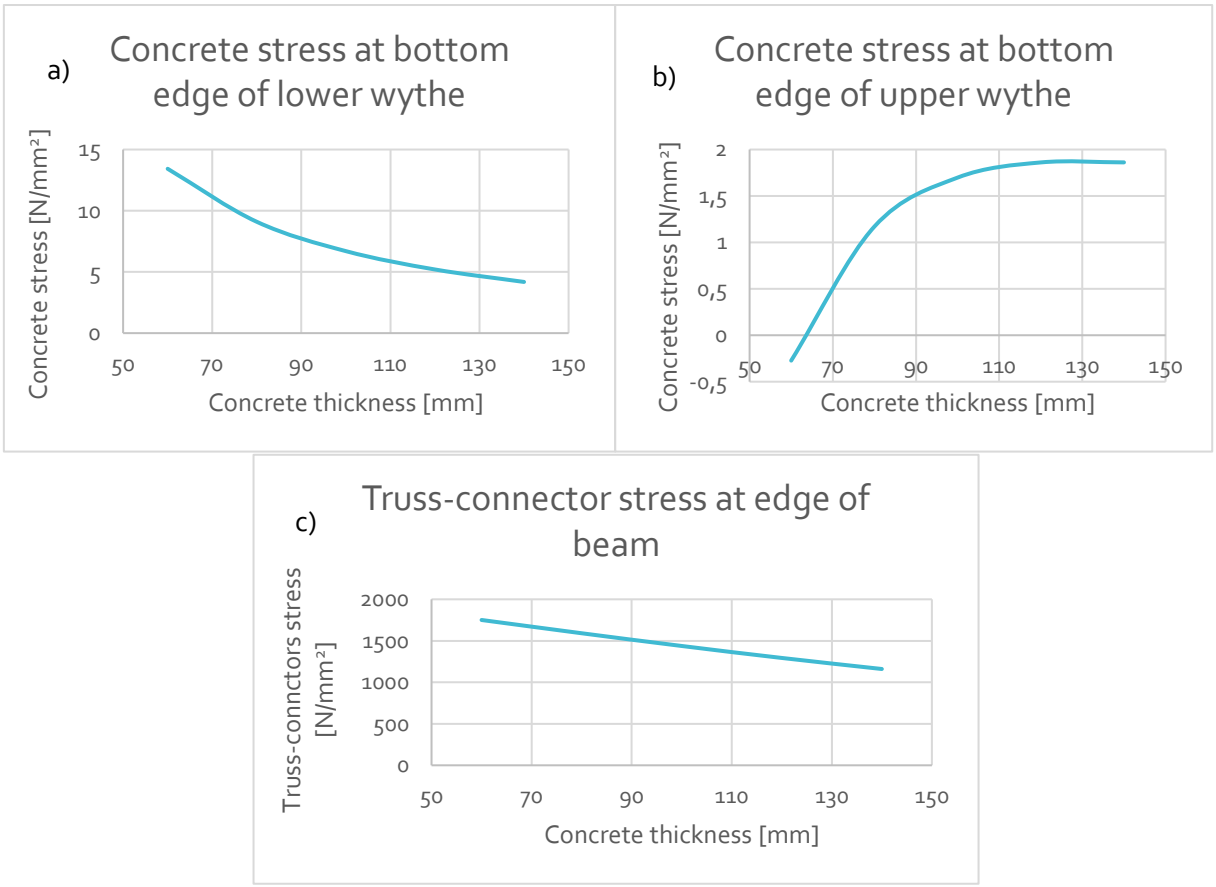

Figure 4-18(a-c): The concrete stresses at the bottom edges of both concrete wythes and the truss-connector stress at the edge of the beam when the concrete thickness is varied

In Figure 4-19, the results are shown for when the span length in varied. As the bending moment at midspan is based on $M = \frac{1}{8} q l^2$, the concrete stress at the outer edges would increase quadratically in the case of a solid element. However, as can be seen in Figure 4-19a, doubling the span length only increases tensile stress at the outer edge of the PCSP by a factor of around 3. This is caused by the increase of the composite factor, reducing the required individual bending of the wythes. This can also be seen in Figure 4-19b, where the stresses in the inner edge of the concrete wythes is reduced when increasing the span length. This hints towards the fact that the added compression force due to the composite effect is higher than the added tension force due to the higher present bending moment. Because both the bending moment at midspan and the composite factor increase when the span length is increased, the stress in the truss-connectors also increase, as can be seen in Figure 4-19c.

Figure 4-20 shows the stresses in concrete and truss-connectors when the diameter of the truss-connectors increase. All of these figures show a clear presence of an asymptote. The asymptotes of Figure 4-20b and Figure 4-20c are in line in a fully composite structure, where the strains are linear through the thickness of the structure. The decrease of the truss-connector stress in Figure 4-20c is logical, as an increase of cross-section area will reduce the total stress on such an element. However, this reduction is not as steep as it would be in a conventional design: an increase of truss-connector diameter increases the composite factor, which in turn increases the force that is required to travel through this intermediate layer. As such, the truss-connector stress is not exactly inversely proportional to the square of the truss-connector diameter.

The analytical model and its gained insights can be used for the Reinbouw project of Lievense | WSP. However, a more detailed analysis of this project must be done first before the model can be used.

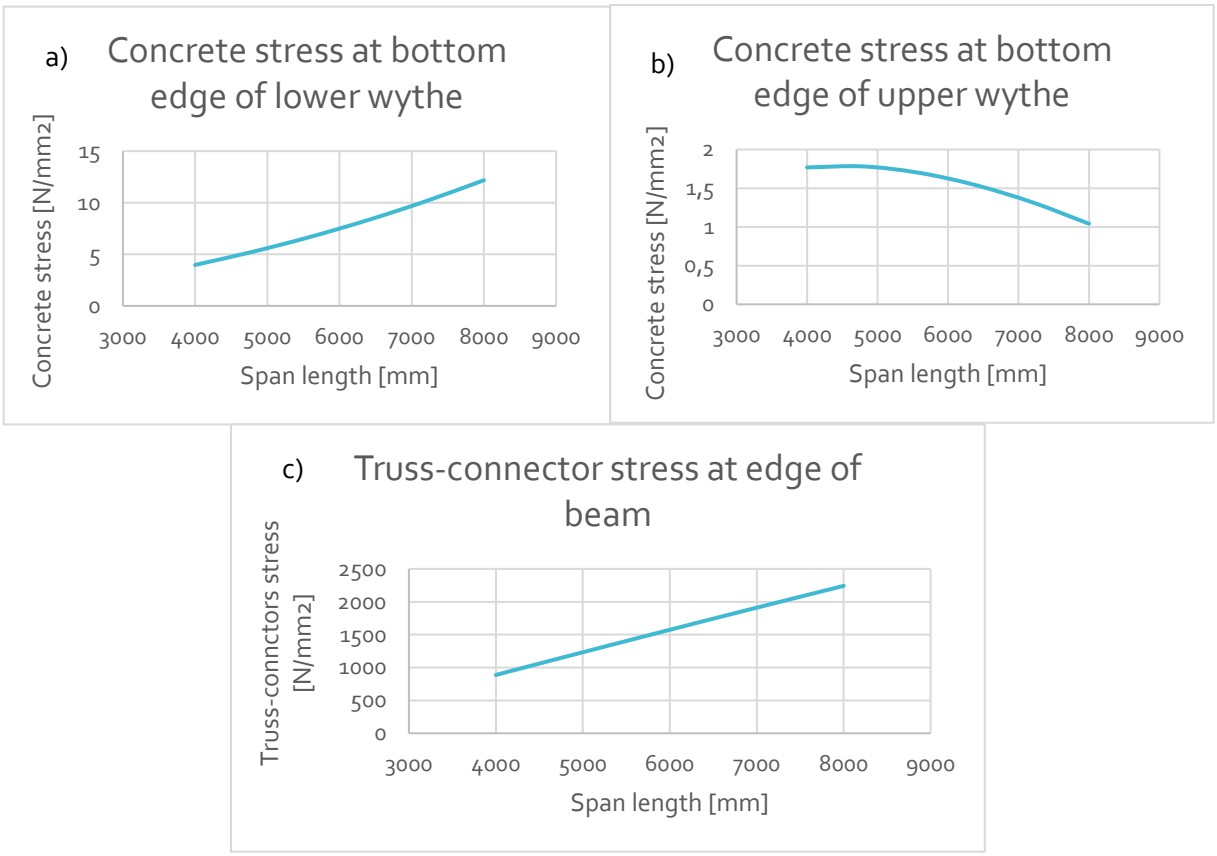

Figure 4-19(a-c): The concrete stresses at the bottom edges of both concrete wythes and the truss-connector stress at the edge of the beam when the span length is varied

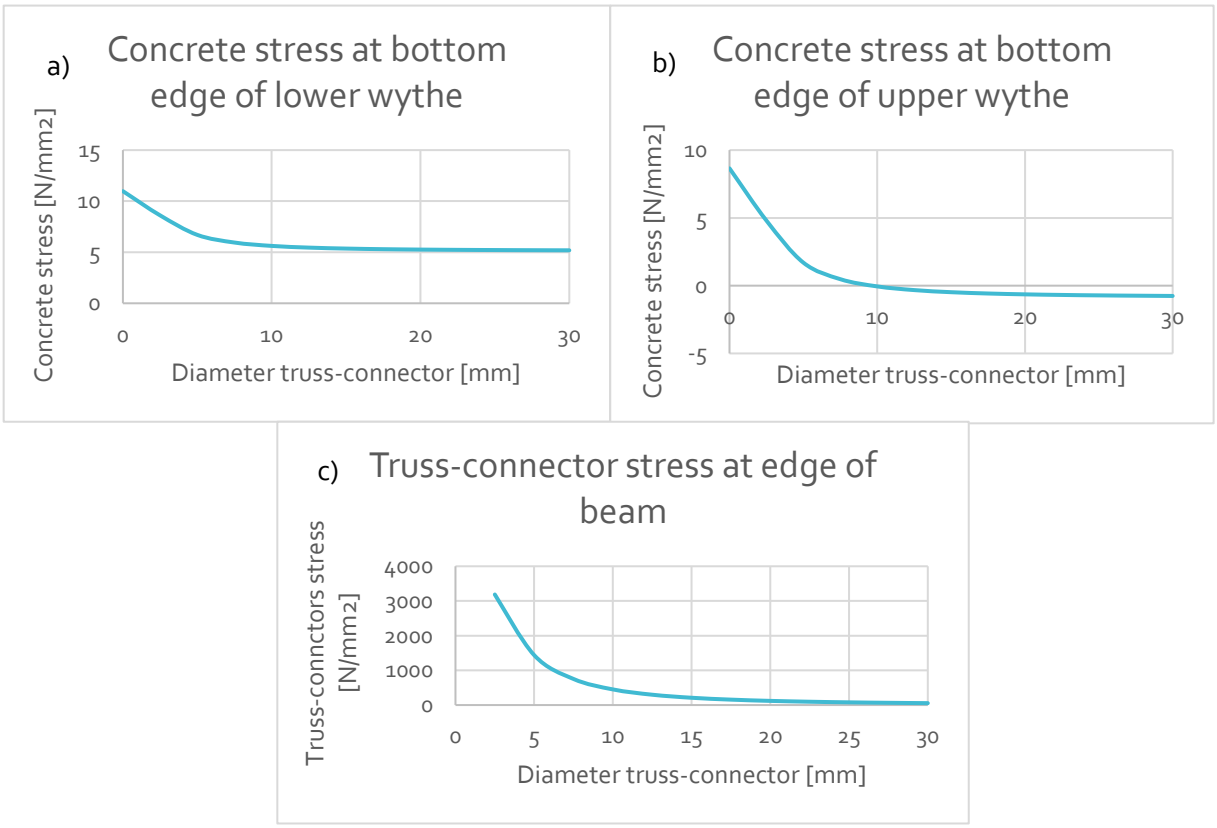

Figure 4-20(a-c): The concrete stresses at the bottom edges of both concrete wythes and the truss-connector stress at the edge of the beam when the truss-connector diameter is varied

5. Case study Lievense | WSP

5.1. Determination of flow of forces in design

As mentioned in Section 1.1 and 2.1, many unusual forces act on the completely prefabricated building. In order to understand what type of forces will be applied to the floor-elements, an analysis of the flow of forces is done on the entire structure. This is also useful, as insight will be gained on where the bottlenecks of the structure are. The case study assumed the concept to have five apartment-units in width, five apartment-units in height, with an additional ground floor for a shopping area underneath.

While most forces have identical flow of forces – for example, permanent and variable load on floors – some other loads in the same direction are applied differently, as is the case with wind-load and skewness of the columns. The different applied forces are as follows:

- All vertical loads
- Horizontal skew load
- Horizontal wind load
- Balcony forces

Vertical load

A top-view of the building is shown in Figure 5-1. In this figure, arrows are drawn to show the flow of forces from the floors to the load-bearing walls. In the case of the unit-elements, the floors function as a two-way slab (green), as the floors are connected to relatively stiff walls along the span. All other floors are considered as a one-way slab (orange), where loads are directly transferred to the walls at the supports. The only exception is the gallery-floor, where the floor-loads are transferred to a steel beam, which in turn transfers it to both the (lower) steel columns and (upper) timber walls (yellow).

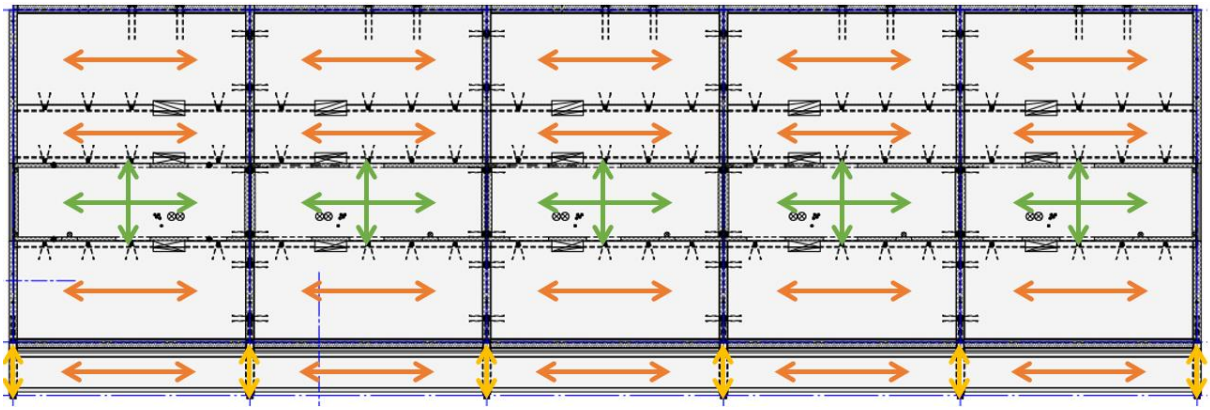

Figure 5-1: Flow of forces horizontal loads top-view

A side-view of the lower part of the building is visualised in Figure 5-2. From the walls, the forces have to be transferred through the ground floor-columns to the foundation (orange). On top of that, there are also permanent loads from the walls in the long direction of the building (yellow). While some of the forces can be directly transferred to the columns and foundation, most loads must be transferred through the lower beam by means of shear forces. From the columns in this figure (green), the loads are transferred to foundation piles. This complete flow of forces already shows initial insight into which pile-foundations require the largest stiffness to result in an equal sagging, as most of the loads will flow to the middle column. When the quantitative loads have been calculated, a more detailed foundation lay-out can be set-up.

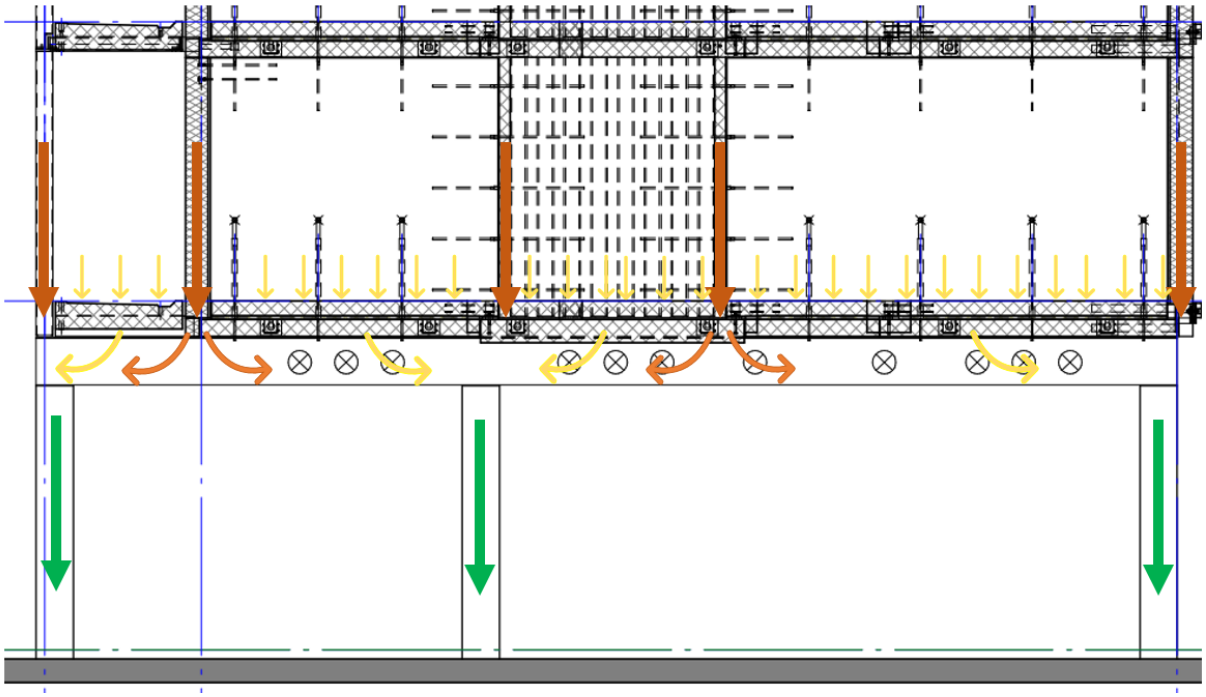

Figure 5-2: Flow of forces horizontal loads side-view

Horizontal skew load

Due to imperfections, walls will never be placed entirely straight. However, this skewness can result in forces in the horizontal direction, as the compression forces in the walls will also push sideways. These forces will be immediately transferred to the floors and result in a horizontal deflection.

When looking at the top view of the ground floor shown in Figure 5-3, it can be seen that there are only three stability walls that protrude through the entire structure. Thus, all horizontal forces have to be transferred to these walls, as columns are not able to resist them. This is done by the floor-elements. However, the connection between intermediate floors is present in the top concrete wythes, while connections next to walls are present in the bottom wythe. This results in these horizontal loads to penetrate through the entire PCSP element, generating shear forces.

After the forces have been transferred to from the floor-elements to the walls, the walls shown in Figure 5-3 will resist the structure by a diaphragm-action, whereby the forces are transferred to the ground.

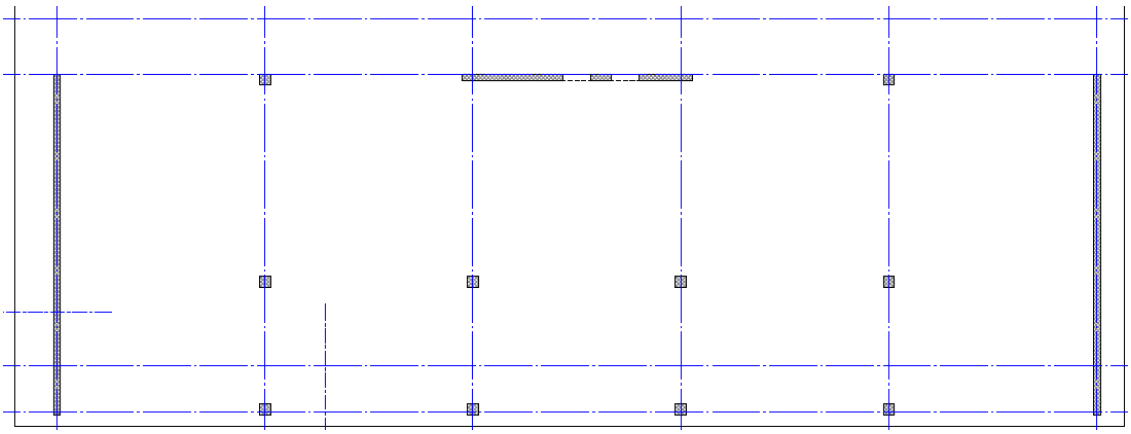

Figure 5-3: Diaphragm walls on ground floor

Horizontal wind load

When the wind blows against any of the sides of the structure, it is assumed the diaphragm effect of all walls will ensure that the apartment-floors will move as one unit. However, the bottleneck in the case of wind on the short direction can be seen in Figure 5-4. The unit-elements possess the only fixed wall in the structure, which in turn has openings for doors. This will result in very high shear stresses above the door-parts.

Afterwards, to resist the horizontal forces and deflection from the apartment-building, the same transfer is required as mentioned in the last section and Figure 5-3.

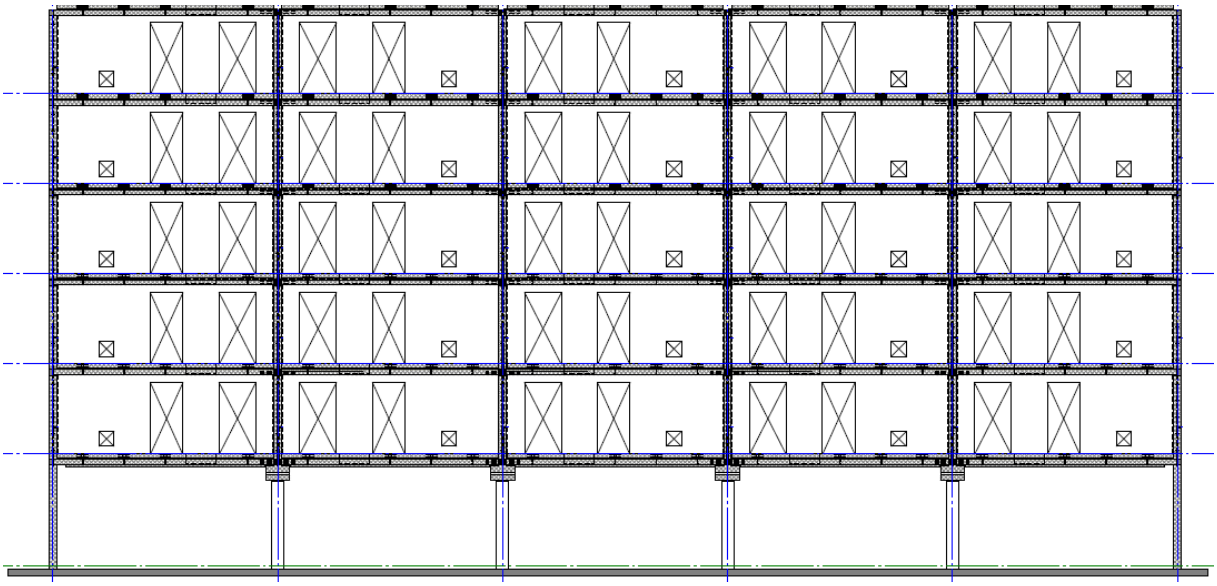

Figure 5-4: Structural bottlenecks during wind in short direction

Balcony forces

The loads present in the balcony cause both a vertical force that are resisted by the surrounding load-bearing walls like in Figure 5-2, and a moment that is resisted by the floor. The latter results in additional shear forces in the PCSPs.

Conclusion

The analysis from this section is required to gain insight in the global behaviour of the structure. Based on these flows of forces, the horizontal and vertical forces can be analysed. Due to complexity and time-restraints, the balcony forces will not be included in this global calculation.

Firstly, the vertical forces are determined by hand-calculations and Excel, and the required pile-foundations are found using Technosoft. These pile-foundations possess a certain relative moment-stiffness, which are important for the determination of the shear forces that protrude through the PCSPs. These are also calculated by hand-calculations. Lastly, the hand-calculations will be compared to a model made in SCIA, to check if initial assumptions like the rigid movement of the structure was correct.

5.2. Design of pile-foundation and determination wind-loads

In order to be able to apply the FE-model and potential simplified expressions to the Reinbouw project of Lievense, it must be known how the floor-elements will be loaded in the project. This section explains all calculations that have been done to determine the pile-foundations and shear-forces due to the wind-load, and the final results of these calculations. The full calculation procedure can be found in Appendix B. These calculations have been done under supervision of Lievense | WSP.

Determination of self-weight and design of pile-foundation

To start off the calculation, loads due to self-weight are determined. All self-weights are loaded on a simplified "beam"-structure, in the short direction of the structure. This "beam" includes the entire cross-section of the building, which means that the height of the fictitious beam is equal to the full height of all walls combined. Based on Figure 5-2, the self-weights are loaded on the beam as given in Figure 5-5. As can be seen, the floor-beam of the second floor is used as a reference-point for all loads. It is important to note that, while the forces are drawn of equal size in the figure, the magnitude differs for each of them. The resulting soil-deformations due to these loads are found by using Technosoft software. Based on trial-and-error, different designs are used for the pile-foundations, to find a lay-out that will result in the most equal sagging of the structure. This is essential for minimizing the bending moments and ensuring serviceability of the structure.

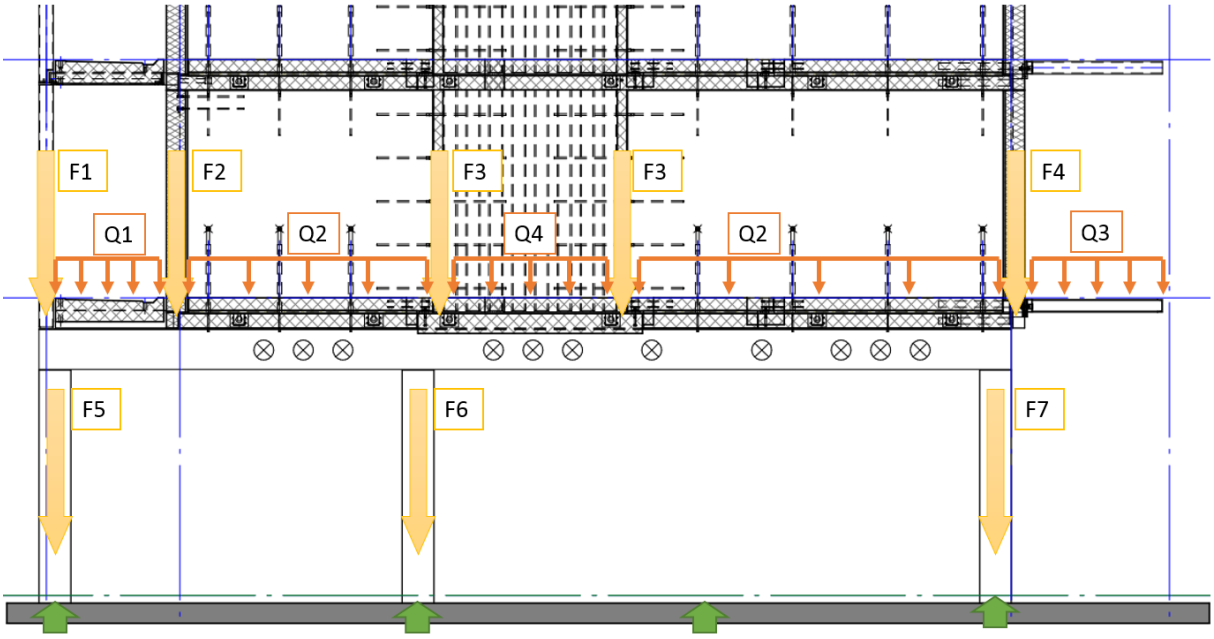

Figure 5-5: Lay-out of loads in cross-section on fictitious beam

As the values of the loads are different for the end and intermediate cross-sections, unique lay-outs have to be designed for each cross-section. The intermediate cross-sections also have two different lay-outs, due to the expectation that the stability-wall causes additional loads in the middle two cross-sections. The magnitude of these loads can be found in the full calculation in Appendix B. Finally, the global pile-foundation can be found in Figure 5-6, and the deflection-results and detailed lay-outs of each cross-section can be found in Figure 5-7 and Figure 5-8 for the inner and outer cross-sections respectively. In these last two figures, it can be seen that the deflections of both cross-sections are of a similar magnitude. This prevents the structure from having initial high shear stresses throughout the building. The stiffnesses and dimensions that are used for the concrete piles are default commercial values for square piles in SLS (Mink, Discussion about the Reinbouw mid-rise project, 2019).

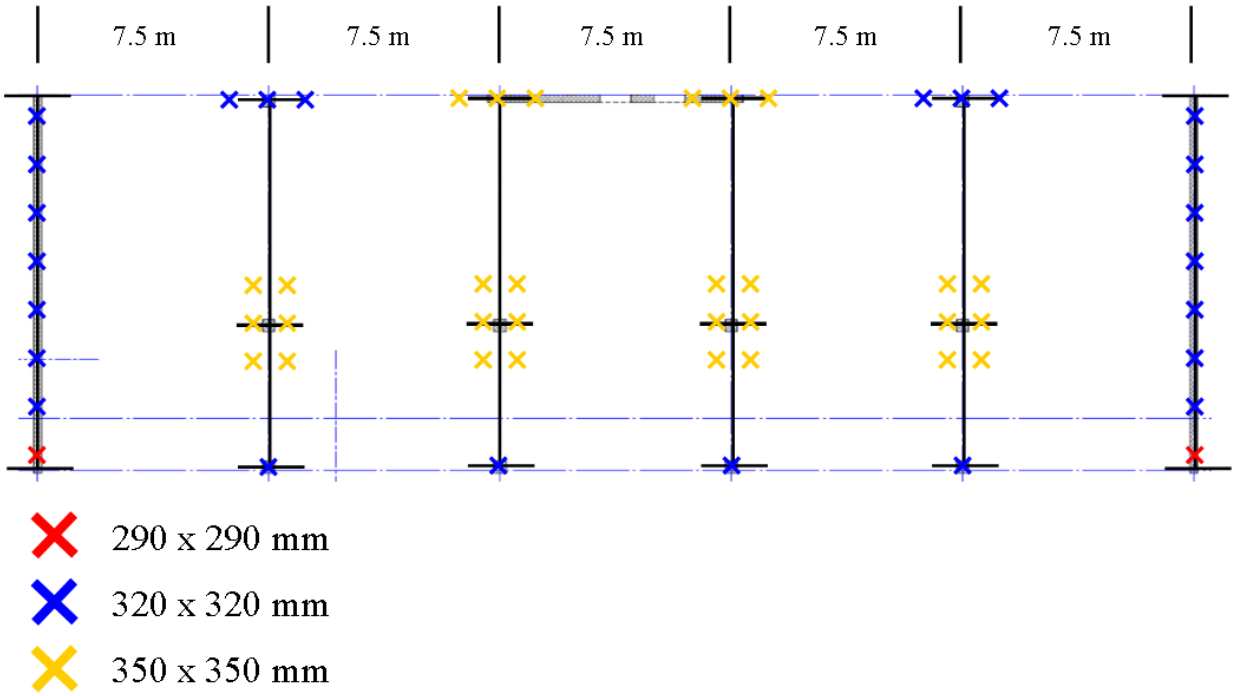

Figure 5-6: Pile-foundation full building including pile-dimensions

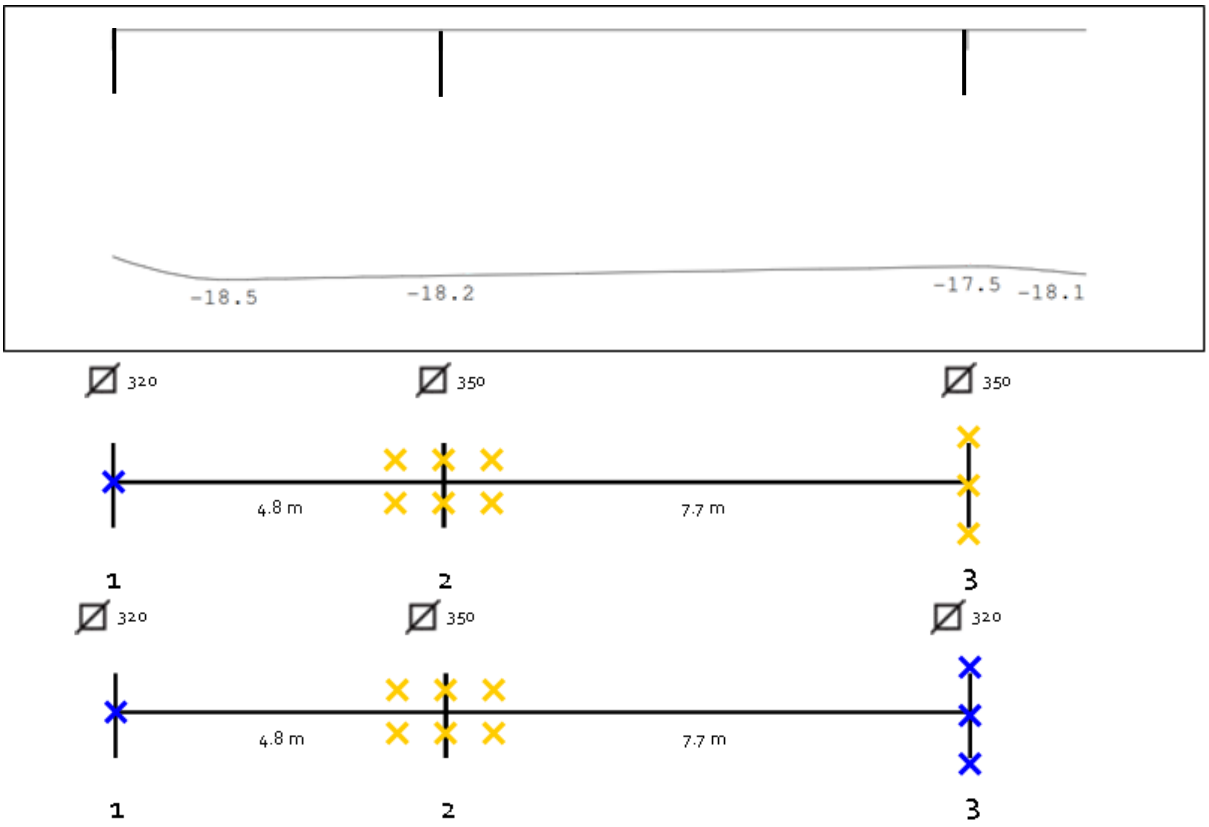

Figure 5-7: Deflection inner cross-section (top) including detailed lay-out strengthened and normal internediate cross-section (middle and bottom, respectively)

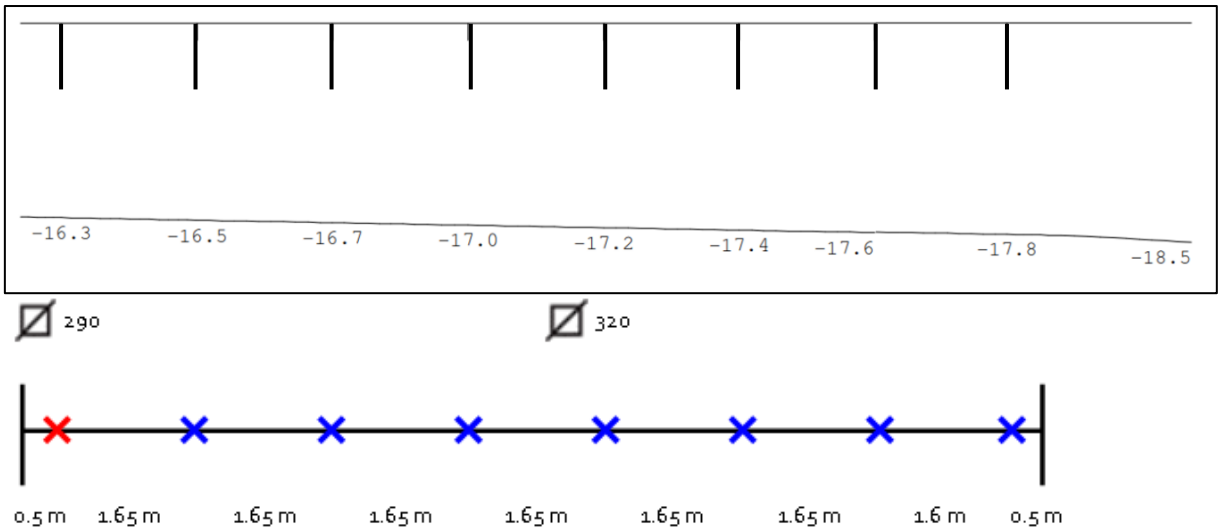

Figure 5-8: Deflection outer cross-section (top) including detailed lay-out outer cross-section (bottom)

Determination shear forces

When wind blows against the long side of this structure, the complete load has to be transferred to the two end-walls, as they also function as stability-walls. However, bending moments will initially still occur in the intermediate cross-sections. As the columns on the ground floor cannot resist any horizontal forces, the bending moment to resist the wind load must already be acquired at the end of the first floor. This means that additional shear forces must be present in the upper floors to gain this additional bending moment. The magnitude of these shear forces are calculated in this part.

The stiffness of each foundation cross-section was determined, because the wind load that each of the cross-sections will resist are determined by the relative stiffnesses of these foundations. The specific magnitude of the wind load and load due to skewness can be found in Appendix B. In the determination of the shear forces, it should be noted that the resulting shear forces should be zero throughout the ground floor, due to the columns not able to resist any of these forces. Based on these equilibriums, the shear forces can be determined by hand-calculations. An example of how these balances are calculated are given in Figure 5-9. Firstly, the shear forces due to wind-load are resisted directly, which is shown on the left side. On the right side, additional shear forces must occur in the floors due to the required increased bending moment in the upper floors. These forces must result in a pure bending effect of an identical magnitude that would usually occur in the ground floor of the structure.

The final shear force results are given in Figure 5-10 and Figure 5-11. While the shear-loads could be based on a linear reaction for the wind loads, a response from a construction like this might also result in a quasi-linear reaction. These results will be used to compare the hand-calculations to the SCIA-model. Based on SCIA, it can be checked if the original assumption of the building moving as one unit was correct, and if the floors show either linear or quasi-linear behaviour in shear.

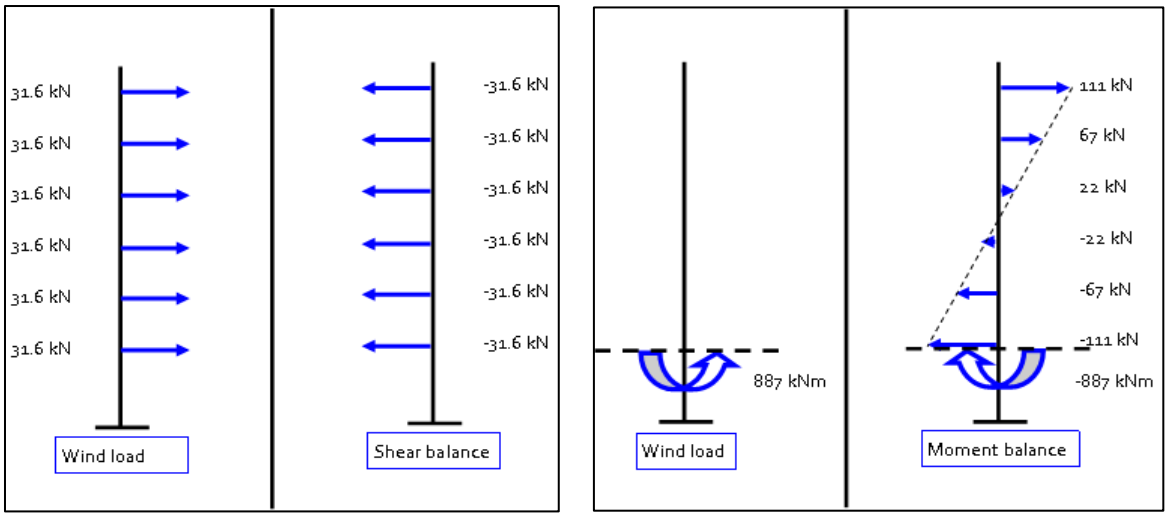

Figure 5-9: Balance forces based on shear and moment equilibriums for the wind load

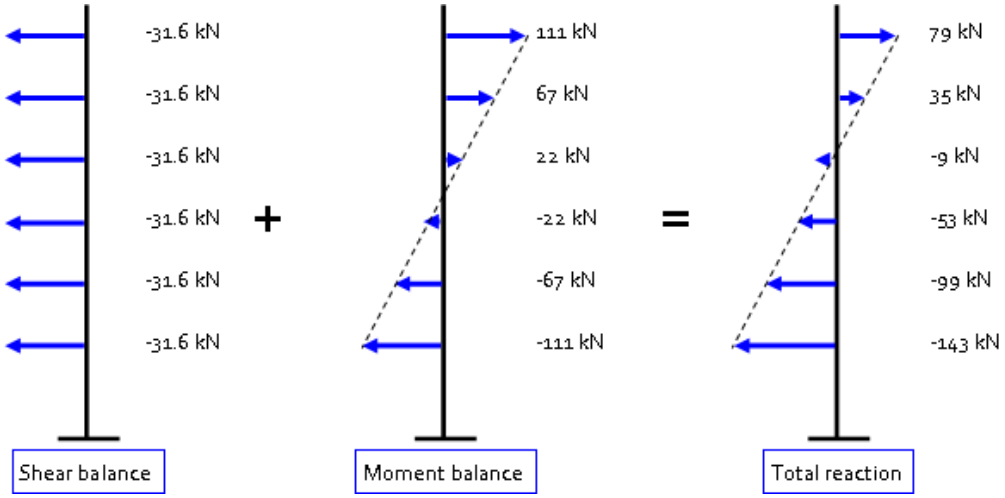

Figure 5-10: Shear-loads on floor-elements using a linear balancing-method

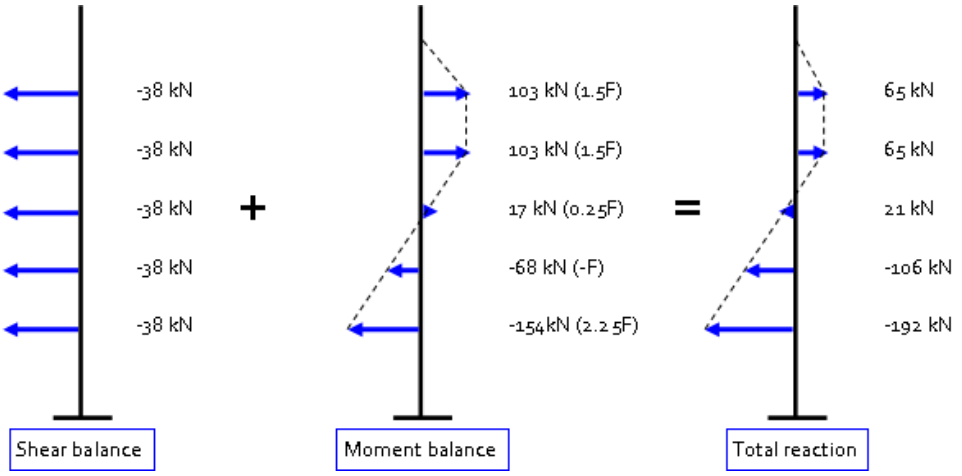

Figure 5-11: Shear-loads on floor-elements using a quasi-linear balancing method

5.3. Modelling of forces due to weakened pile-foundations

In this part, the structure is built in SCIA with a multitude of functions. The main calculations and considerations can all be found in Appendix C. Firstly, it is be used to verify the assumptions from the hand-calculations. As can be seen in Figure 5-12, the entire structure does behave as one unit, which confirms this assumption. Additionally, in Figure 5-13 and Figure 5-14, it can be seen that the structure can be modelled as a "bending beam", where the distributed load is equal to the wind load. Based on these considerations, the effect of weakened pile-foundations can be calculated.

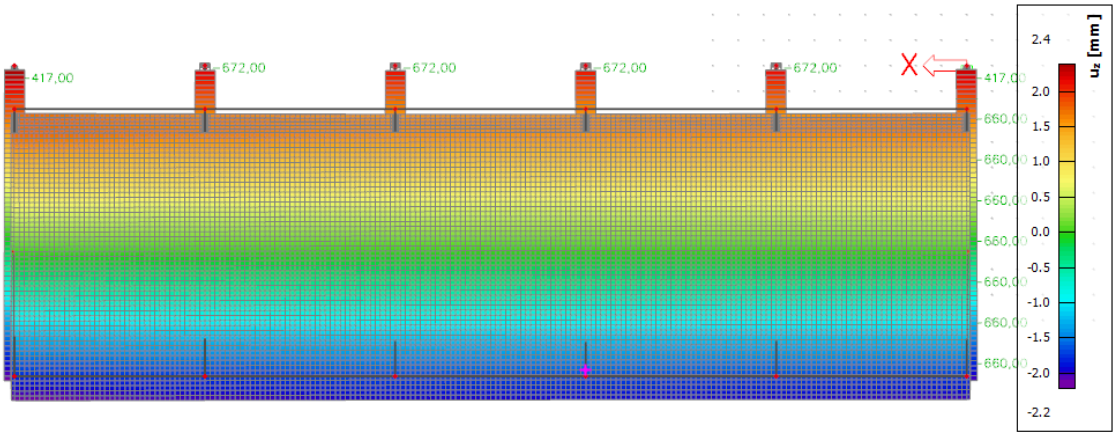

Figure 5-12: Top-view of structure, showing downwards deflection

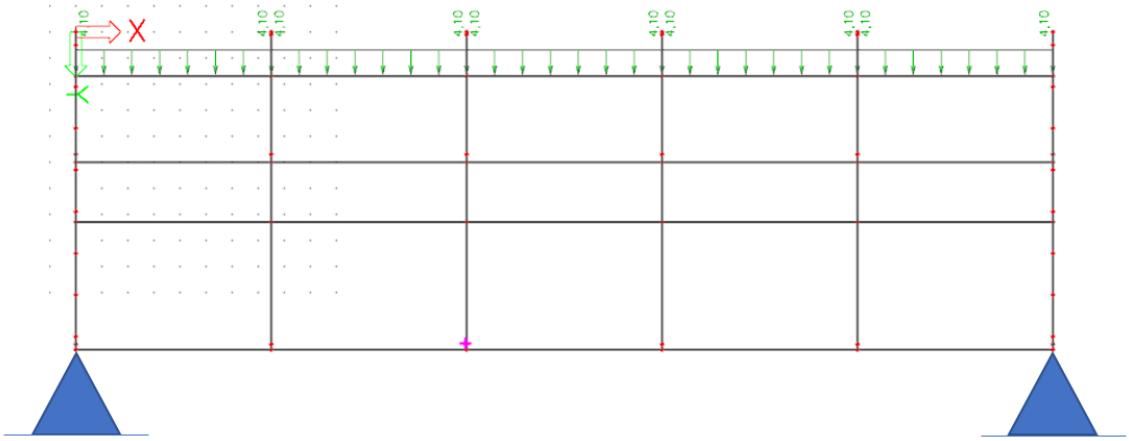

Figure 5-13: Top view of structure, showing visualisation of "bending beam"

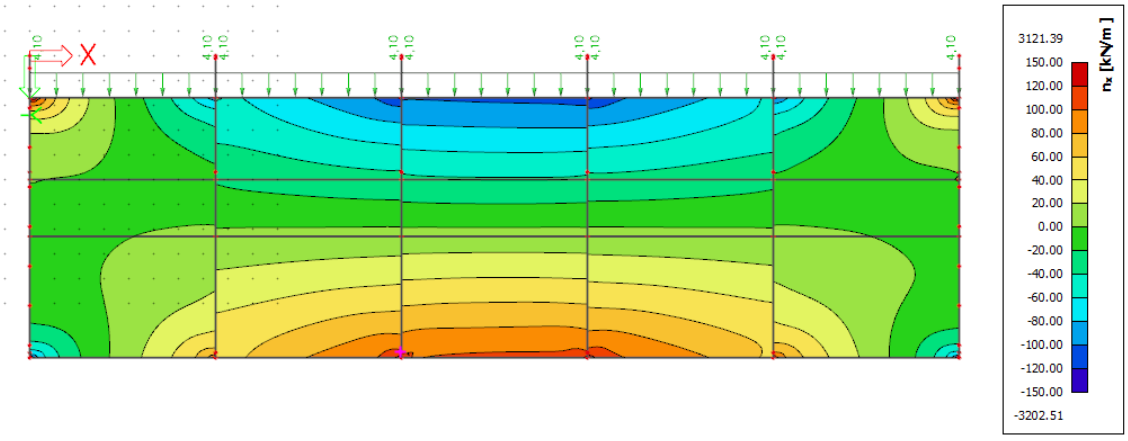

Figure 5-14: Top view of structure, showing stresses in x-direction

When the walls from the unit-structure are included in the SCIA-model, the bending behaviour shown before is reduced and less clear. A comparison between the model-results with and without unit-walls can be found in Figure 5-15 and Figure 5-16 respectively. As such, to keep the model easy-to-read, it has been decided to not include the unit-walls in the calculation for the weakened pile-foundations.

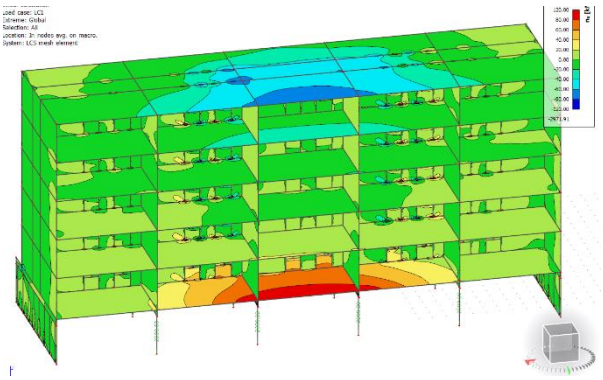

Figure 5-15: Stresses when unit walls are present

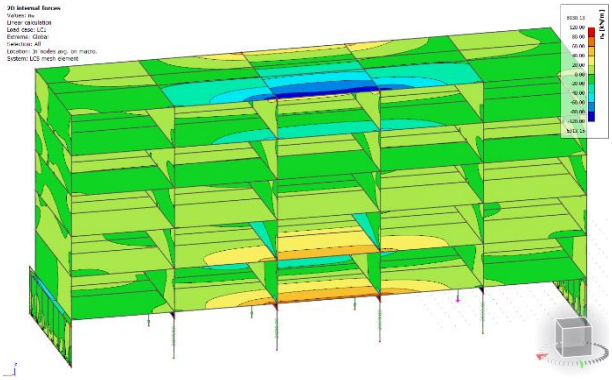

Figure 5-16: Stresses when unit walls are not present

The results of the wind-load calculation from Section 5.2 can be used to relate the present shear forces due to wind-loads to the occurring forces due to weakened pile-foundations. For this calculation, different variations of weakened pile-foundations were checked, and the governing situation has been used to calculate the maximum shear force that will be applied on the floor-elements. From the results, it seems that the largest reactions occurred when there was a sideways movement due to the weakened pile-foundations. If the weakened pile-foundations only caused a downward movement, it only caused a compression force in the floors.

While all different variations and detailed calculations can be found in Appendix C, the variation that caused the highest amount of shear forces per cross-section can be found in Figure 5-17 and Figure 5-18. The accompanied bending moment through the entire structure is visualised in Figure 5-19, and the final shear forces, combined with the shear forces due to wind loads, can be found in Figure 5-20.

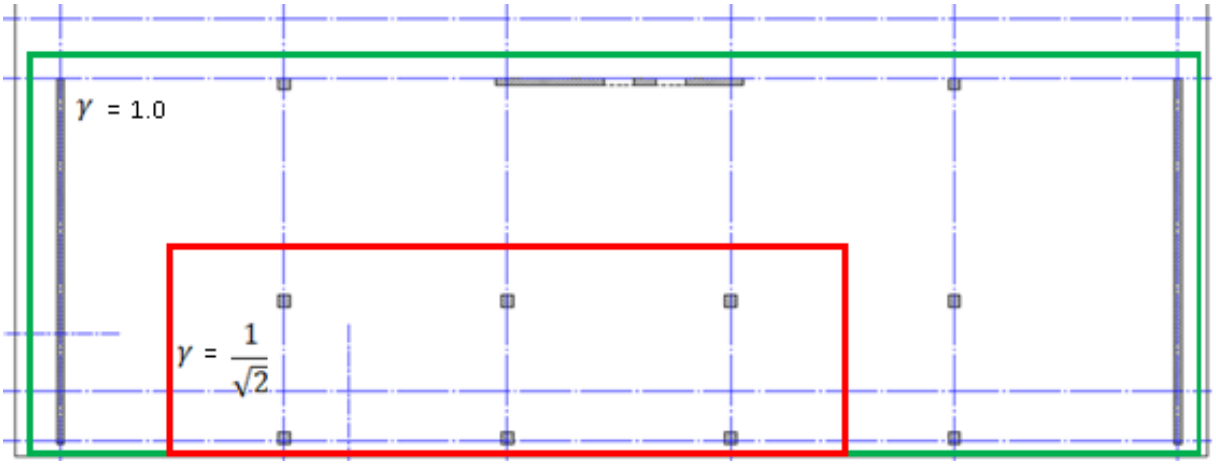

Figure 5-17: Lay-out of weakened-pile variation that cause highest response

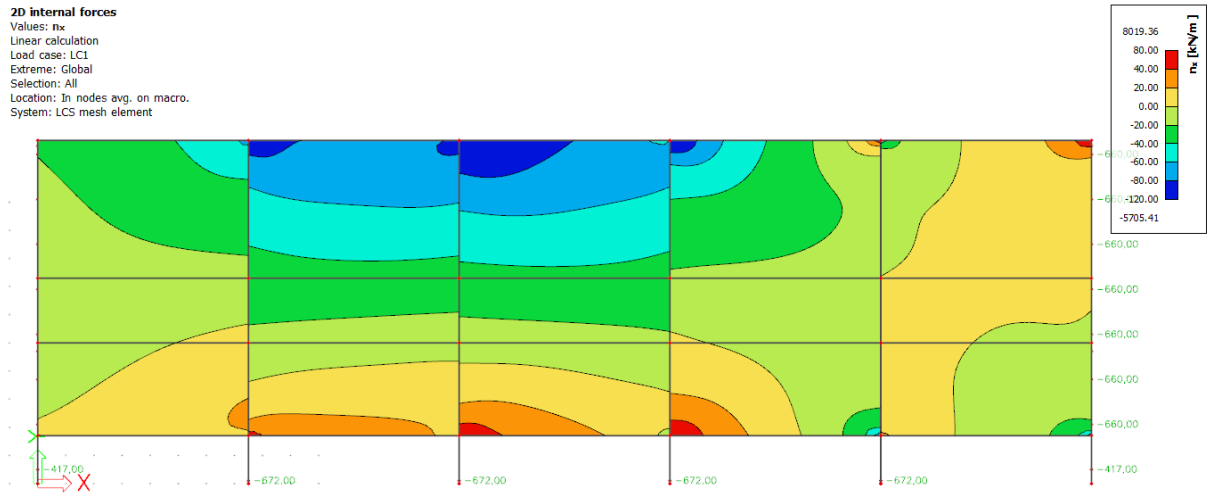

Figure 5-18: Results of weakened-pile variation that caused highest response

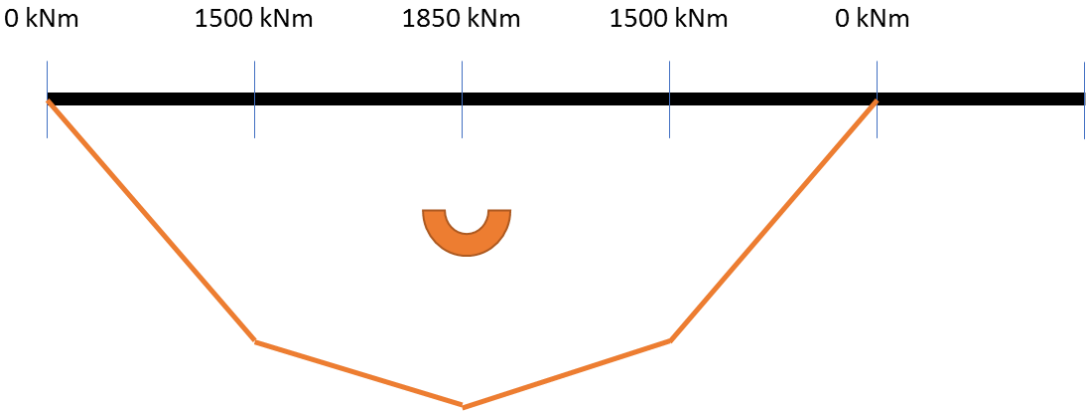

Figure 5-19: Calculated bending moment based on governing variation

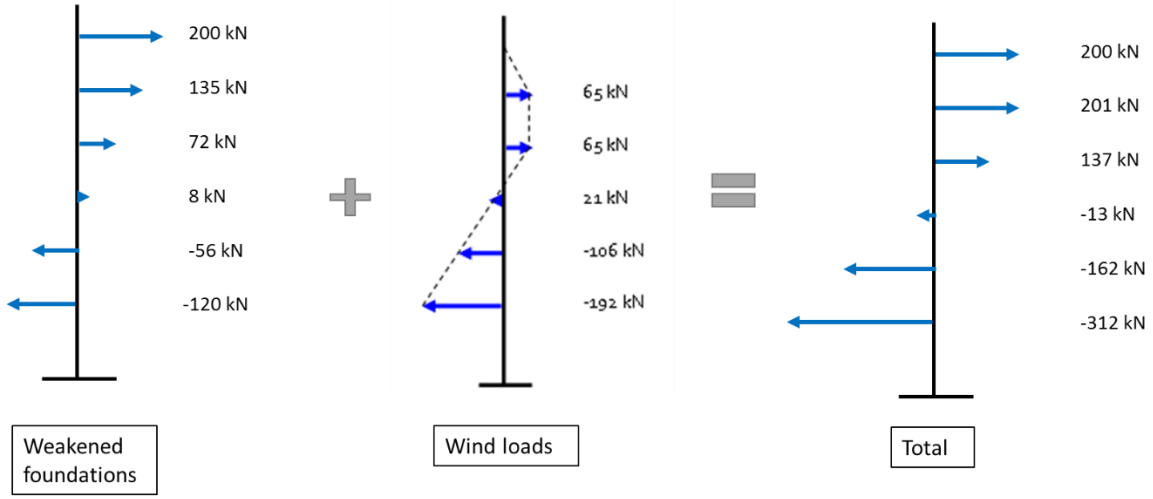

Figure 5-20: Total shear load on cross-sections due to weakened pile-foundations and wind-loads

This governing load of 312 kN can be used by Lievense | WSP as a guideline for the shear-force that their floors have to resist. The rest of the analyses and considerations from this chapter can also be used for insight into the behaviour of the Reinbouw project structure. Using this and the rest of this report, a collection of recommendations can be set up for Lievense | WSP for their use of the PCSP-floors in their project, both on a theoretical and practical level.

5.4. Application of analytical model to case study

After extensive analysis and development, multiple insights and models have been created regarding the use and application of PCSPs. In order to give advice to Lievense | WSP on the use of PCSP-floors in a fully prefabricated structure, all acquired information in this research is applied to the Reinbouw project, and recommendations for designs are given.

Application in project Reinbouw

As mentioned in the analysis of the Reinbouw project structure, the design causes the structure to function like a house of cards, resulting in a unique flow of forces in certain situations. In regards to the PCSP floors, the most notable bottleneck is the potential axial forces in the floors, causing a shear force, as the axial force has to flow from one concrete wythe to another.

Two main causes for these types of loads are wind loads and forces caused by weakened pile-foundations, as calculated in Section 5.2 and 5.3 respectively. Although the highest individual force is caused in the upper floor by the weakened pile-foundations, the highest combination can be found in the second floor, where the load is equal to 312 kN. It is noteworthy to mention that this load is applied perpendicular to the span-direction, meaning that the truss-connectors meant for resisting the bending forces, are not applied in the same direction. However, the current design makes use of angled truss connectors, as shown in Figure 5-21. The resistance and stiffness of these types of truss connectors have not been researched in this paper due to time constraints. Additionally, the dimensions of these truss-connectors are one of the unknown elements of the design. While an effort was made to develop an FE-model that could predict the shear-behaviour of PCSPs, this was unsuccessful. If the plan is to apply the current floor-design to the structure, it is recommended to carry out additional shear-experiments to ensure sufficient resistance.

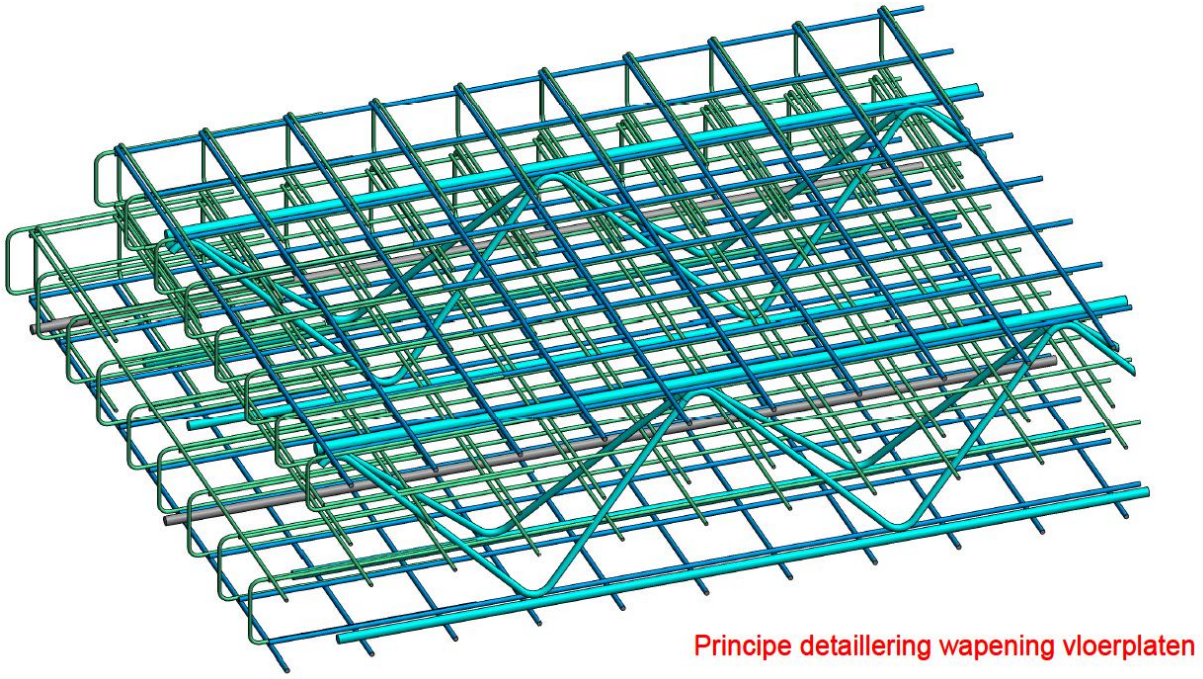

Figure 5-21: Preliminary truss-connector design without dimensions for the Reinbouw project

Linear prediction model

The analytical prediction model that has been developed in Excel can be used to advise on the dimensions of the required truss-connectors or prestressing. Although only linear bending behaviour is included in this analytical model, this can still be used to develop an initial floor-design, to check its non-linear behaviour more in-depth at a later stage.

Some of the input-parameters for the model are already fixed in the design of Lievense | WSP (Lievense | WSP, 2019):

- Span length: 7500 mm
- Concrete thickness: 170 mm
- Insulation thickness: 40 mm

Most other parameters have to be determined based on practical values or calculations. For prefab elements, the concrete strength class is set as C45/55. The truss-connector-steel is assumed to be strength class B500, and the initial centre-to-centre distance is set at 800 mm, as this distance has been used often in experiments of PCSP-floors. The insulation-stiffness is set at the same value as all previous comparisons and experiments. Lastly, the load is calculated by a combination of self-weight and the variable load of a living area:

$$q = 2 * t_c * b * \rho_c + q_{res} * b + q_{walls}$$

$$q = 2 * 0.36 * 0.8 * 25 + 2.0 * 0.8 + 0.8 = 9.6\ kN/m$$

Where:
$\boldsymbol{q}$: Total distributed load on the PCSP-floor [kN/m]

$\boldsymbol{t_c}$**:** Thickness of concrete wythes [m]

$\boldsymbol{b}$: Centre-to-centre distance of truss-connectors [m]

$\boldsymbol{\rho_c}$: Density of concrete [kN/m]

$\boldsymbol{q_{res}}$: Distributed load in residential areas [kN/m]

$\boldsymbol{q_{walls}}$: Distributed load due to walls [kN/m]

As such, all parameters can be found in Figure 5-22. The two parameters not filled in yet are the truss-diameter and the prestressing, which are the two main points of interest for design. While the truss-connectors increase the composite-factor, the prestressing is used to prevent the concrete from cracking too much. As input, the diameter of the truss-connector has been varied from 0 to 30 mm, while no prestressing is set initially, to check if this is required.

CALCULATION-INPUT

Span length:	7500	mm	Truss diameter:		mm
Width (c.t.c.):	800	mm	Truss stiffness:	200000	N/mm^2
Concrete thickness:	170	mm			
Insulation thickness:	40	mm	Applied load:	9.6	N/mm
Concrete stiffness:	36283	N/mm^2			
Insulation stiffness:	5	N/mm^2			

STRENGTH-LIMITS

Concrete prestressing:		N/mm^2
Concrete tensile strength:	1.77	N/mm^2
Concrete compressive strength:	30	N/mm^2
Truss strength:	500	N/mm^2

Figure 5-22: Fixed input of Lievense | WSP design for the Reinbouw project

As can be seen in the results in Section 4.2, a considerable truss-diameter is required to connect the concrete wythes when these wythes have a high thickness. When checking the truss-connector stress as shown in Figure 5-23, it's also clear that this value decreases significantly until a truss-diameter of 10 mm. Additionally, visualised in the figure with a red line, a truss-diameter of at least 12 mm is required to prevent the truss-connectors to yield at the edges. A diameter of 10 mm could also still result in similar results – as only the far edges of the truss-connectors would yield – but this non-linearity was not included in the model, and designs like this must be used with caution. Figure 5-24 shows the tensile stresses of the concrete at the bottom edge. In this figure, it is clear that significant cracking will occur in this floor. As such, the calculated deflection of the mathematical Excel-model is not in line with realistic results. However, a potential solution would be to apply around 2 MPa of prestressing in the concrete wythes. In this case, no cracks will occur due to this loading and the behaviour of the PCSP can be predicted by the mathematical model. A potential design-recommendation for the Lievense | WSP floor-design can be found in Figure 5-25.

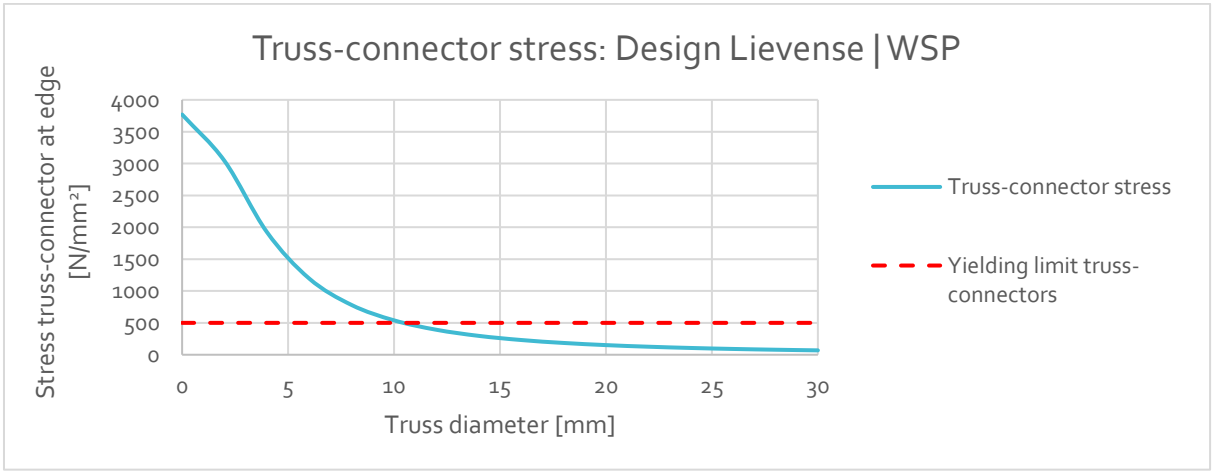

Figure 5-23: Truss connector stresses when varying truss-diameter

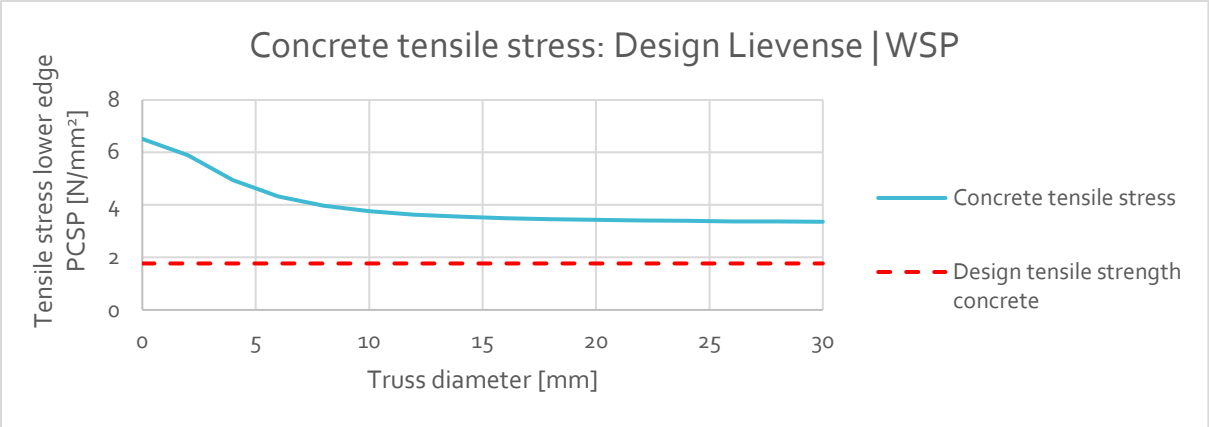

Figure 5-24: Concrete tensile stresses when varying truss-diameter

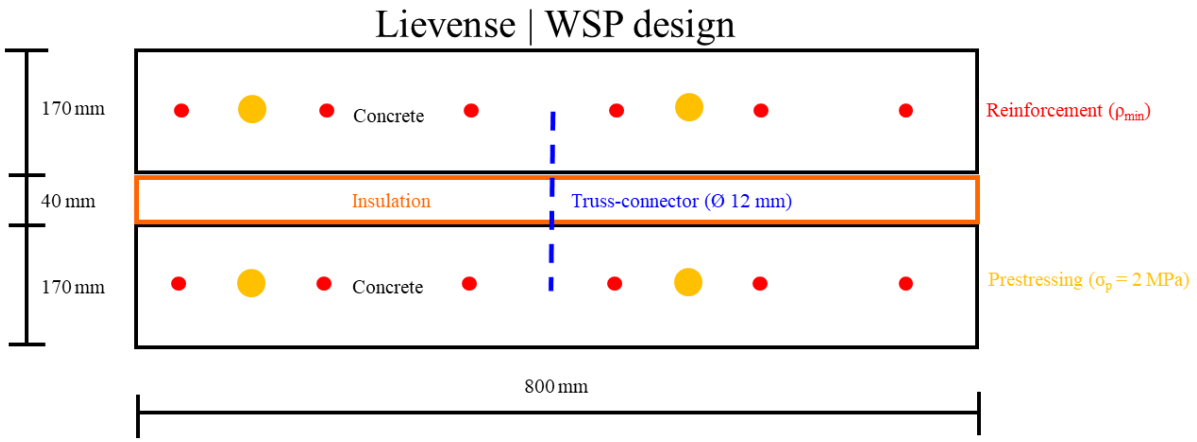

Figure 5-25: Recommendation possible Lievense | WSP design

Non-linear insights

If not enough prestressing is applied to prevent cracking, the Excel-model cannot ensure correct results anymore. However, some insights are still gained from analysing the non-linear FE-model that was developed and checked in Section 3.1 and 3.2 respectively. Instead of only the concrete, the non-linear behaviour of the truss-connectors is also essential for the behaviour of the PCSP.

In the case that the truss-connectors show non-linear behaviour, the only change that occurs is that the composite effect is reduced. However, the magnitude of this reduction is harder to predict, as this non-linearity initially only occurs at the edges of PCSPs. This means that the stiffness of the intermediate layer cannot be assumed as constant over the span, and as such, the general behaviour of the floor along the span also changes. Still, the most important aspect are the stresses at mid-span, as the presence of cracks have a much higher effect on the stiffness of the PCSP than the non-linearity of the truss-connectors. In the current design, it seems like non-linearity in the trusses will not be present, so this will not be a bottleneck in the design.

When the thickness of concrete wythes is increased, the crack-width also increases when only one reinforcement bar is used. Especially if no prestressing is being used – causing much higher tension stresses – the crack-widths might become too large for only one reinforcement bar. In order to gain enough insight into this, it is recommended to perform experiments or do more detailed research with the non-linear FE-model. The reason why this can't be calculated by simple formulas as a tensile tie model, is that the cooperation between the two concrete wythes and the truss-connectors change significantly when cracking occurs.

6. Discussion

Many different insights and conclusions have been gained from this research, that can be compared to earlier research. Firstly, it is said in literature that the truss connectors were essential to the linear stiffness of the PCSPs (Hopkins et al., 2017). From the parameter-studies done in Section 3.4 and 4.3, the conclusion is the same. Without truss-connectors, a full composite PCSP is never reached. A relatively small amount of truss-connector area increases the stiffness of the PCSP-structure significantly. Secondly, the essential elements for the non-linear phase of the PCSPs are more difficult to compare and analyse. However, literature has mentioned that post-tensioning behaviour of concrete is the reason for the complicated global behaviour of these floors (Hamed, 2016). This is also clear from the analysis of the FE-model in Section 3.1: after concrete cracks, a significant increase in deflection is found. The effect and magnitude of non-linear truss-connectors is harder to analyse, and also has not been explicitly mentioned in previous research. Thirdly, although the non-linear FE-model of this research was not able to consistently predict the behaviour of experiments, it did follow the behaviour of an earlier-developed FE-model for PCSPs. Still, it should be noted that the FE-model that is developed in Chapter 3 behaves a lot more brittle than the FE-model that it is compared to.

Although the initial plan of this research was to predict the non-linear behaviour of PCSPs using a FE-model, this focus was later changed to developing a much simpler model, predicting the linear behaviour using Excel. Insights into the non-linear behaviour were still gained, but uncertainties are still largely present in this aspect of PCSPs. While the FE-model was able to predict the linear part almost perfectly, the non-linearity showed some deviations. This was not caused by the general behaviour; the FE-model showed similar steps in cracking and non-linearity as the experiments. However, when looking purely at the load-displacement diagram, the FE-model seems to deviate from results regularly. This might be caused by experimental variations, but not enough experiments have been compared to non-linear models in order to confirm or deny this claim. In the case of shear-experiments, it seems that the FE-model was not able to predict the interaction between layers correctly. While comparing this shear-experiment, there were also some difficulties finding values for certain parameters of this experiment, which might have caused deviations between expectation and result.

When focusing on the linear Excel-model, the accuracy of this model is almost perfect, especially in the range where a logical amount of truss-connectors are applied. However, there are still some limitations to this model. First and foremost, the model is only able to determine linear behaviour. Additionally, as the model is largely based on linear assumptions, applying non-linear behaviour to this model might be difficult to accomplish. As the non-linearity and ductility of PCSPs adds a lot of resistance to the element, the linear model is not able to fully make use of its resistance. Lastly, some assumptions are present in the Excel-model that reduces freedom of design: only a simply supported PCSP with identical concrete wythes and truss-connectors with a constant diameter and an angle of 45° are able to be predicted. However, for some of these assumptions, potential room for improvement is possible.

The Reinbouw project from Lievense | WSP possesses multiple unique design-challenges, of which one is the PCSP-floors. The shear force that protrudes through these floors has not been researched or tested in this paper. As such, no confident statements can be made about the shear-resistance and stiffness of these types of floor. However, there are other bottlenecks in the structure as discussed in Section 5.1, which might cause a different flow of forces as initially expected. In most cases, this would cause a lower load on the floors, as the unit-walls have been ignored in the calculation from Section 5.3. This means that the shear loads on the PCSP-structure are expected to be of a similar or lower magnitude as calculated in this research.

Luckily, the PCSP-design of Lievense | WSP can still be put into the mathematical Excel-model to determine the bending behaviour of this element. When doing this, it can be seen that a high level of stiffness can be easily acquired with an acceptable amount of truss connectors. However, the bottom edge of the concrete will still crack significantly, requiring prestressing or non-linearity to resist part of the load. Given the high span length for a concrete structure, it was expected that prestressing might be necessary to prevent too much cracking.

7. Summary & conclusion

Although Precast Concrete Sandwich Panels are weight-efficient and possess good insulation characteristics, the behaviour of these panels are relatively unknown. There is no simple expression or model to calculate the linear composite factor. Additionally, the non-linear behaviour has not been consistently predicted correctly by either analytical or finite-element models yet. Lievense | WSP wants to use these PCSPs in their fully prefabricated structure, but are unsure about the requirements for these types of floors. In order to use PCSPs to their full extent, more analysis and development had to be done in order to increase the applicability of PCSPs. As such, it was researched how simple expressions can be set-up for the behaviour of precast concrete sandwich panels, and to what extent these expressions can be used in a fully pre-fabricated structure.

In order to research the current issues in the prediction of the PCSP-behaviour, a literature-study was initially set up to analyse the behaviour of PCSPs. Based on the knowledge gained from this analysis, an advanced, non-linear Finite Element model was developed in order to predict the linear and non-linear behaviour of PCSPs. This model includes the non-linearity of all materials but the insulation, and has been compared to experiments from literature. Afterwards, an analytical model was developed with the goal to predict the linear behaviour without any complicated input from the user. This has in turn been compared to the earlier-developed FE-model, where only the linear behaviour was enabled for this comparison. Lastly, a number of calculations were done for the project of Lievense | WSP, where hand-calculations, Technosoft and SCIA were used to find the present shear forces in the floor-systems.

From the literature-study, the truss-connectors connecting the two concrete wythes were mentioned as the most essential parameter to the total stiffness of these panels. When these truss-connectors are applied, the insulation layer does not play an essential role in the stiffness anymore. It was also clear that the main cause for incorrect non-linear predictions were caused by a complicated tension-stiffening model from the concrete wythes. This could cause an over- or under-estimation of the PCSP-stiffness of around 20% in the worst cases. Already developed expressions to calculate the level of composite effect could not be used for PCSPs, as the design that is assumed for these expressions is significantly different when compared to PCSPs.

When developing the FE-model, an effort was made to add non-linear effects step-by-step, to ensure that each element was added correctly. An important aspect from this development-process was that the truss-connectors had to be modelled as reinforcement-bars to ensure a realistic stiffness-behaviour. When comparing the FE-model to various experiments, it showed that the linear behaviour was perfectly predicted. Although some experiments also compared very well with the developed model in the non-linear behaviour, the FE-model also over- or underestimated the stiffnesses in some experiments. This might be caused by the complicated tension-stiffening model of the concrete, or by strength variations in the concrete itself. However, the FE-model was still able to be used to find non-linear insights regarding PCSPs, as the general non-linear ductility and qualitative behaviour of the FE-model showed similar results to the experiments. While it is said that the concrete cracking plays an important role in literature, the plasticity of the truss connectors indirectly have an influence on this as well. Essentially reducing the stiffness of truss-connectors due to plasticity, the composite factor of the PCSP reduces, and the concrete stress increases. The magnitude of this stress-increase due to this plastic behaviour is a possible future research for this subject. Additionally, as the linear stiffness of the shear-experiments was over-estimated by the FE-model with a factor of around six, the prediction of shear behaviour of PCSPs is also a possible future research.

In the development of the linear prediction model, the goal was to develop a model that could be used in practice, by people that have close to no knowledge of the underlying behaviours of these floors. As such, a model in Excel was developed, where an easy-to-use interface is present for input, and only insightful output is shown, while all other calculations are done in the background. This analytical model has been compared with the FE-model – which was already confirmed to correctly predict linear parts of experiments – and showed a perfect comparison to a broad set of floor-designs. Although the model does not include non-linear behaviour, it warns the user when limits are reached. Without the application of truss-connectors, increasing the concrete thickness of the PCSPs from 60 to 140 mm would decrease the composite factor for a value of around 0.28. Increasing the span length from 4000 to 8000 mm would increase the composite factor for around 0.31. The effect of increasing the insulation thickness from 40 to 80 mm depends on the concrete thickness, where the reduction of the composite factor is 0.02 and 0.06 for a concrete thickness of 60 and 140 mm respectively. When truss-connectors are applied, most PCSP-designs will possess a composite factor of above 0.95 when 12 mm diameter bars are being used every 800 mm. However, when concrete wythes with a thickness of 140 mm or higher are being used, the increase in composite-action due to the application of trusses decreases significantly, causing a decrease in composite factor from 0.96 to 0.91 compared to when 140 mm and 60 mm wythes are used respectively. When more insight is gained in the actual effect of non-linearity on the composite behaviour and stiffness, an additional research could potentially try to apply these effects on the already present linear prediction-model.

To start off the analysis of the Reinbouw project of Lievense | WSP, a general flow of forces was set up to understand how the structure functioned generally. This also included a general analysis of the structure, to find bottlenecks in the structure that should be taken into account in the final design. Based on the flow of forces, a pile-foundation design was calculated. This lay-out was then used to calculate the wind-load on each layer of the building. On top of this, an additional calculation was done to analyse the effect of weakened pile-foundations, and to find the resulting forces in the floors that are caused by this. From this analysis, it was clear that considerable axial forces will be present in the floor-systems of the structure. Due to the way the floors are connected, this results in shear-forces in the span-length of the PCSPs. This is something that must be more thoroughly analysed before these floors can be confidently used in this design. When using the analytical Excel-model to predict the bending-behaviour of the floor-design, it is concluded that 12 mm diameter truss-connectors are required over every 800 mm width to ensure that no plasticity occurs in these trusses. Additionally, even with the 12 mm truss-connectors, 2 MPa prestressing is required in the concrete to prevent cracking of the lower wythe. In regards to non-linear behaviour, experiments are recommended in order to check concrete cracking to ensure that no unexpected behaviour occurs in these designs.

In conclusion, the applicability of PCSPs have been increased due to all above-mentioned methods and results. One of the first questions that arose, was what were the most important features of PCSPs that change their behaviour in comparison to solid concrete floors. It can be said that the truss connectors are the most essential factor for the linear stiffness, while the individual concrete cracking of the wythes causes the largest unpredictability in the non-linear phase. When thinking about the application of the different elements and materials in the FE-model, it became clear that the truss-connectors must be modelled as reinforcement to ensure that the model correctly predicted the behaviour of the interaction between the two concrete wythes. In regards to the analytical prediction model and its development, it was not possible to develop this model in Maple. This was more successful when using Microsoft Excel, and this also seems the most useful, due to the low complexity of Excel as a software. The main insights that could be gained from the model have been mentioned in the previous paragraph: required truss-connector diameters to prevent plasticity can be determined, or general stiffness-behaviour can be calculated for input for other modelling-programs.

Finally, the main research-question is returned to: how simple expressions can be set up and used in a fully prefabricated structure. It has not been possible to develop simple expressions yet. However, the simple analytical model allows for easy input by users without much background-knowledge of the behaviour, which has been used to advice on the floor-designs of the fully prefabricated structure of Lievense | WSP. The development of simple expressions based on this analytical model seems like the logical next step in future research.

Acknowledgements

This thesis was the final part of my Msc Structural Engineering at the Delft University of Technology. Before and throughout the progress of this thesis, many people have helped me to get to this point that I would like to thank here.

Firstly, I would like to give my thanks to the TU Delft-part of my graduation committee: Eva Lantsoght, Yuguang Yang and Jan Rots. Even during the COVID-19 crisis, they have managed to help me to develop the report that can be read here. Eva Lantsoght has guided and advised me with multiple problems that I faced throughout the entire process of my thesis. Yuguang Yang and Jan Rots ensured that my tendency to focus on details did not bring any harm to the quality of this thesis, and gave insights in how to calculate certain elements of my models. Next to my committee, I would like to give special thanks to Max Hendriks, for his quick and elaborate responses to my questions regarding DIANA.

Secondly, I would like to thank the company where I was able to work on my thesis for these last months: Lievense | WSP. The office in Apeldoorn – in the time I was able to work there – had a welcoming environment and it was nice to get to know everyone there. I would like to give special thanks to Rob Mink, who has guided me through the Reinbouw project and made sure to also introduce me to the practical aspects of becoming an structural engineer. Additionally, I would like to thank Marielle Snoek for introducing me to Lievense | WSP and for finding this opportunity for a graduation-project in their company.

Lastly, I would like to thank my family and friends, inside and outside my studies, that supported me throughout the entire process of my study. Special thanks to my parents, as they took me back in during the entire COVID-19 crisis, and allowed me to vent about all the different models whenever they were not cooperating.

References

Abspoel, R. (2018, February 21). Steel Structures 3: Lecture 4 Composite structures Steel-Concrete. Delft, Zuid-Holland, The Netherlands.

Bajracharya, R., Lokuge, W., Karunasena, W., Lau, K., & Mosallam, A. (2013). *Structural evaluation of Concrete Expanded Polystyrene sandwich panels for slab applications.* Syndey, Australia: Australasian Conference on the Mechanics of Structures and Materials.

Bush, T., & Stine, G. (1994). *Flexural behavior of composite precast concrete sandwich panels with continuous truss connectors.* Norman, Oklahoma: Precast/Prestressed Concrete Institute.

Choi, K.-B., Choi, W.-C., Feo, L., Jang, S.-J., & Yun, H.-D. (2015). *In-plane shear behavior of insulated precast concrete sandwich panels reinforcement with corrugated GFRP shear connectors.* Seongnam-si: Elsevier.

Designing Buildings. (2019, September 25). *Concrete slabs in buildings*. Retrieved from Designing Buildings wiki: https://www.designingbuildings.co.uk/wiki/Concrete_slabs_in_buildings

Einea, A., Salmon, D., Fogarasi, G., Culp, T., & Tadros, M. (1991). *State-of-the-Art of Precast Concrete Sandwich Panels.* Omaha, Nebraska: University of Nebraska.

Einea, A., Salmon, D., Fogarasi, G., Culp, T., & Tadros, M. (1994). *A new structurally and thermally efficient precast sandwich panel system.* Omaha, Nebraska: Precast/Prestressed Concrete Institute.

Ekenel, M. (2014). *Testing and acceptance criteria for fiber-reinforced composite grid connectors used in concrete sandwich panels.* Whittier: Journal of Materials in Civil Engineering.

Eurocodeapplied.com. (n.d.). *Table of concrete design properties*. Retrieved from Eurocode 2: https://eurocodeapplied.com/design/en1992/concrete-design-properties

Gilbert, R., & Ranzi, G. (2011). *Time-Dependent Behaviour of Concrete Structures.* Abingdon: Spon Press.

Gruijl, J. d. (2019, February 18). *Circularity in construction is gaining importance, but it is not well known yet*. Retrieved from USP Marketing Consultancy | Marktonderzoek, Inzichten & Advies: https://www.usp-mc.nl/nl/artikel/776/circularity-in-construction-is-gaining-importance-but-it-is-not-well-known-yet/

Hamed, E. (2016). *Modeling, Analysis, and Behavior of Load-Carrying Precast Concrete Sandwich Panels.* Sydney: American Society of Civil Engineers.

Hellenberg Hubar, S. v., Korthagen, P., & Verbaten, M. (2019, January 25). *Detailengineering plaatnaden breedplaatvloeren.* Retrieved from Cement Online: https://www.cementonline.nl/article/14657/YjFjZjA2YTk5NjgwNDVjNGQ1Y2JjMWQ4ZmIyODhkM2M=

Hopkins, P., Norris, T., & Chen, A. (2017). *Creep Behavior of insulated concrete sandwich panels with fiber-reinforced polymer shear connectors.* Pennsylvania: Elsevier.

Huang, Q., & Hamed, E. (2019). *Nonlinear finite element analysis of composite precast concrete sandwich panels made with diagonal FRP bar connectors.* Sydney, Australia: Elsevier.

Kubbinga, B., Bamberger, M., Noort, E. v., Reek, D. v., Blok, M., Roemers, G., . . . Faes, K. (2019). *A Framework For Circular Buildings.* Amsterdam: Circle Economy.

Learn About Structures. (2020). *5.2 The Bernoulli-Euler Beam Theory*. Retrieved from Learn About Structures: https://learnaboutstructures.com/Bernoulli-Euler-Beam-Theory

Lievense | WSP. (2019, October 9). Bouwfasering. Apeldoorn, Gelderland, Nederland.

Linssen, J. (2019). Het dossier breedplaatvloeren belicht. *Cement*, 1-8.

Meester, J. (2019, October 22). Investigation into the cause of the failure of parking garage Eindhoven Airport. Delft, Zuid-Holland, Nederland.

Mink, R. (2019, September 19). Discussion about the Reinbouw mid-rise project. (B. Schrooten, Interviewer)

Mink, R. (2019, November 27). Overleg en discussie project Reinbouw Hoogbouw. (B. Schrooten, Interviewer)

NEN. (2005, December| 1). *EN 1992-1-1:2005.* Retrieved from NEN: https://connect.nen.nl/Standard/Detail/167115?compId=14489&collectionId=0

NEN. (2011, November). *NEN-EN 1995-1-1:2011.* Retrieved from NEN Connect: https://connect.nen.nl/Family/Detail/30424?compId=10037&collectionId=0

Newell, S., & Goggins, J. (2019). *Experimental study of hybrid precast concrete lattice girder floor at construction stage.* Galway: Elsevier.

Northwest Foam Products inc. (n.d.). *EPS Specs | Physical Properties of EPS*. Retrieved from Building Code Classification: https://www.northwestfoam.com/eps-specs-physical-properties.php.html

NOS.nl. (2017, September 27). *Instorting Eindhoven was technische fout, onderzoek naar andere parkeergarages.* Retrieved from NOS.nl - Nieuws, Sport en Evenementen: https://nos.nl/artikel/2194738-instorting-eindhoven-was-technische-fout-onderzoek-naar-andere-parkeergarages.html

Qiu, C., Ding, C., He, X., Zhang, L., & Bai, Y. (2018). *Axial performance of steel splice connection for tubular FRP column members.* Clayton: Bridge Engineering Institute.

Salmon, D., Einea, A., Tadros, M., & Culp, T. (1997). Full-scale testing of precast concrete sandwich panels. *ACI Structural Journal, 94*(4), 354-362. Retrieved from https://www.concrete.org/publications/internationalconcreteabstractsportal/m/details/id/486

Soetens, T., & Matthys, S. (2014). Different methods to model the post-cracking behaviour of hooked-end steel fibre reinforced concrete. *Construction and Building Materials, 73*, 458-471. doi:https://doi.org/10.1016/j.conbuildmat.2014.09.093

Ulfkjær, J., & Brincker, R. (1995). *Fractuce energy of normal strength concrete, high strength concrete and ultra high strength concrete ultra ductile steel fibre reinforced concrete.* Freiburg: AEDIFICATIO Publishers.

Yang, Y. (2019, December 20). Kick-off meeting Master's Thesis. (B. Schrooten, Interviewer)

Yun, H., Jang, S., & You, Y. (2012). Direct Shear Responses of Insulated Concrete Sandwich Panels with GFRP Shear Connectors. *Applied Mechanics and Materials, 204-208*, 803-806. doi:https://doi.org/10.4028/www.scientific.net/AMM.204-208.803

A. Appendix: User-interface analytical model

The model for practical use can be divided into three main parts:

1. Input & limit strengths
2. Calculations
3. Output

The input & limit strengths can be seen in Figure A-1. This is the only part of the model where users should edit values. Although the limit strengths do not have an influence on the calculation-part, they are important to show the limitations of the (linear) prediction model.

CALCULATION-INPUT

Span length:	7200	mm	Truss diameter:	12	mm
Width (c.t.c.):	800	mm	Truss stiffness:	200000	N/mm^2
Concrete thickness:	140	mm			
Insulation thickness:	40	mm	Applied load:	10	N/mm
Concrete stiffness:	31000	N/mm^2			
Insulation stiffness:	5	N/mm^2			

STRENGTH-LIMITS

Concrete prestressing:	0	N/mm^2
Concrete tensile strength:	1.77	N/mm^2
Concrete compressive strength:	30	N/mm^2
Truss strength:	410	N/mm^2

Figure A-1: Input & limit strengths for mathematical model

The calculations are found in Figure A-2. As mentioned before, the details of these calculation-steps can be found in Appendix 0. Generally, the goals is not to view these intermediate calculations to the users of the model, as only the input and output is important.

CALCULATION (DO NOT CHANGE)

Step 1 & 2: Determination initial deflection and rotation

Deflection when assuming full composite action: 5.17722997 mm

Deflection when assuming no composite action: 30.8520643 mm

Assumed deflection: 18.0146472 mm

q-load based on single concrete wythe: 2.91952055 N/mm

Assumed rotation: 0.00800651 -

Step 3: Determination axial distance

Initial axial distance (1 wythe to centre-line): 0.72058589 mm

Fictitious stiffness intermediate layer: 162.079633 N/mm^2

Maximum reaction force intermediate layer: 3687042.94 N

Maximum reaction force concrete wythe: 1042447.58 N

Actual axial distance (1 wythe to centre-line): 0.15882747 mm

Step 4: Calculation bending-response intermediate layer on concrete wythes

Actual axial distance (full PCSP): 0.31765494 mm

Shear strain intermediate layer at edge: 0.007941374 -

Mean shear strain intermediate layer: 0.004526583 -

Mean shear stress intermediate layer: 0.282179575 N/mm^2

Compression/Tension force in concrete wythe: 812677.1748 N

Additional stress in concrete wythes: 7.256046204 N/mm^2

Bending moment based on initial load (Step 1): 37836986.3 Nmm

Bending moment based on reaction intermediate layer: 146281891.5 Nmm

Total bending moment: 184118877.8 Nmm

Step 5 & 6: Calculating the actual composite action

q-load based on total bending moment (step 4): 28.41341 N/mm

Mid-span deflection assuming full composite effect: 14.71027 mm

Mid-span deflection assuming no composite effect: 87.66123 mm

Composite factor (based on assumed deflection step 1): 0.954704 -

Additional calculations:

Stress outer edge compressive wythe: -14.4953 N/mm^2

Stress inner edge compressive wythe: -0.01683 N/mm^2

Stress inner edge tensile wythe: 0.016827 N/mm^2

Stress outer edge tensile wythe: 14.49527 N/mm^2

Stress truss connectors at edge: 1123.08 N/mm^2

Figure A-2: Calculations for mathematical model

The output can be found in Figure A-3. In this output, both the direct results from the calculations are showed, as well as the strength checks based on the limit strengths that are set as input. If the concrete-strength limits are exceeded, a "Warning!"-text will show, to inform the user that the model might not be able to show correct results for this design and load. In this case, it is advised to check the design with a more detailed, non-linear model. If the truss-strength limit is slightly exceeded, a "Caution"-text will show, to inform the user that correctness of the model might decrease. However, the results are not immediately untrustworthy for two reasons: first, compared to the FE-model, the truss-stresses are overestimated in the mathematical model. Secondly, as the stress on the truss-connector only specifies the stress at the edges – where the stress is the highest – a small exceedance means that only the outer truss-connector possesses a slightly lower stiffness. If the truss-limit strength is greatly exceeded, the same "Warning!"-text is shown as the concrete-check.

OUTPUT (DO NOT CHANGE)			
Composite factor:	0.954704184	-	
Ficticious bending stiffness:	6.50405E+13	Nmm^2	
Deflection at midspan:	6.34019254	mm	
Stress outer edge upper wythe	-5.10155839	N/mm^2	
Stress inner edge upper wythe	-0.00592216	N/mm^2	
Stress truss-connectors at edge	395.264042	N/mm^2	
Stress inner edge lower wythe	0.005922164	N/mm^2	
Stress outer edge lower wythe	5.101558391	N/mm^2	Warning!

Figure A-3: Output for mathematical model

In contrast to FE-models, this mathematical model in Excel does not require a lot of knowledge to be used. As such, it can be easily used by people in practice to get an estimate for how the need to design their PCSP-floors. This also means that this model can be used for insight in the case of the Reinbouw project from Lievense | WSP. However, as this structural design is unique in itself, research must be done on the flow of forces of the Reinbouw project, and the resulting forces that occur due to this behaviour.

B. Appendix: Calculation Reinbouw High-rise concept

Self-weight of an intermediate wall

Initially, a lay-out was drawn for a cross-section of the structure like Figure B-1 (cross-section short side), in which all point- and distributed loads were shown. The reference-beam was taken as the lower beam, where the columns and foundation underneath this beam were included by use of additional point loads underneath the reference-beam. This visualisation can also be found in Figure B-1. While the loads are all focused on one "beam", the stiffnesses of the entire structure are still taken into account. For example, the part that is loaded by Q2 and Q4 will include the walls from all floors. To simplify the calculation, only the self-weights have been included in this calculation.

Based on the horizontal load-transfer mentioned in Section 5.1, the different point- and distributed loads consist of the following:

- F1: Columns steel + 4 floors of ½ gallery
- F2: Walls HSB + 4 floors of ½ gallery
- F3: Walls unit element
- F4: Walls HSB
- F5: Column concrete + ½ ground floor left + ½ eff. foundation beam
- F6: Column concrete + ½ ground floor left + ¼ ground floor right + ¾ eff. foundation beam + foundation footing
- F7: Column concrete + ¼ ground floor right + ¼ eff. foundation beam + foundation footing
- Q1: Floor gallery + lower beam
- Q2: 5 upper normal floors + normal roof + 5 floors of normal walls + lower beam
- Q3: 5 balconies
- Q4: 5 upper unit floors + unit roof + 5 floors of unit walls + lower beam

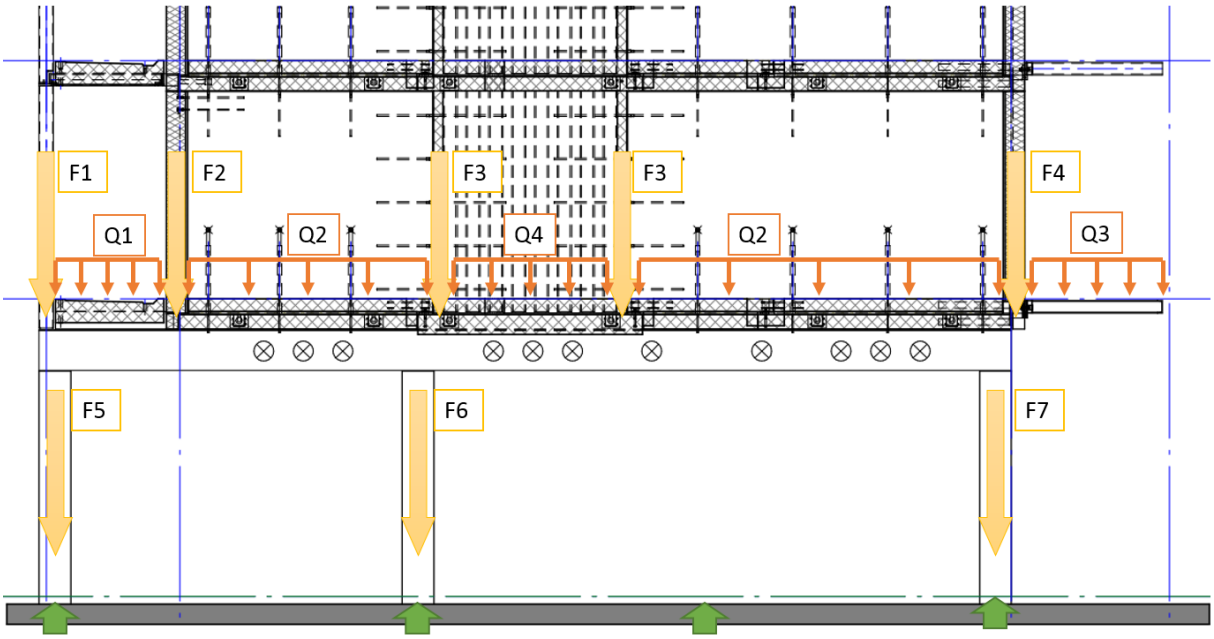

Figure B-1: Load lay-out case study including point loads (yellow), distributed loads (orange), and foundation reaction forces (green)

As can be seen in the figure, an additional pile can be seen in between the beams carrying point loads F6 and F7. This means that part of the foundation beam and ground floor is resisted by this pile, not contributing to the loads of the structure calculation shown above. The method for including this in

the calculation is applying only ¼ of the total floor area to both point loads surrounding the area, instead of ½.

The calculation-process was iterative, with the goal for the author to gain insight in how a project is initially calculated. An expected pile lay-out was developed so that pile-stiffnesses were available. After all loads were calculated and used as input in Technosoft, the pile lay-out was changed to ensure an optimal deflection of the entire structure. Together with some feedback on the calculation itself, the final calculation could be made, which is also given below. As the process of the intermediate calculations were almost identical, it has been chosen to only include the final calculations and values.

The calculation-process

The process starts with the determination of the dimensions of each structural element. Then, the loads will be calculated based on these dimensions. The loads will be used as input for Technosoft, together with the pile- and "beam"-stiffnesses, where the deflection of the entire structure will be analysed.

In the digital excel sheet, the dimensions and load-calculation are done in the same sheet and columns. Thus, both of these can be found in Figure B-2 and Figure B-3 for the normal and unit elements respectively. These elements have to be summarized to find the total values for the point- and distributed loads. This is done in Figure B-5 for the distributed loads, and Figure B-4 for the point loads.

Finally, these values are used as input for Technosoft. Other required input is the "beam"- and pile-stiffness. For the global structure, a simple beam is modelled where all forces from Figure B-1 are applied to. While the stiffnesses of the gallery is based on one gallery-floor, the balconies have a combined stiffness, and all walls are assumed to fully contribute their stiffness to the applied load. These assumptions result in the following dimensions for the "beam"-element:

- Gallery-floor: B*H 800x500 (C40/50)
- Apartments: B*H 250x15800 (C40/50)
- Balconies: B*H 11350x120 (C40/50)

The goal of this calculation is to find a pile-layout that will result in the most equal sagging of the full structure. In this design, a large amount of piles can only be placed on the positions where the columns are present. As such, the final pile lay-out for the intermediate walls is as follows:

For the two inner intermediate cross-sections:

- Position F5: ⌀ 320 mm
- Position F6: 6 * ⌀ 350 mm
- Position F7: 3 * ⌀ 350 mm

For the two outer intermediate cross-sections:

- Position F5: ⌀ 320 mm
- Position F6: 6 * ⌀ 350 mm
- Position F7: 3 * ⌀ 320 mm

The additional pile between F6 and F7 is ⌀ 290 mm. The difference between the inner and outer cross-sections are due to the stability wall that is placed in between the two inner cross-sections on the position of F7. This will result in additional stresses and loads, which is why this pile lay-out is stronger than the outer cross-sections.

The final deflection of the outer intermediate cross-sections is given in Figure B-6.

2.1 Permanent loads

Flat roof (6th floor)	Floor-element	d =	340	mm	=	8,50	kN/m²			
	Gravel	d =	60	mm	=	1,08				
	Insulation (type unknown)				=	0,10				
	Roof cover				=	0,05	+			
					G_k =	9,73	kN/m²			
2nd-5th floor	Floor-element	d =	340	mm	=	8,50	kN/m²			
							+			
					G_k =	8,50	kN/m²			
1st floor	Floor-element	d =	340	mm	=	8,50	kN/m²			
							+			
					G_k =	8,50	kN/m²			
Ground floor	Hollow core slab (VBI 260)	d =	260	mm	=	6,50	kN/m²			
	Finishing layer	d =	70	mm	=	1,40	+			
					G_k =	7,90	kN/m²			
Gallery floor	Floor-element	d =	300	mm	=	7,50	kN/m²			
							+			
					G_k =	7,50	kN/m²			
Steel balcony	Top- and bottomlayer	d =	10	mm	=	0,79	kN/m²			
	Beam along q-load	d_rel =	2,55507	mm	=	0,20				
	Beam in q-load, front	d_rel =	1,64	mm	=	0,13				
	Beam in q-load, back	d_rel =	0,83333	mm	=	0,07				
					G_k =	1,18	kN/m²			
Lower beam	Concrete	d =	500	mm	G_k =	12,50	kN/m²			
Walls	HSB incl. glass				G_k =	2,50	kN/m²	A =	1E+08 mm²	= 281,3 kN
	HSB full				G_k =	3,00	kN/m²	A =	1E+08 mm²	= 337,5 kN
	Concrete normal walls	d =	250	mm	G_k =	6,25	kN/m²			
	Concrete unit walls short direction	d =	320	mm	G_k =	8,00	kN/m²			
	Concrete unit walls long direction	d =	150	mm	G_k =	3,75	kN/m²	A =	1E+08 mm²	= 421,9 kN
Columns	Steel column gallery	A =	6580	mm²	G_k =	0,52	kN/m²	l =	13 m	= 6,715 kN
	Concrete columns ground floor	A =	160000	mm²	G_k =	4	kN/m²	l =	2,91 m	= 11,64 kN
Foundation	Footings	d =	800	mm	G_k =	20,00	kN/m²			
	Beams	d =	500	mm	G_k =	12,50	kN/m²			

Figure B-2: Dimensions and loads normal elements

Flat roof (6th floor)	Floor-element	d =	360	mm	=	9,00	kN/m²
	Gravel	d =	60	mm	=	1,08	
	Insulation (type unknown)				=	0,10	
	Roof cover				=	0,05	+
					G_k =	10,23	kN/m²
2nd-5th floor	Floor-element	d =	360	mm	=	9,00	kN/m²
							+
					G_k =	9,00	kN/m²
1st floor	Floor-element	d =	360	mm	=	9,00	kN/m²
							+
					G_k =	9,00	kN/m²

Figure B-3: Dimensions and loads unit elements

F1

	width	length	6.10b		
	m	m	FGk	FQk	
steel columns	0,00	0,00	6,71	0,00	kN
gallery-floor (2nd-5th fl.)	1,24	30,00	279,56	0,00	kN
			286,28	0,00	kN

F2

	width	length	6.10b		
	m	m	FGk	FQk	
gallery-floor (2nd-5th fl.)	0,84	30,00	189,56	0,00	kN
facade longitudinal	7,50	14,30	268,13	0,00	kN
			457,69	0,00	kN

F3

	width	length	6.10b		
	m	m	FGk	FQk	
unit wall long dir.	7,20	13,10	353,70	0,00	kN
			353,70	0,00	kN

F4

	width	length	6.10b		
	m	m	FGk	FQk	
facade longitudinal	7,50	15,80	296,25	0,00	kN
			296,25	0,00	kN

F5

	width	length	6.10b		
	m	m	FGk	FQk	
concrete columns	0,00	0,00	11,64	0,00	kN
ground floor gallery-side	2,58	7,50	153,01	0,00	kN
foundation-beams	0,5	10,2	63,75	0,00	kN
			228,40	0,00	kN

F6

	width	length	6.10b		
	m	m	FGk	FQk	
concrete columns	0,00	0,00	11,64	0,00	kN
ground floor gallery-side	2,58	7,50	153,01	0,00	kN
ground floor balcony-side	1,75	7,50	103,69	0,00	kN
foundation-footing	3,10	3,40	210,80	0,00	kN
foundation-beams	0,5	3,875	24,22	0,00	kN
			503,36	0,00	kN

F7

	width	length	6.10b		
	m	m	FGk	FQk	
concrete columns	0,00	0,00	11,64	0,00	kN
ground floor balcony-side	1,75	7,50	103,69	0,00	kN
foundation-footing	2,20	2,20	96,80	0,00	kN
foundation-beams	0,5	6,475	40,47	0,00	kN
			252,60	0,00	kN

Figure B-4: Determination point loads

q1

	width	G_k		6.10a	
	m	kN/m²	G_k	$Q_{k,1}$	
gallery-floor	7,5	7,50	56,25	5,25	kN/m'
lower beam	0,8	12,50	10,00	0,00	kN/m'
			66,25	5,25	kN/m'

q2

	width	G_k		6.10a	
	m	kN/m²	G_k	$Q_{k,1}$	
flat roof n	7,5	9,73	72,98	0,00	kN/m'
5th floor n	7,25	8,50	61,63	7,40	kN/m'
4th floor n	7,25	8,50	61,63	7,40	kN/m'
3rd floor n	7,25	8,50	61,63	7,40	kN/m'
2nd floor n	7,25	8,50	61,63	7,40	kN/m'
1st floor n	7,25	8,50	61,63	7,40	kN/m'
constr. wall 5 floors n	15	6,25	93,75	0,00	kN/m'
lower beam	0,8	12,50	10,00	0,00	kN/m'
			484,85	36,98	kN/m'

q3

	width	G_k		6.10a	
	m	kN/m²	G_k	$Q_{k,1}$	
steel balcony 5th floor	2,27	1,18	2,68	2,27	kN/m'
steel balcony 4th floor	2,27	1,18	2,68	2,27	kN/m'
steel balcony 3rd floor	2,27	1,18	2,68	2,27	kN/m'
steel balcony 2nd floor	2,27	1,18	2,68	2,27	kN/m'
steel balcony 1st floor	2,27	1,18	2,68	2,27	kN/m'
			13,39	11,35	kN/m'

q4

	width	G_k		6.10a	
	m	kN/m²	G_k	$Q_{k,1}$	
flat roof u	7,5	10,23	76,73	0,00	kN/m'
5th floor u	7,5	9,00	67,50	5,25	kN/m'
4th floor u	7,5	9,00	67,50	5,25	kN/m'
3rd floor u	7,5	9,00	67,50	5,25	kN/m'
2nd floor u	7,5	9,00	67,50	5,25	kN/m'
1st floor u	7,5	9,00	67,50	5,25	kN/m'
constr. wall 5 floors u	15	8,00	120,00	0,00	kN/m'
lower beam	0,8	12,50	10,00	0,00	kN/m'
			544,23	26,25	kN/m'

Figure B-5:Determination distributed loads

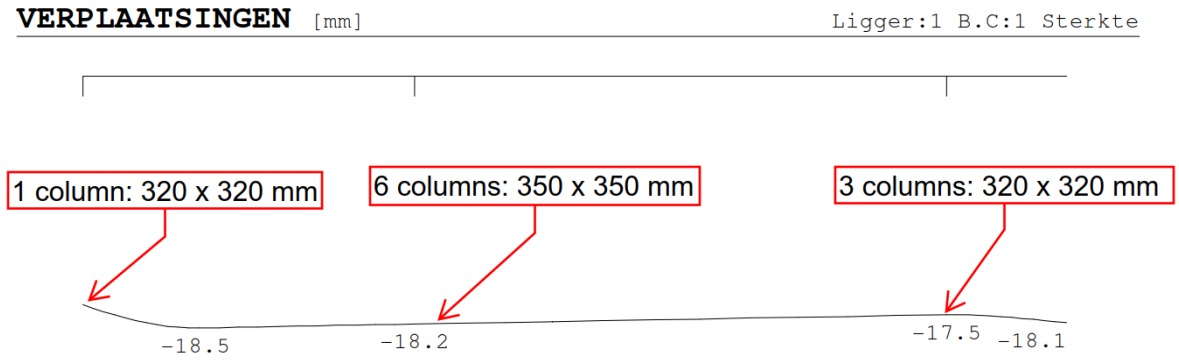

Figure B-6: Final lay-out and deflection outer intermediate wall

Self-weight of an end-wall

Instead of the columns present in intermediate walls, the end walls consist of a wall that progresses to the foundation. Additionally, extra weight is present in these walls, due to exterior aesthetics that are applied. Lastly, only half of the floor-loads are applied on these walls, due to these walls being at the end of the structure. Thus, the self-weight calculation has to be redone for end-walls. The load lay-out is given in Figure B-7, where some parameters have been changed in comparison to the intermediate wall:

- F1: Columns steel + 4 floors of ¼ gallery
- F2: Walls HSB + 4 floors of ¼ gallery
- F3: Walls unit element
- F4: Walls HSB
- Q1: ½ Floor gallery + lower beam
- Q2: 5*½ upper normal floors + ½ normal roof + 5 floors of normal walls + lower beam
- Q3: 5*½ balconies
- Q4: 5*½ upper unit floors + ½ unit roof + 5 floors of unit walls + lower beam
- Q5: Normal end wall + ground floor + foundation beam
- Q6: Unit end wall + ground floor + foundation beam

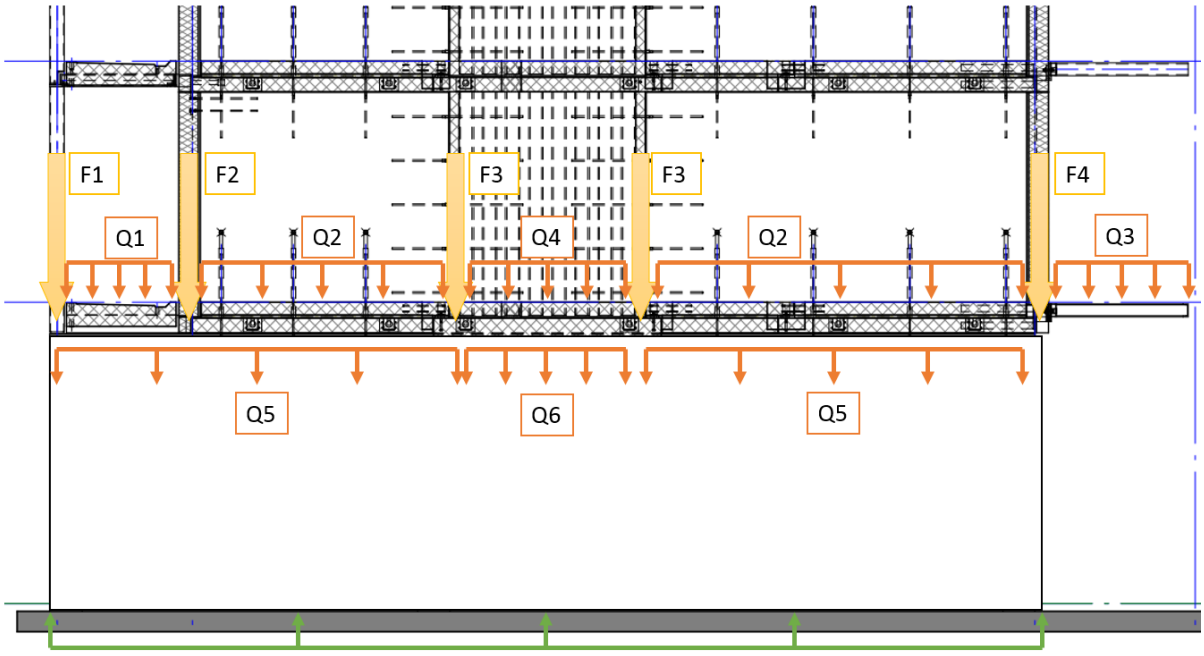

Figure B-7: Load lay-out case study including point loads (yellow), distributed loads (orange), and foundation reaction forces (green)

The reason why the foundation reaction forces are shown as a distributed load is because the amount of piles can be placed on any position of the cross-section due to the wall being connected to the ground. These walls also contribute to the "beam"-element. The left area is now being resisted by the wall from the ground floor, instead of the gallery floor. The newly found dimensions are as follows:

- Gallery-floor: B*H 250x3800 (C40/50)
- Apartments: B*H 250x18800 (C40/50)
- Balconies: B*H 11350x120 (C40/50)

The calculation of the additional wall-elements can be found in Figure B-8, and the determination of the load-values is shown in Figure B-9 and Figure B-10. Now, multiple considerations have to be taken into account. Next to the already mentioned equal sagging in the short direction, there is now also the additional requirement that the sagging must be equal along the long direction of the building. This means that the pile lay-out of the end-walls must result in similar deflections as the intermediate walls. However, due to the wall structure being connected to the floor, the piles can be placed anywhere along the cross-section. By trial-and-error, the final pile lay-out is given in Figure B-11. All of the piles are dimensions 320 by 320 mm, with an exception for the fully left pile, which is 290 by 290 mm. The deflection of the end walls is given in Figure B-12.

Exterior wall n	Concrete	d =	250 mm	6,25 kN/m²
	Stone cladding			1,80
				+
				G_k = 8,05 kN/m²
Exterior wall u	Concrete	d =	320 mm	8,00 kN/m²
	Stone cladding			1,80
				+
				G_k = 9,80 kN/m²

Figure B-8: New wall-loads due to exterior aesthetics

q1

	width	G_k		
	m	kN/m²	G_k	
gallery-floor	3,75	7,50	28,13	kN/m¹
lower beam	0,8	12,50	10,00	kN/m¹
			38,13	kN/m¹

q2

	width	G_k		
	m	kN/m²	G_k	
flat roof n	3,75	9,73	36,49	kN/m¹
5th floor n	3,625	8,50	30,81	kN/m¹
4th floor n	3,625	8,50	30,81	kN/m¹
3rd floor n	3,625	8,50	30,81	kN/m¹
2nd floor n	3,625	8,50	30,81	kN/m¹
1st floor n	3,625	8,50	30,81	kN/m¹
wall 5 floors incl. cladding r	15	8,05	120,75	kN/m¹
lower beam	0,8	12,50	10,00	kN/m¹
			321,30	kN/m¹

q3

	width	G_k		
	m	kN/m²	G_k	
steel balcony 5th floor	1,135	1,18	1,34	kN/m¹
steel balcony 4th floor	1,135	1,18	1,34	kN/m¹
steel balcony 3rd floor	1,135	1,18	1,34	kN/m¹
steel balcony 2nd floor	1,135	1,18	1,34	kN/m¹
steel balcony 1st floor	1,135	1,18	1,34	kN/m¹
			6,69	kN/m¹

q4

	width	G_k		
	m	kN/m²	G_k	
flat roof u	3,75	10,23	38,36	kN/m¹
5th floor u	3,625	9,00	32,63	kN/m¹
4th floor u	3,625	9,00	32,63	kN/m¹
3rd floor u	3,625	9,00	32,63	kN/m¹
2nd floor u	3,625	9,00	32,63	kN/m¹
1st floor u	3,625	9,00	32,63	kN/m¹
wall 5 floors incl. cladding u	15	9,80	147,00	kN/m¹
lower beam	0,8	12,50	10,00	kN/m¹
			358,49	kN/m¹

Figure B-9: Determination first half distributed loads

q5

	width	G_k	G_k	
	m	kN/m²		
wall 1 floors incl. cladding r	3,75	8,05	30,19	kN/m¹
ground floor	3,625	7,90	28,64	kN/m¹
foundation beams	0,5	12,50	6,25	kN/m¹
			65,08	kN/m¹

q6

	width	G_k	G_k	
	m	kN/m²		
wall 1 floors incl. cladding ι	3,75	9,80	36,75	kN/m¹
ground floor	3,625	7,90	28,64	kN/m¹
foundation beams	0,5	12,50	6,25	kN/m¹
			71,64	kN/m¹

F1

	width	length	G_k		
	m	m	kN/m²	FGk	
steel columns	0,00	0,00	0,00	6,71	kN
gallery-floor (2nd-5th fl.)	1,24	15,00	7,50	139,78	kN
				146,50	kN

F2

	width	length	G_k		
	m	m	kN/m²	FGk	
gallery-floor (2nd-5th fl.)	0,84	15,00	7,50	94,78	kN
facade longitudinal	3,75	14,30	2,50	134,06	kN
				228,84	kN

F3

	width	length	G_k		
	m	m	kN/m²	FGk	
unit wall long dir.	3,60	13,10	3,75	176,85	kN
				176,85	kN

F4

	width	length	G_k		
	m	m	kN/m²	FGk	
facade longitudinal	3,75	15,80	2,50	148,13	kN
				148,13	kN

Figure B-10: Determination second half distributed loads and point loads

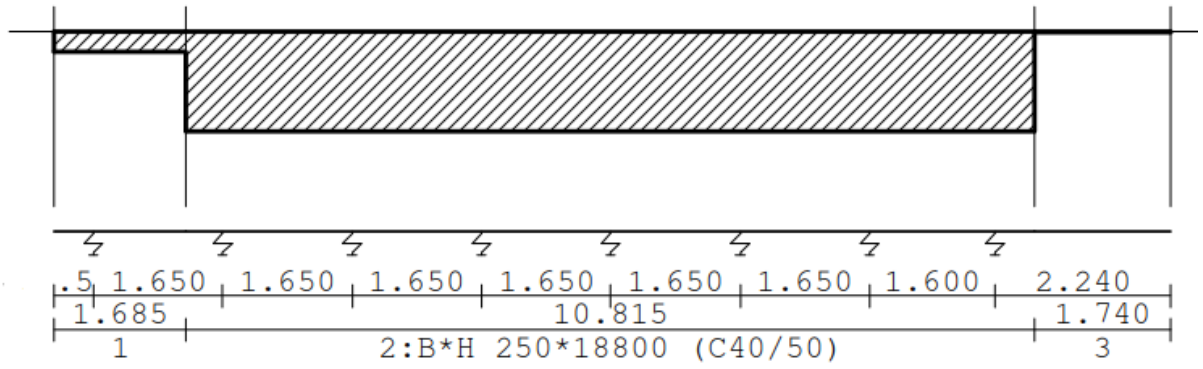

Figure B-11: Final lay-out pile foundation end-wall

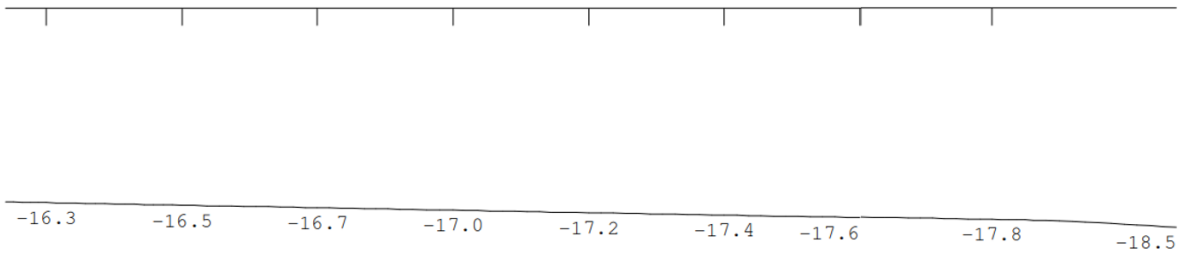

Figure B-12: Final deflection end-walls

Wind load and skewness walls

For this calculation, it is assumed that the building in infinitely stiff. This means that a horizontal load will result in a solid rotation of the structure. This solid rotation will be resisted by the pile-foundations determined in the last calculation. The amount of horizontal load each part resists, depends on the relative stiffnesses between the foundations. These stiffnesses are calculated here, after which the loads on each

Firstly, a small change is made in the foundation lay-out. To resist wind-loads on the short side of the structure, one stability-wall is placed on the balcony-side of the structure, which is supported by the two inner pile foundations. As it is expected that this will cause additional loads on these piles, these two pile foundations will be additionally strengthened by replacing the three 320 x 320 mm piles on this position by three 350 x 350 mm piles. Thus, there will be three cross-sections that need to be calculated:

1. Normal inner cross-section (using 320 x 320 mm piles at the balcony-side)
2. Strengthened inner cross-section (using 350 x 350 mm piles at the balcony-side)
3. Outer cross-section

<u>Normal cross-section</u>

Before the relative stiffness of each pile cross-section are mentioned, extra attention is given to the pile on the gallery-side, as this pile is indirectly connected to a relatively weak beam in the gallery. This beam will bend, and as such not take part fully in the solid rotation of the structure. In the end, this will result in a pile-foundation that is less stiff. The magnitude of this reduction is as follows:

Stiffness of 320x320 pile: $\gamma = 40000\ kN/m$

If it is assumed that a load of 1000 kN is applied to this pile, this will result in a deflection of:

$$w = \frac{F}{\gamma} = \frac{1000}{40000} * 1000 = 25\ mm$$

Additionally, the 1.6 m long beam will be loaded by the pile-foundation like a cantilever with this same load, resulting in the following deflection:

$$w = \frac{F * L^3}{3 * EI} = \frac{1000 * 10^3 * 1600^3}{3 * 14000 * \frac{1}{12} * 800 * 500^3} = 12\ mm$$

The total deflection is thus $25 + 12 = 37\ mm$.

Putting this back into the pile-formula to determine the fictitious stiffness of the pile:

$$\gamma_f = \frac{F}{w} = \frac{1000}{0.025 + 0.012} = 27000\ kN/m \approx 25000\ kN/m$$

This approximation is equal to pile-dimensions of 260 x 260 mm. Thus, the lay-out of the piles can be found in Figure B-13 and their relative stiffnesses are as follows:

- 320 mm piles including beam: 25000 kN/m
- 350 mm piles: 50000 kN/m
- 320 mm piles: 40000 kN/m

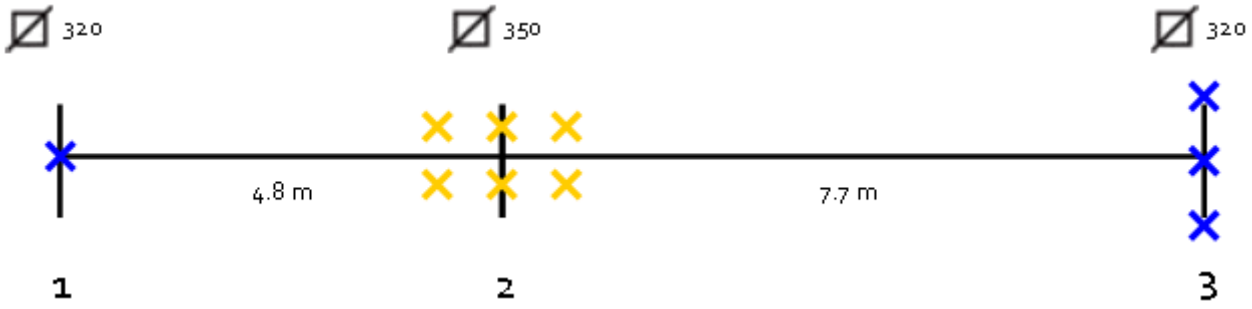

Figure B-13: Pile lay-out of normal inner cross-section

Based on these foundations, the centre of gravity can be determined, after which a relative moment of inertia can be calculated. The reference-point is set at pile-group 1. Additionally, relative stiffnesses are set for the piles to simplify the calculation. Thus, the calculation is as follows:

- Pile-group 1: $1 * 0.5 *$ 0 $= 0$
- Pile-group 2: $6 * 1 *$ 4.8 $= 28.8$
- Pile-group 3: $3 * 0.8 *$ 12.5 $= 30$
- Total: $8.9 *$ x $= 58.8$

This results in a distance of **6.6 m** from pile-group 1. With this information, the moment of inertia can be determined:

$$I = 1 * 0.5 * 6.6^2 + 6 * 1(6.6 - 4.8)^2 + 3 * 0.8(12.5 - 6.6)^2$$

$$\boldsymbol{I = 125 \ldots\ldots m^4}$$

The same is done for the strengthened inner cross-sections, of which the lay-out is shown in Figure B-14.

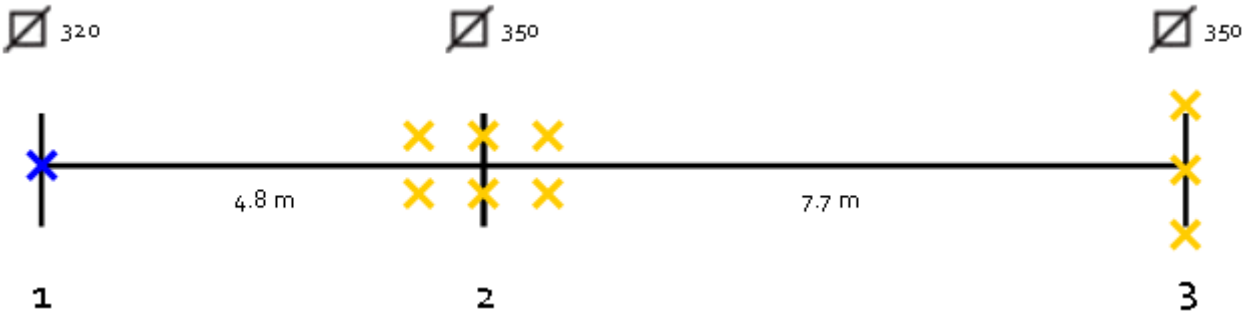

Figure B-14: Pile lay-out of strengthened inner cross-section

Thus, the calculation is as follows:

- Pile-group 1: $1 * 0.5 *$ 0 $= 0$
- Pile-group 2: $6 * 1 *$ 4.8 $= 28.8$
- Pile-group 3: $3 * 1 *$ 12.5 $= 37.5$
- Total: $9.5 *$ x $= 66.3$

This results in a distance of **7.0 m** from pile-group 1. With this information, the moment of inertia can be determined:

$$I = 1 * 0.5 * 7.0^2 + 6 * 1(7.0 - 4.8)^2 + 3 * 1(12.5 - 7.0)^2$$

$$\boldsymbol{I = 144 \ldots\ldots m^4}$$

For the determination of the moment of inertia of the outer walls, the piles are spread along the cross-section, as is shown in Figure B-15. The stiffnesses of these piles are as follows:

- 290 mm pile: 32000 kN/m
- 320 mm piles: 40000 kN/m

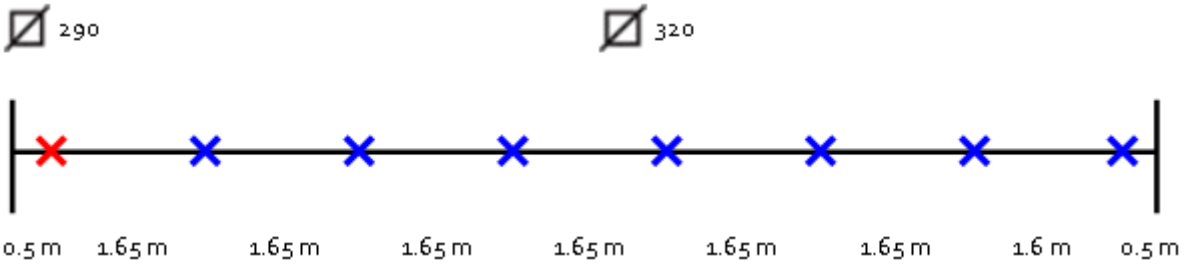

Figure B-15: Pile lay-out of outer cross-section

Thus, the calculation is as follows:

$$z = \frac{0.8 * (0.5) + 1.0 * (2.15 + 3.8 + 5.45 + 7.1 + 8.75 + 10.4 + 12.0)}{7.8} = 6.4\, m$$

This results in a distance of **6.4 m** from the left edge. With this information, the moment of inertia can be determined:

$$I = 0.64 * (5.9^2) + 0.8 * (4.25^2 + 2.6^2 + 0.95^2 + 0.7^2 + 2.35^2 + 4^2 + 5.6^2)$$

$$\boldsymbol{I = 86 \ldots\ldots m^4}$$

As the wind-load will blow against the entire 40 m of the building, this width will be divided between all relative stiffnesses:

"Total" relative stiffness: $I = 710 \ldots \ldots m^4$

Width taken by normal inner cross-section: $\frac{125}{710} * 40 = \mathbf{7.0\ m}$

Width taken by strengthened inner cross-section: $\frac{144}{710} * 40 = \mathbf{8.1\ m}$

Width taken by outer cross-section: $\frac{86}{710} * 40 = \boldsymbol{4.9\ m}$

As an initial calculation, the wind load is simplified as $q = 1.2 * 1.07 \approx \boldsymbol{1.3\ kN/m^2}$

This results in a total moment of:

Outer cross-sections: $\frac{1}{2} * 4.9 * 1.3 * 21.3^2 = 1445\ kNm$

Inner normal cross-sections: $\frac{1}{2} * 7.0 * 1.3 * 21.3^2 = 2065\ kNm$

Inner strengthened cross-sections: $\frac{1}{2} * 8.1 * 1.3 * 21.3^2 = 2390\ kNm$

Which is equal to a total moment on the building of $\sum M_{stab} = 11800\ kNm$.

However, the ground floor only consists of columns in the inner cross-sections. As these structures will not be able to transfer the moment to the ground floor, these loads have to be transferred by shear forces in the floor-elements. The magnitude of these shear forces are calculated in the following part.

Wind load

Including additional regulations due to wind blowing around a structure, the total moment in the strengthened inner cross-section is determined as $M_{t/m\,0}$. Due to the restriction that no moment may occur in the column, the shear force reactions by the floor are split into two parts:

- The shear balance, that balances out the vertical equilibrium;
- A (linear) moment reaction, that ensures that no moment occurs in the ground floor.

The shear balance is easily calculated by taking the loaded area per floor:

$F_{shear} = 3.0 * (1.3 * 8.1) = \boldsymbol{31.6\ kN}$

The total moment that needs to be balanced out can be calculated as follows:

$M_{t/m\,0} = 18.0 * (1.3 * 8.1) * (3.3 + 9.0) = 2331\ kNm$

The required balance-forces can be found using the following equation:

$15F_m + 12 * 0.6F_m + 9 * 0.2F_m - 6 * 0.2F_m - 3 * 0.6F_m = 2331\ kNm$

Solving this results in $\boldsymbol{F_m = 111\ kN}$.

Combining both parts results in the total shear force reactions due to wind load, which is given in Figure B-16.

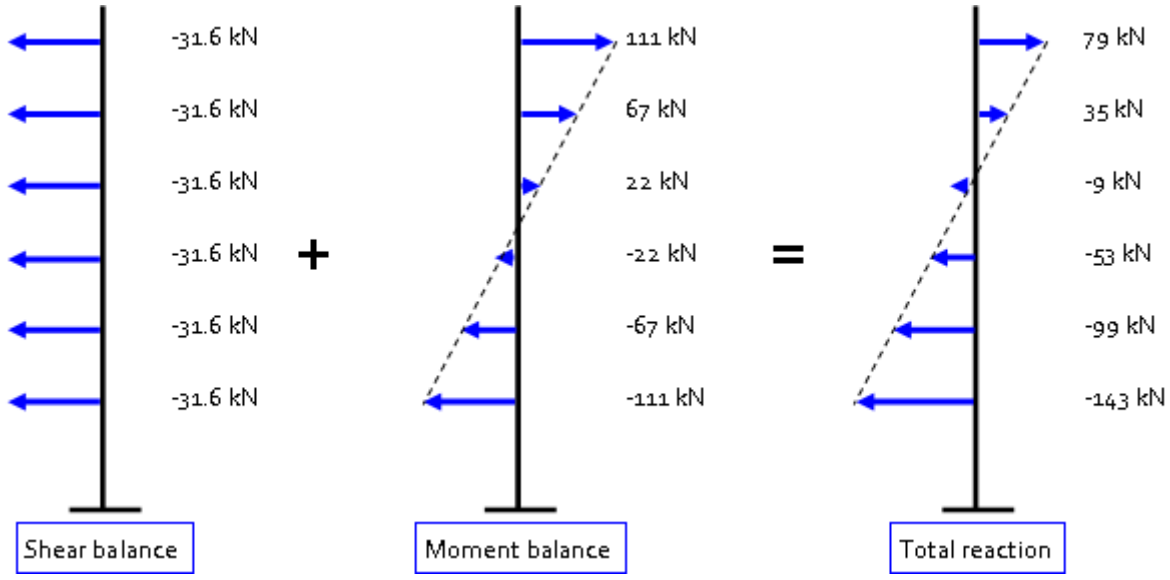

Figure B-16: Resulting shear forces due to wind-load

Skewness columns

This same calculation has to be made for the skewness of the columns. However, two important differences are present:

- Skewness of the columns will not occur in the roof-structure, so only five floors will be loaded;
- The behaviour of the moment-forces are quasi-linear instead of linear (Mink, Discussion about the Reinbouw mid-rise project, 2019).

As an initial calculation, it is assumed that the same load is applied in the case of the wind load. As only 5 floors will resist this force, the total shear balance-force is equal to:

$$F_{shear} = 31.6 * \frac{6}{5} = \mathbf{38\ kN}$$

The total moment that needs to be balanced out can be calculated as follows:

$$M_{t/m\,0} = 38 * (4.8 + 7.8 + 10.8 + 13.8 + 16.8) = 2052\ kNm$$

The required balance-forces can be found using the following equation:

$$(12 + 9)1.5F_m + 6 * \frac{1}{4}F_m - 3 * F_m = 2052\ kNm$$

Note that this equation is based on the quasi-linear behaviour of skewness-forces.

Solving above equation results in $\boldsymbol{F_m = 68\ kN}$.

Combining both parts results in the total shear force reactions due to wind load, which is given in Figure B-17.

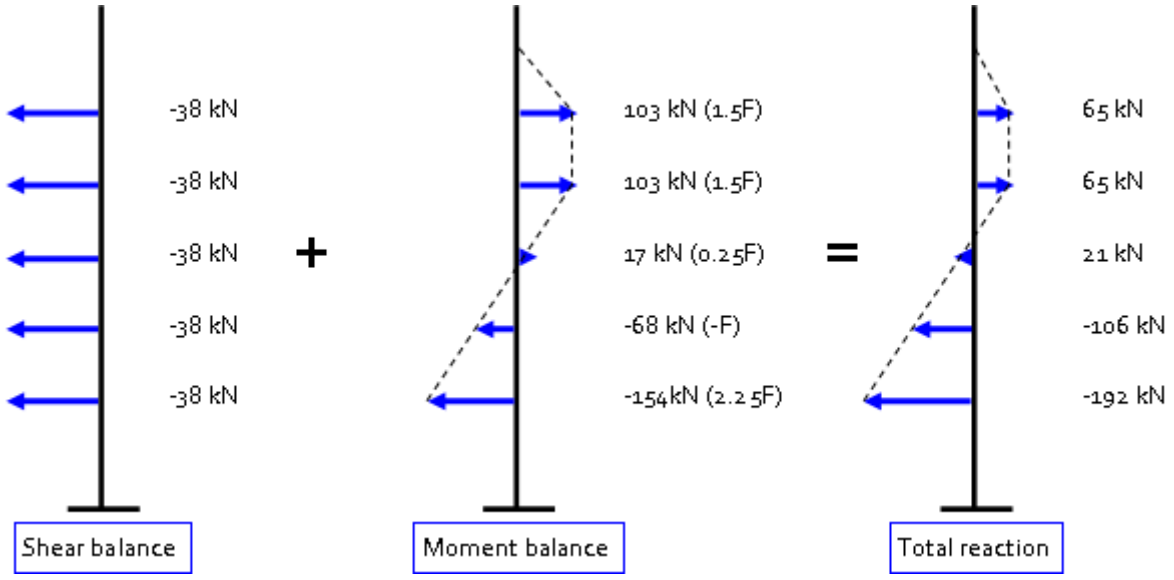

Figure B-17: Resulting shear forces due to skewness columns

C. Appendix: Calculation weakened pile-foundations

In this appendix, the full procedure and calculation from Section 5.3 is shown. In SCIA, the full pre-fabricated project of Lievense | WSP has been modelled, which is shown in Figure C-1. In this model, self-weight loads are not placed onto the floors themselves, but instead applied directly on the foundation springs. This will initially result in an equal sag of the full structure. However, changes in the soil-stiffness will cause the changed flow of forces to be clearly visible.

This model has multiple functions. Firstly, it will be used to check if the assumptions from the hand-calculations are correct. If this is the case, the wind-load and their resultant shear-forces can be related to the effect of weakened soil-areas in the foundation.

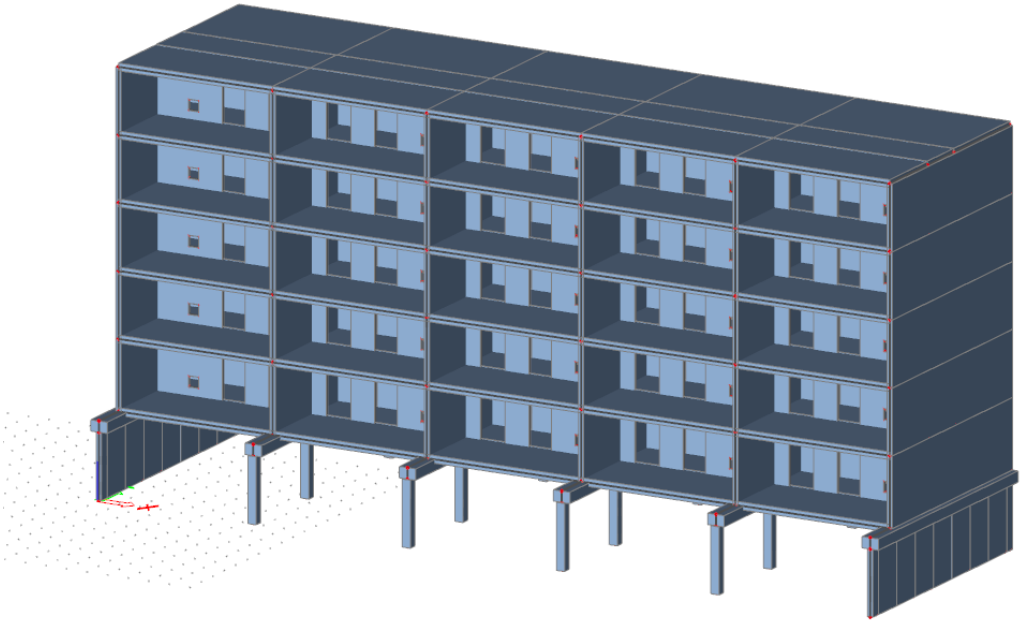

Figure C-1: SCIA model of the pre-fabricated project of Lievense | WSP

Verification of assumptions

Firstly, the most simple test to check if the structure behaves as one unit – and thus, linear – is to check the deflection by a wind load. When loaded by only a wind load, the top view of the structure can be found in Figure C-2. The contour-plot shows a complete linear deflection, verifying that the building behaves a one unit.

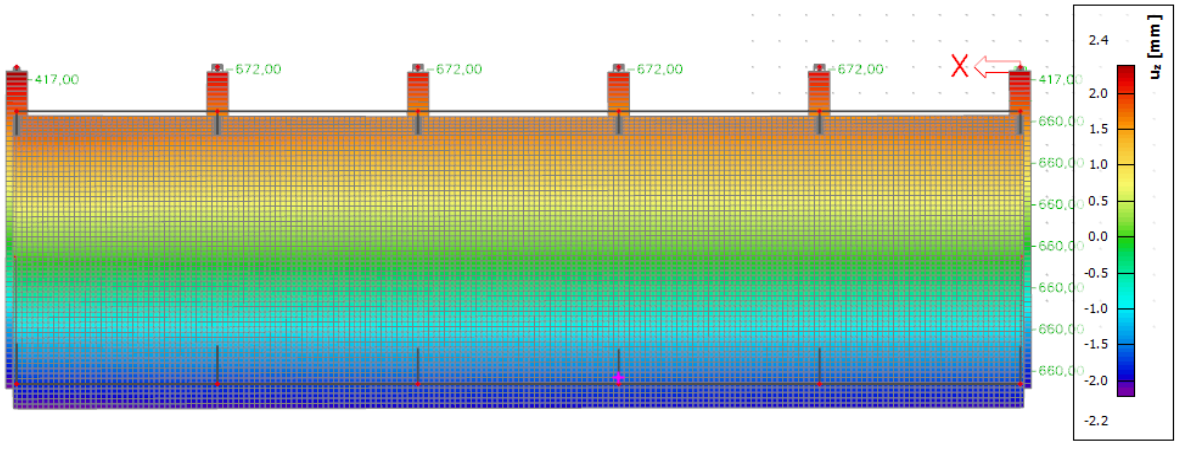

Figure C-2: Deflection (u_z) due to wind-load

Additionally, if viewed from the top, the structure can be seen as a simply supported span, where the wind-load is a distributed load on the "beam", as shown in Figure C-3. The reasoning for this is that only the edge-walls are able to resist shear-forces to the ground. All wind-loads on the inner walls must thus be transferred to the outer walls. However, this essentially causes a bending moment with compression at the top edge and tension at the bottom throughout the floors. This is also visible when looking at the SCIA-model in Figure C-4.

This behaviour is important, as it shown the global behaviour of the structure. When viewing all floors simultaneously as shown in Figure C-5, a clear change of sign in this "bending moment" can be found. More importantly, the proportion of the normal stresses on the different floors are very close to the proportion of shear forces in Figure B-16. This is another verification that the structure behaves essentially as one unit, meaning the linear balancing-method can be used as relative values to calculate the shear-forces that occur due to weakened foundation due to soil.

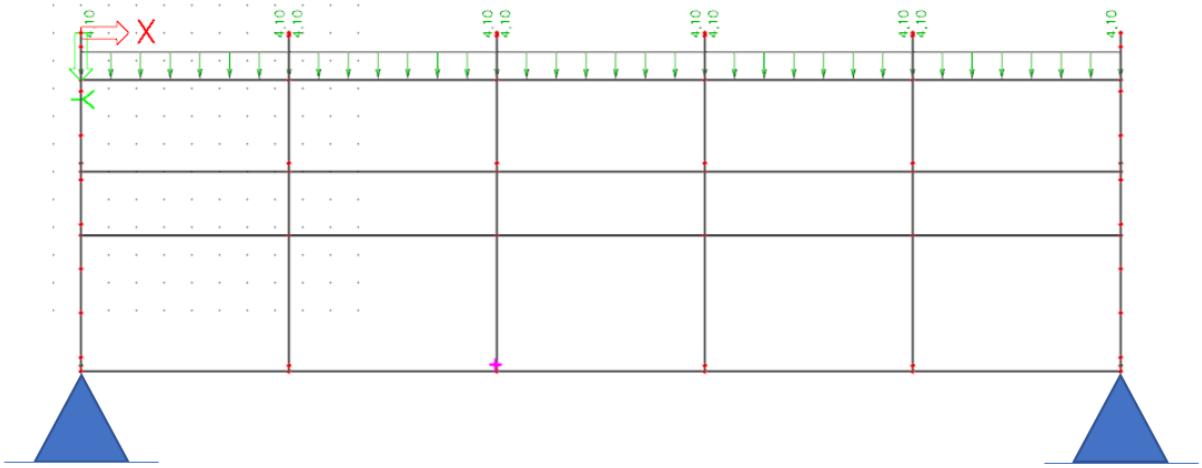

Figure C-3: Simply supported beam-model from top-view

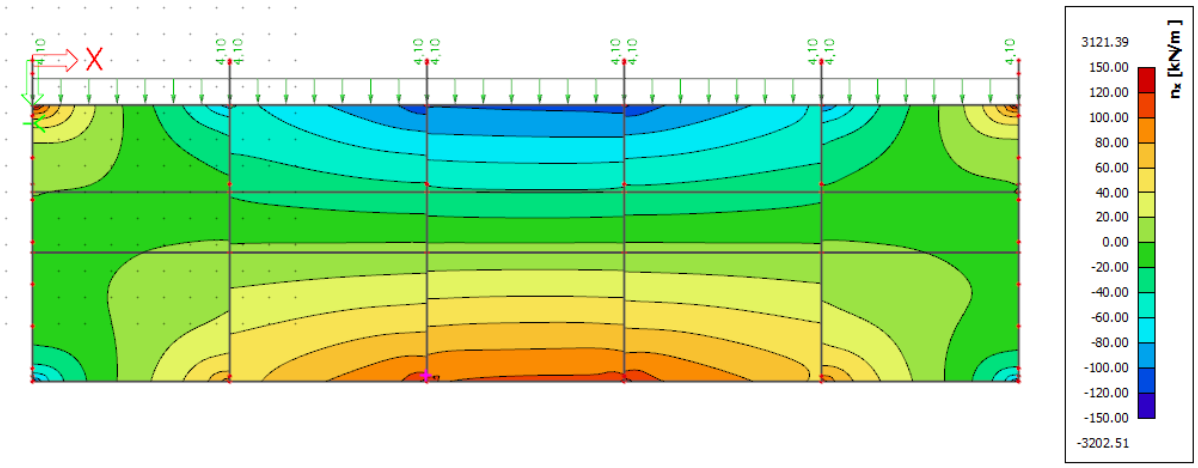

Figure C-4: Visible "bending moment" from top-view

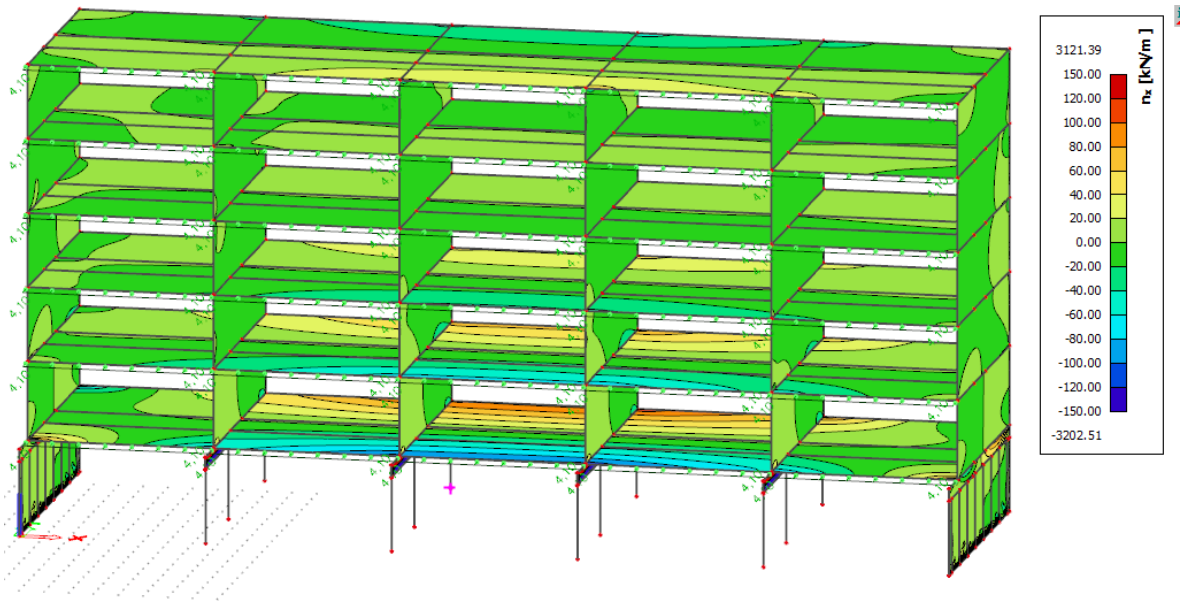

Figure C-5: Proportion of "bending moments" in each floor

Effect of unit-walls

Weaker pile-foundations can cause both concentrated horizontal and vertical displacements. While the horizontal displacements are mainly resisted by the floor-elements, the unit-walls are expected to resist the vertical displacements. Still, as these displacements might be dependent on each other, a stiffer unit wall might influence the loads on the floor-elements. In this part, the effect of the unit walls on the general response of the structure is discussed.

As a comparison, two models are set up, possessing the same weakened pile-foundations. The original situation including reaction forces without any weakened pile-foundations is given in Figure C-6a. The reaction-forces with and without unit walls can be found in Figure C-6b and c respectively. Here, it can be seen that a significant portion of the reaction forces are transported to non-weakened pile-foundations when unit walls are applied. This means that the surrounding pile foundations help resist the unequal deflection when unit walls are applied. As the goal is to find the worst-case scenario with the highest deflections, it is more useful to not use unit walls in this calculation.

When looking at Figure C-7 and Figure C-8, it can also be seen that the "bending" behaviour of the structure is also much more clear when unit walls are not applied. This observation is yet another reason to use the alternative without unit walls, to simplify the calculation.

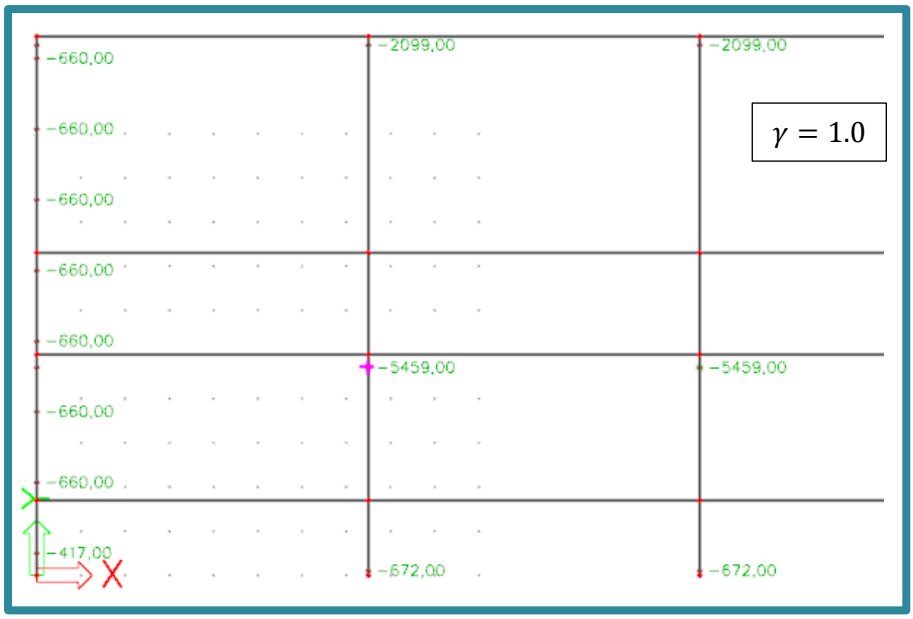

a) Applied forces on pile foundations

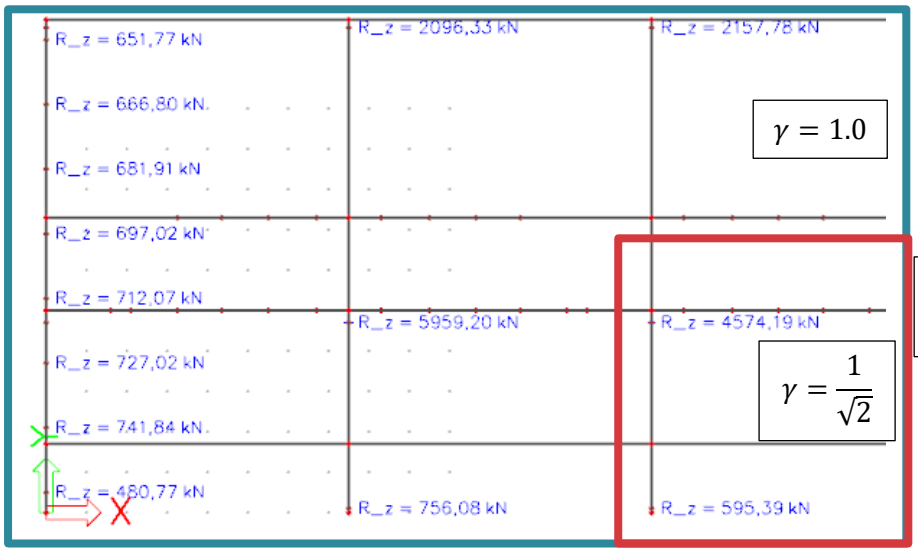

b) Foundation response with unit walls

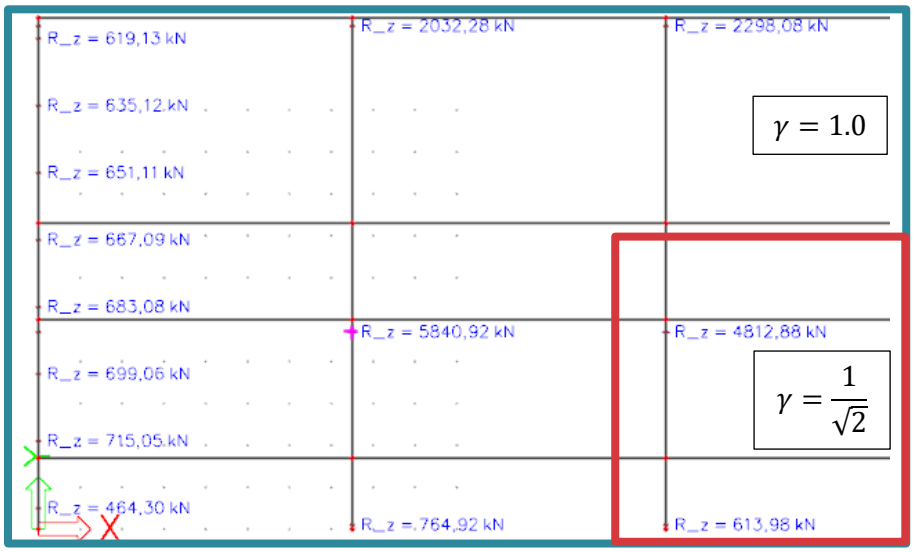

c) Foundation response without unit walls

Figure C-6(a-c): Pile foundation loads and responses with and without unit walls

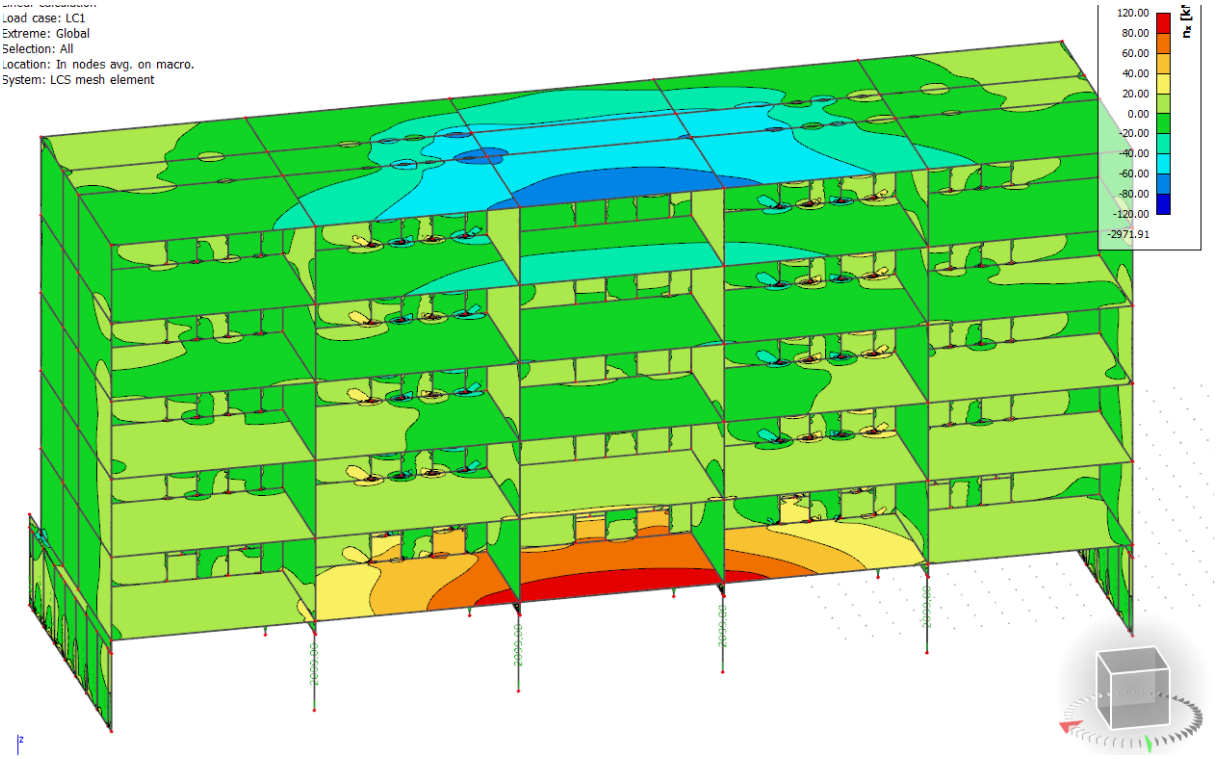

Figure C-7: Internal forces (n_x) of the structure with unit walls

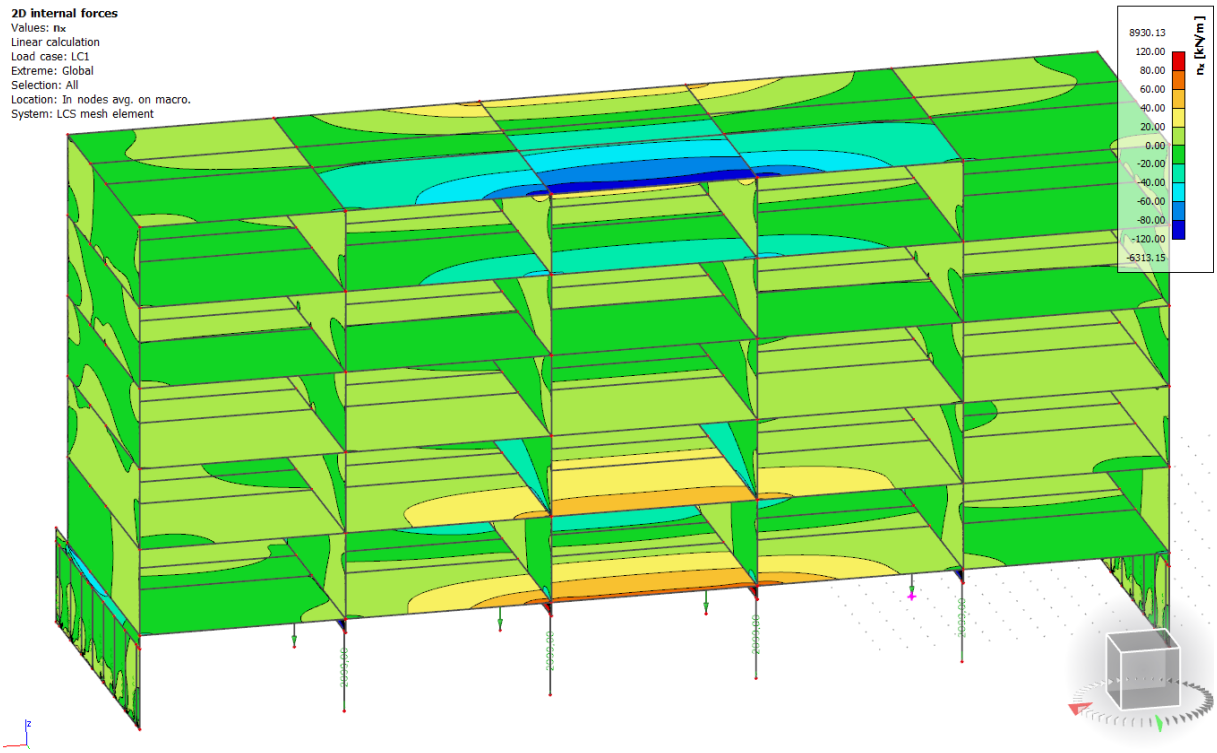

Figure C-8: Internal forces (n_x) of the structure without unit walls

Determination characteristic shear-load

As mentioned before, the unequal soil-deflection causes significant shear-forces in the structure. In this part, it is analysed in what case the highest shear forces occur. The magnitude of these shear-forces are based on the theory explained in the last part, where the occurring "bending moments" in the floors are translated into an additional "wind-load", adding up to the expected shear loads that occur in PCSPs.

Firstly, many different variations of unequal soil-deflections were checked. The following main questions were asked:

- Which side of the structure causes the most "bending moment", the gallery- or balcony-side?
- What size of weakened pile-foundation-groups causes the highest "bending moment"?

To keep a valid amount of different variations, pile-groups will only be weakened in rectangular pairs. In the situation where the piles under the diaphragm-walls are weakened, a number of piles causing an equal stiffness to the inner pile-groups are weakened.

To answer the first question, different variations of weakened pile-groups were modelled. For each of these, the middle two rows of pile groups were used for this comparison. The following variations were modelled:

1. Two pile-groups at gallery-side (1)
2. Two pile-groups at middle (2)
3. Two pile-groups at balcony-side (3)
4. Four pile-groups at gallery-side and middle (1+2)
5. Four pile-groups at middle and balcony-side (2+3)
6. All six pile-groups (1+2+3)

The weakened pile-groups per variation are shown numbered in Figure C-9.

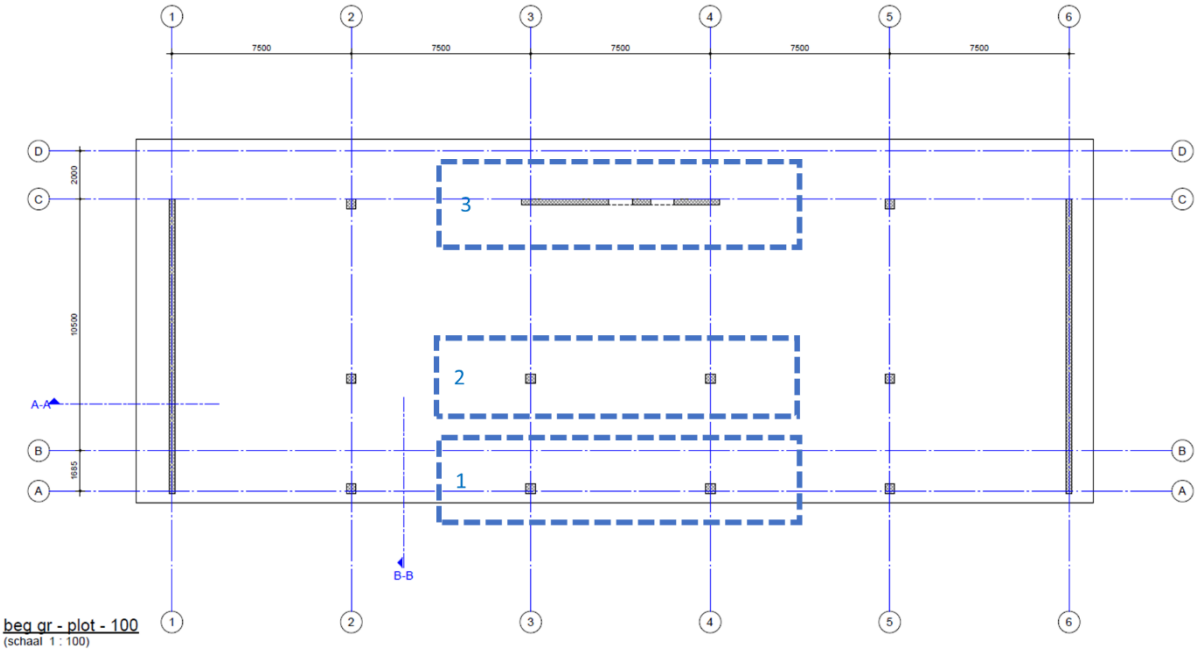

Figure C-9: Weakened pile-groups for first group of variations

The results of all 6 variations can be found in Figure C-10 and Figure C-11. For each result, the same limits of the contour plot are used. It can be seen that variation 1 causes essentially no stresses. Variation 2 and 3 do cause a significant bending moment in the structure, each in the opposite direction of each other. Variation 4 causes the largest reaction of all variations, as this is the combined response of both variation 1 and 2, which caused a bending in the same direction. Both variation 5 and 6 show an almost stable compression in the middle floor. As pile-group 1 from Figure C-9 possesses close to no stiffness, both variations act in a way that the two entire middle cross-section sag equally. This causes no sideward deflection, but only downward, causing a compression force in the inner floors instead. As the goal is to find the variation with the highest bending moment in the structure, variation 4 is chosen as the governing situation. Now, it must be checked which grouping of pile-groups in the width-direction causes the largest bending reaction.

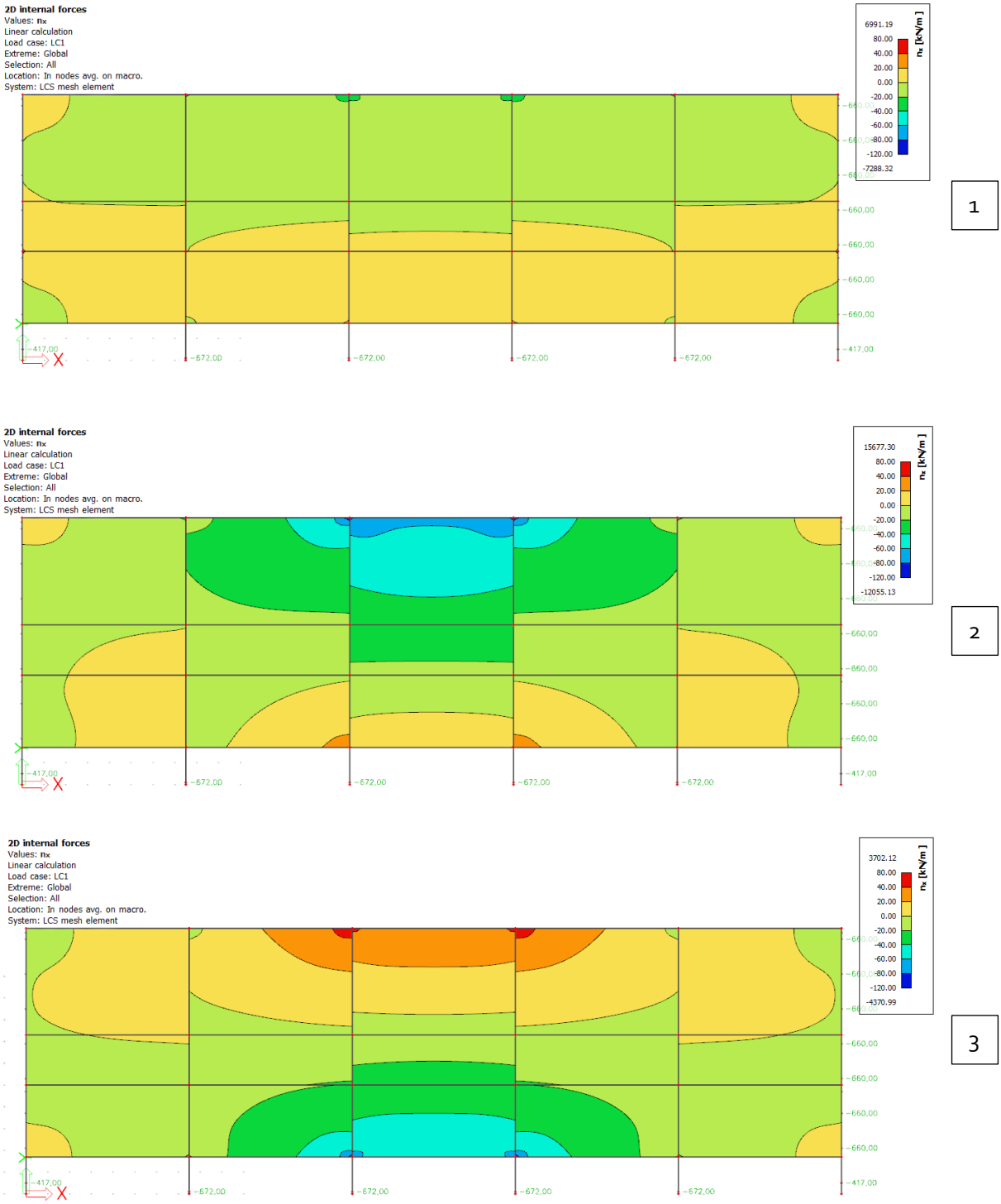

Figure C-10: Results from question 1: variation 1 to 3

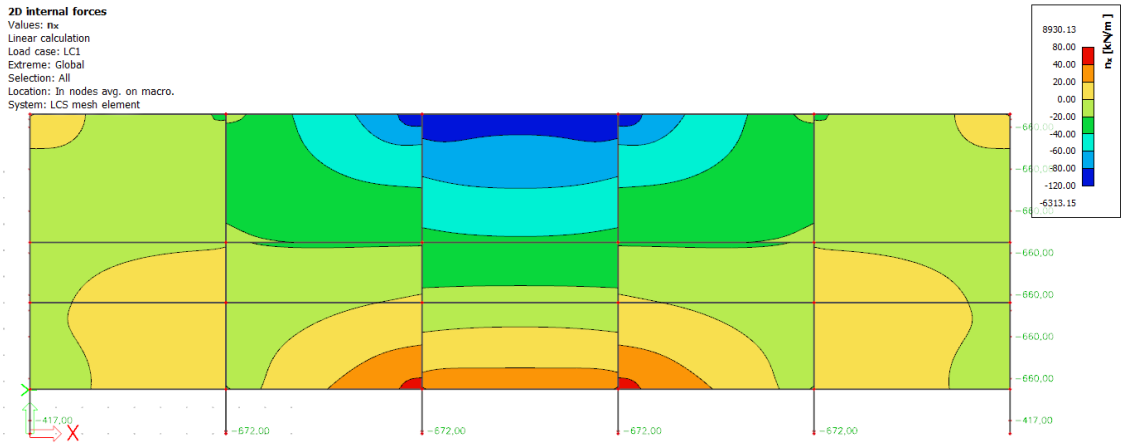

4

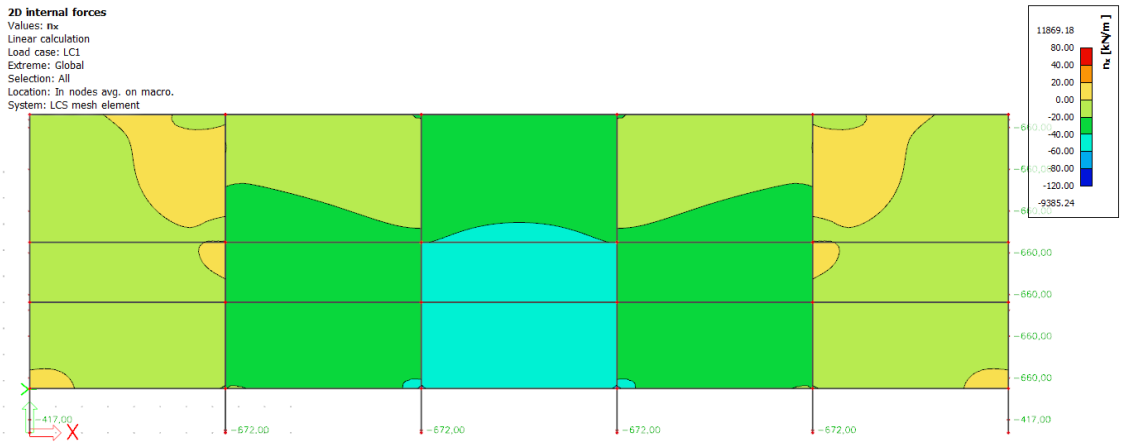

5

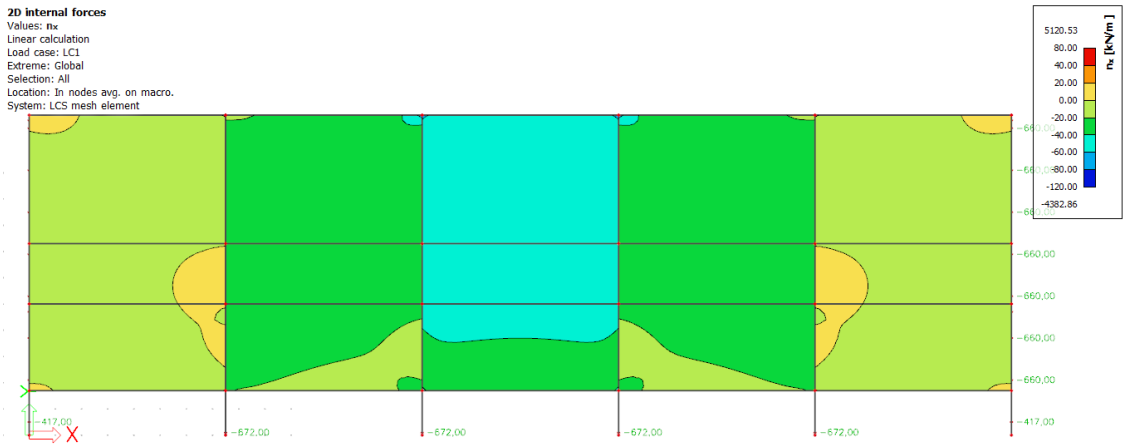

6

Figure C-11: Results from question 1: variation 4 to 6

To answer the second question, the set of pile-groups in the width-direction that cause the highest bending moments had to be found. As the diaphragm walls act as the supports in this case, these are not included in the variations. Additionally, due to symmetry, some combinations don't have to be considered. Thus, the following variations were developed:

1. Two pile-groups of inner left side (1)
2. Two pile-groups of intermediate left side (2)
3. Four pile-groups of inner and intermediate left side (1+2)
4. Four pile-groups of both inner sides (1+3)
5. Six pile-groups of both inner sides and intermediate left side (1+2+3)
6. All eight pile-groups (1+2+3+4)

The weakened pile-groups per variation are shown numbered in Figure C-12.

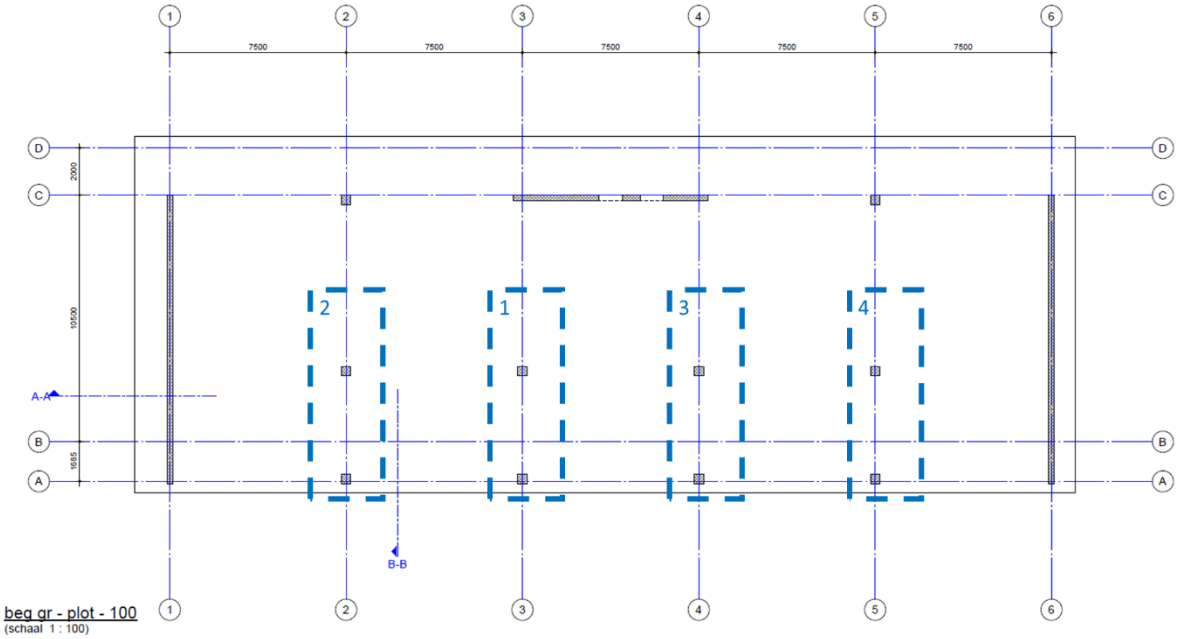

Figure C-12: Weakened pile-groups for second group of variations

The results of all 6 variations can be found in Figure C-13 and Figure C-14. The results from these variations are a bit harder to interpret, due to the effects of a sideways unequal deflection causing significantly higher stresses at edges. However, the goal is still to find the linear bending moment reaction. As can be seen in variation 1 to 3, the stress starts increasing non-linearly when getting closer to the edge. These results seem more like a high reaction force instead of a bending moment. Variation 4 has already been seen from question 1. However, when looking at variation 5, the results show a high linear response at one of the pile cross-sections. Weakening all eight pile-groups in variation 6 lowers the total bending response, as the building makes more of a global rotation instead of causing a reaction moment. As the goal is to find the variation with the highest bending moment in the structure, variation 5 is chosen as the governing situation.

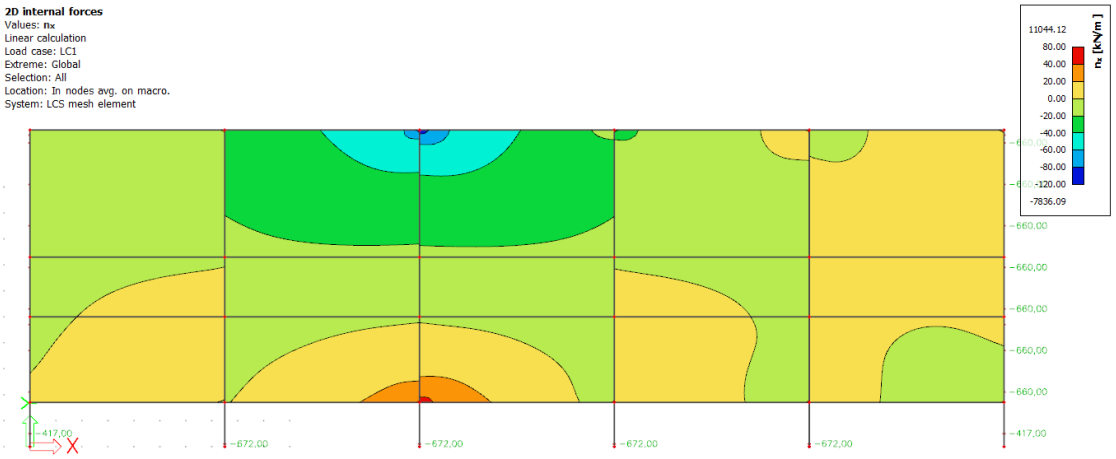

1

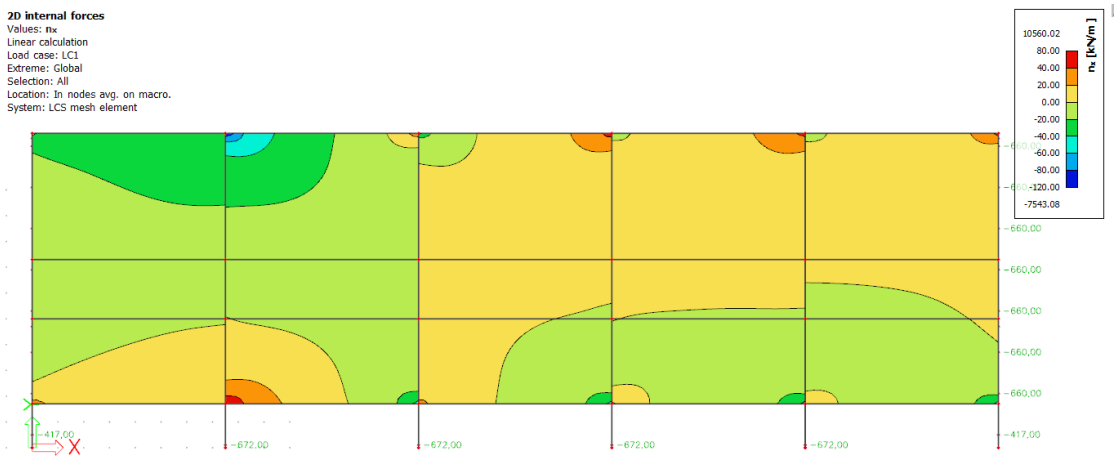

2

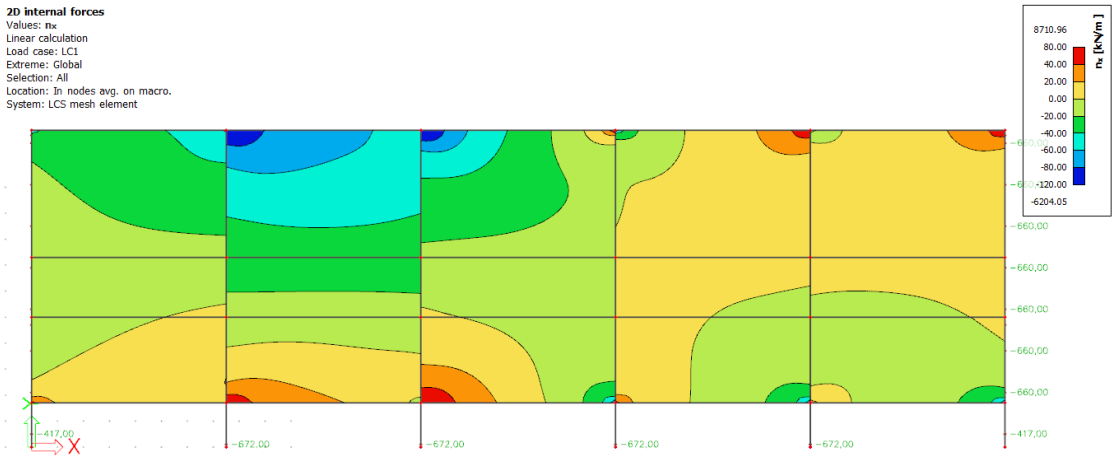

3

Figure C-13: Results from question 2: variation 1 to 3

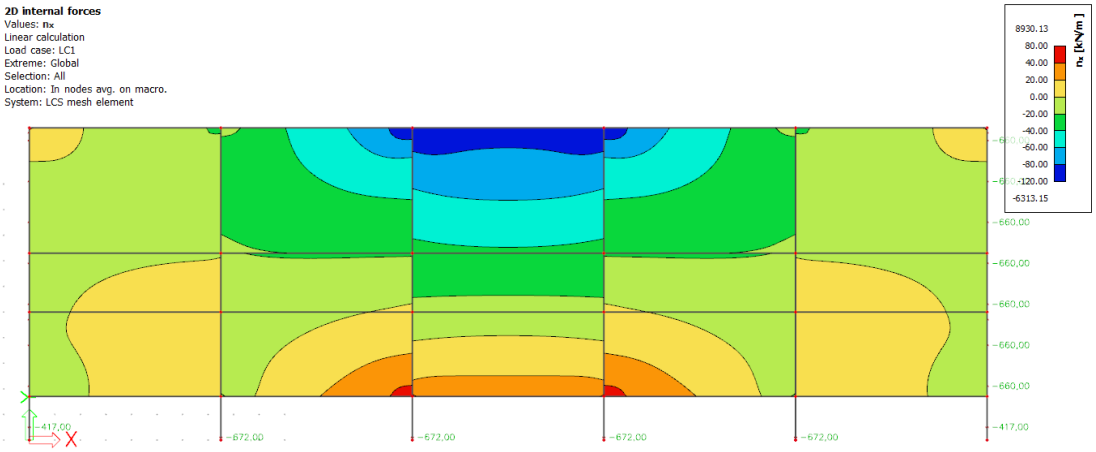

4

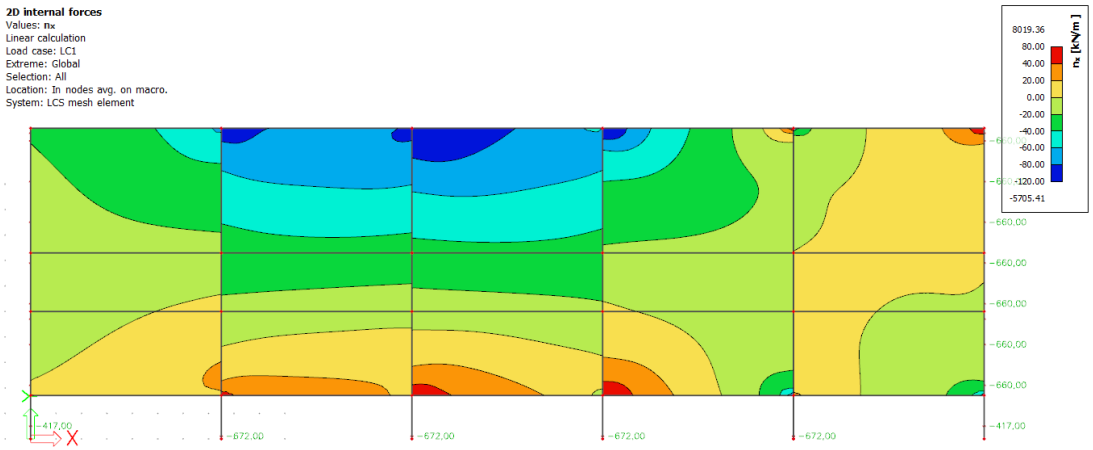

5

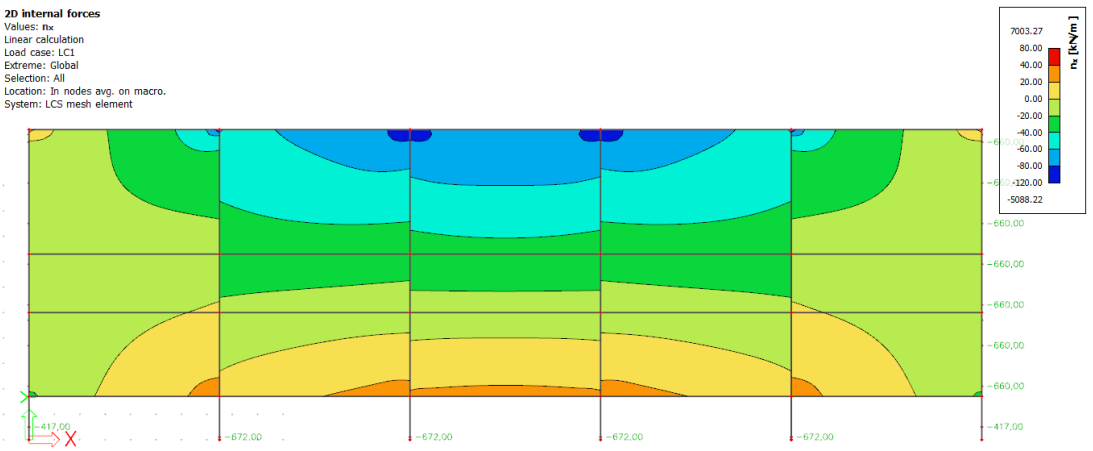

6

Figure C-14: Results from question 2: variation 4 to 6

In order to calculate the shear-responses from each cross-section, the bending stresses in the floor must first be calculated into a bending moment. From Figure C-14 - variation 5, the following bending moments are found:

$$M_{2,4} = \frac{4}{6} * 80 * 5.25^2 \approx 1500\ kNm$$

$$M_3 = \frac{4}{6} * 100 * 5.25^2 \approx 1837.5\ kNm$$

The moment from cross-section 1, 5 and 6 are assumed to be zero. The bending moment schema that comes from these values is found in Figure C-15.

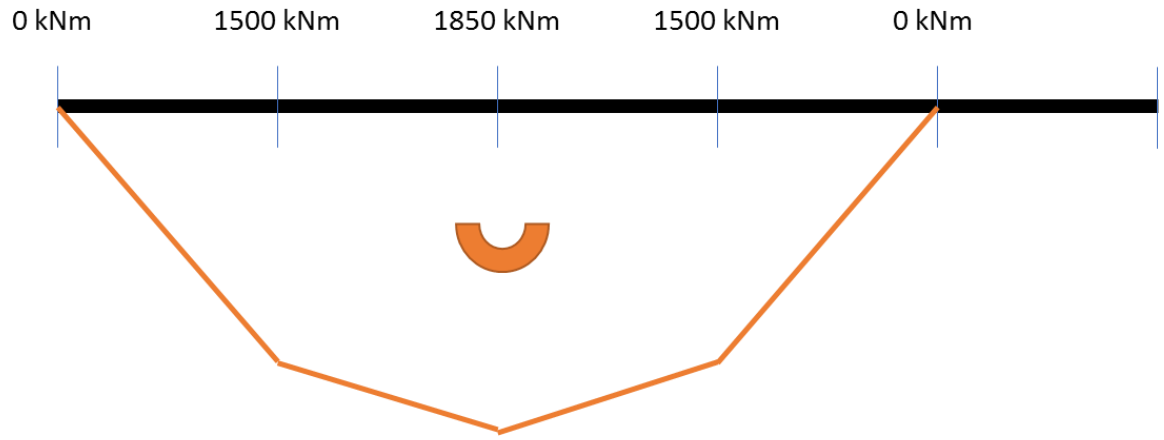

Figure C-15: Bending moments due to weakened pile-foundations

Based on these values, the resulting reaction forces from the cross-sections can be calculated:

$$F_1 = \frac{1500}{7.5} = 200\ kN$$

$$F_{2,4} = \frac{1500 - 350}{7.5} = 153\ kN$$

$$F_{3,5} = \frac{350 + 350}{7.5} = 93\ kN$$

This means that 200 kN is the governing force on the top floor. As it has been confirmed at the start of this appendix that the structure behaves as one unit – and as such linearly – the full shear force on each floor can be calculated. From the model, it is given that the 1st floor has bending stresses of 60 kN/m instead of 100 kN/m. This results in a total response due to weakened pile-foundations and wind loads as shown in Figure C-16. From this, it can be seen that the governing shear force in a floor-element is equal to **312 kN**.

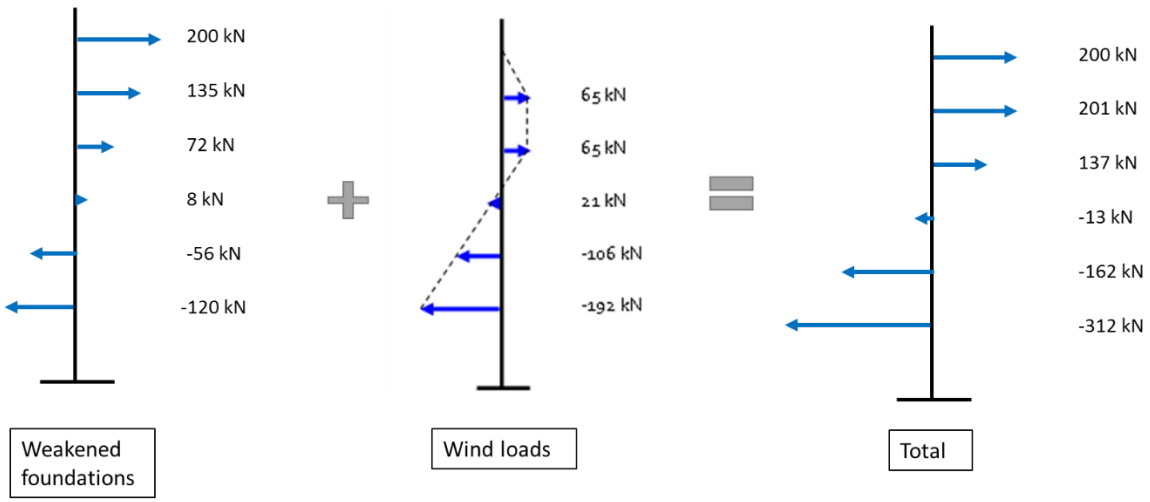

Figure C-16: Total shear values in floors